

AD-A139 539

THE CHEMISTRY OF NITROGEN COMPOUNDS IN COMBUSTION
PROCESSES(U) SRI INTERNATIONAL MENLO PARK CA
T G SLANGER 02 MAR 84 ARO-17561.3-CH DAAG29-81-K-0001

1/0

UNCLASSIFIED

F/G 7/2

NL

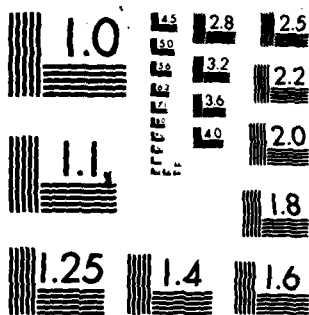
END

DATE

FILED

4-84

DTIC



MICROCOPY RESOLUTION TEST CHART
NATIONAL BUREAU OF STANDARDS-1963-A

AD A139539

Unclassified

SECURITY CLASSIFICATION OF THIS PAGE (When Data Entered)

REPORT DOCUMENTATION PAGE		READ INSTRUCTIONS BEFORE COMPLETING FORM
1. REPORT NUMBER ARO 17561.3-CH	2. GOVT ACCESSION NO. AD-A139539	3. RECIPIENT'S CATALOG NUMBER
4. TITLE (and Subtitle) The Chemistry of Nitrogen Compounds in Combustion Processes		5. TYPE OF REPORT & PERIOD COVERED Final Report 1 Nov 80 - 31 Oct 83
		6. PERFORMING ORG. REPORT NUMBER
7. AUTHOR(s) Tom G. Slanger		8. CONTRACT OR GRANT NUMBER(s) DAAG29-81-K-0001
9. PERFORMING ORGANIZATION NAME AND ADDRESS SRI International		10. PROGRAM ELEMENT, PROJECT, TASK AREA & WORK UNIT NUMBERS N/A
11. CONTROLLING OFFICE NAME AND ADDRESS U. S. Army Research Office Post Office Box 12211 Research Triangle Park, NC 27709		12. REPORT DATE
		13. NUMBER OF PAGES
14. MONITORING AGENCY NAME & ADDRESS (if different from Controlling Office)		15. SECURITY CLASS. (of this report) Unclassified
		15a. DECLASSIFICATION/DOWNGRADING SCHEDULE
16. DISTRIBUTION STATEMENT (of this Report) Approved for public release; distribution unlimited.		
17. DISTRIBUTION STATEMENT (of the abstract entered in Block 20, if different from Report)		
18. SUPPLEMENTARY NOTES The view, opinions, and/or findings contained in this report are those of the author(s) and should not be construed as an official Department of the Army position, policy, or decision, unless so designated by other documentation		
19. KEY WORDS (Continue on reverse side if necessary and identify by block number) Photochemistry Nitrogen Compounds Reaction Kinetics Combustion		
20. ABSTRACT (Continue on reverse side if necessary and identify by block number) The major tasks under the current contract have in general involved the photochemistry and kinetics of nitrogenous molecules, using F ₂ and KrF excimer lasers as initiating sources.		

DTIC
ELECTE
MAR 30 1984

DTIC FILE COPY

84 03 20 027

SRI International



ARO 17561.3-CH

March 2, 1984

Final Report

THE CHEMISTRY OF NITROGEN COMPOUNDS
IN COMBUSTION PROCESSES

By: Tom G. Slanger

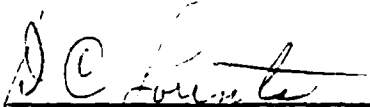
Prepared for:

U.S. ARMY RESEARCH OFFICE
P. O. Box 12221
Research Triangle Park, N. C. 27709

Attn: Dr. George Wyman

Contract No. DAAG29-81-K-0001
SRI Project No. 2373
MP 84-034

Approved:


D. C. Lorents, Director
Chemical Physics Laboratory

G. R. Abrahamson
Vice President
Physical Sciences Division



A-1

333 Ravenswood Ave. • Menlo Park, CA 94025
415 326-6200 • TWX 910-373-2046 • Telex 334-486

CONTENTS

SUMMARY.....	11
INTRODUCTION.....	1
RESULTS AND DISCUSSION.....	2
The Photodissociation of NO_2 in the 2480-2900 Å Region.....	2
Photoexcitation of NO at 1576 Å.....	3
C_2N_2 Photodissociation.....	12
C_2N_2 Quenching and Radiative Lifetimes of $\text{CN}(\text{A}^2\Pi)$	29
$\text{CN}(\text{A}^2\Pi, v=1)$ Quenching	33
The Heat of Formation of NCO.....	37
The $\text{C}_2\text{N}_2\text{-O}_2$ System.....	38
The Herzberg I System of O_2	60
CONCLUSIONS.....	64
PUBLICATIONS.....	67
REFERENCES.....	68

SUMMARY

The major tasks under the current contract have in general involved the photochemistry and kinetics of nitrogenous molecules, using F_2 and KrF excimer lasers as initiating sources. The results of this three-year program are summarized below.

- NO_2 has been dissociated at 2485 Å, revealing in its nascent NO vibrational distribution a very strong inversion, in which vibrational levels near the thermodynamic limit of $v = 8$ are strongly populated. These observations suggest a new technique for atmospheric and combustion monitoring of NO_2 and may be applicable to other polyatomic systems.
- Resonance excitation of NO by the 1576-Å F_2^+ laser line has been observed and the spectroscopy clarified. By this method, collisional cascading in NO, originating at the $B'^2\Delta$ state, can be studied, and the $B'^2\Delta-B'^2\Pi/B'^2\Delta-X'^2\Pi$ branching ratio has been determined. This observation provides a method for monitoring the intensity of the principal F_2 laser line in a totally unambiguous manner.
has been studied *A subscript 3 Sigma u(+)*
- We attempted to study the $O_2(A^3\Sigma_u^+)$ state by laser-induced fluorescence (LIF). However, we found that even under the best conditions, in which 0.6 cm^{-1} wide, 6 mJ pulses of 2489 Å radiation were tuned to the O_2 absorption lines, it was not possible to detect an emission signal. This observation sets a minimum value on the rate coefficient for quenching $O_2(A^3\Sigma_u^+)$ in the $v = 8$ level by O_2 .
A subscript 3 Sigma u(+)
- Radiative lifetimes of the $CN(A^2\Pi)$ state have been measured for $v = 0-5$. The data give, for the first time, good agreement with theoretical predictions. *Contin*

- 111
- A 3000 script 2 pi
- Quenching rate coefficients of $\text{CN}(A^2\Pi)$ by C_2N_2 have been determined for $v = 0-5$, these coefficients increase rapidly with vibrational level, except for an anomaly at $v = 4$. For the $v = 1$ level, CO_2 , N_2 , H_2 , O_2 and NO have been investigated as quenchers.
 - An evaluation of the heat of formation of NCO indicates that the most recent determination is inconsistent with kinetic requirements and must be re-interpreted.
 - Photodissociation of C_2N_2 at 1576 \AA populates $\text{CN}(A^2\Pi)$ up to the one-photon limit of $v = 5$, with a strong maximum occurring at $v=2$. However, there is secondary production of $\text{CN}(A)$, and it appears that levels up to $v = 9$ are generated by energy pooling of vibrationally excited ground state CN molecules. Each vibrational level of the $\text{CN}(A)$ state has a unique dependence on laser power. Relatively intense and immediate emission from the $\text{CN}(B^2\Sigma^+)$ state is also observed, which is not possible with a one-photon process. We concur with the work of Jackson and Halpern¹⁰ who have concluded from their work at 1930 \AA that C_2N_2 can be doubly excited at moderate laser fluxes to give the $\text{CN}(B)$ state.
 - Simultaneous photodissociation of C_2N_2 and O_2 at 1576 \AA results in greatly enhanced $\text{CN}(A)$ and $\text{CN}(B)$ emission intensities over those obtained in the absence of O_2 , due to slow secondary processes. Emissions were also seen from $\text{CO}(A^1\Pi)$, $\text{NO}(A^2\Sigma^+)$, $\text{NCO}(A)$, $\text{NCN}(A)$ and $\text{CCN}(A)$, over times exceeding 1 ms after the laser pulse. It is believed that highly exothermic chemical reactions, possibly involving $\text{N}(^2\text{D})$ and NCO , are responsible for the CO and NO excitation, whereas the most likely energy carrier that populates the triatomic excited states is vibrationally excited CO . The chemistry of the triatomic molecules is believed to play a large part in the overall energy flow of this system.

INTRODUCTION

Nitrogen compounds as a class are of considerable importance in combustion processes because many of them have high heats of formation, which often make their reactions quite exothermic. The purpose of this three-year study has been to explore photodissociative methods for generating some of the more interesting chemical species, then to obtain information on reaction kinetics and pathways, energy flows, and radiative lifetimes of excited molecules, and finally to determine which of the active species were likely to be the principal energy carriers under combustion conditions.

In this study, we concentrated on two starting materials, cyanogen (C_2N_2) and nitrogen dioxide (NO_2), and have been able to investigate other intermediates, including CN, C₂N, NCN, NCO, CO, and NO, in a variety of electronically and vibrationally excited levels.

Most of the work performed has involved excimer laser photodissociation of the parent molecules, using a 1576-Å F_2 laser for C_2N_2 and a 2485-Å KrF laser for NO_2 . This has enabled us to obtain temporal information on the very rapid processes taking place in these systems, and it is evident that both physical and chemical interactions are important. For example, the triatomic molecules NCO, NCC, and NCN are chemically produced in an $C_2N_2-O_2$ system, whereas the distributions of the various CN electronic and vibrational levels that we see are a consequence of physical quenching processes.

Although the lasers we used have not had especially high intensity (typically 10-20 mJ) and have not in general involved focusing, we nevertheless find that multiphoton effects are very marked. In the case of NO_2 our results form the basis of a possible diagnostic scheme for NO_2 in the atmosphere or in flames, whereas with C_2N_2 we were able to demonstrate the number of photons required to excite the various excited states that we observe.

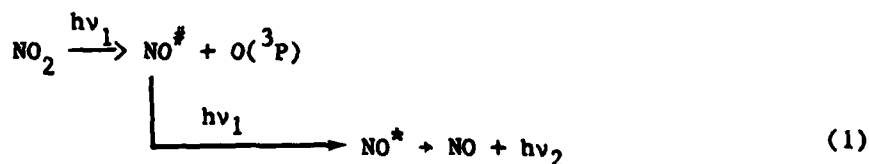
We have attempted to use laser-induced fluorescence (LIF) techniques to generate the important $A^3\Sigma_u^+$ state of O_2 . Although not successful, we have established a firm lower limit for the rate at which O_2 quenches this state.

RESULTS AND DISCUSSION

Photodissociation of NO₂ in the 2480-2900 Å Region

Appendix A is a recently published article on this study. To summarize, we have obtained a nascent NO vibrational distribution for the process $\text{NO}_2 \rightarrow \text{NO}^\# + \text{O}(^3\text{P})$. It is very nonstatistical, with most of the NO molecules possessing vibrational energy near the thermodynamic limit. For instance, at 2485 Å, NO can be produced with up to eight quanta of vibrational energy, and we find that most of the molecules are in $v = 6-8$, with a peak at $v = 7$. This also seems to be the case at lower input energies; where $v = 5$ is the upper limit, there is in fact a large population in $v = 5$. These observations are consistent with earlier studies performed at wavelengths above 3000 Å.^{1,2}

These studies have also demonstrated a potentially useful and general phenomenon. Although such experiments are normally performed by a "pump and probe" technique - one light source photodissociates NO₂ while a second uses LIF to sample the resulting NO - we have shown that NO can be detected, and NO₂ thereby inferred, with a single laser. Because NO₂ exhibits continuous absorption in the 2000-4000 Å region, tuning to an NO₂ feature is unnecessary, and if the laser wavelength is selected to coincide with an NO absorption line, then the same wavelength will photodissociate NO₂ and give an LIF signal from NO. The process is



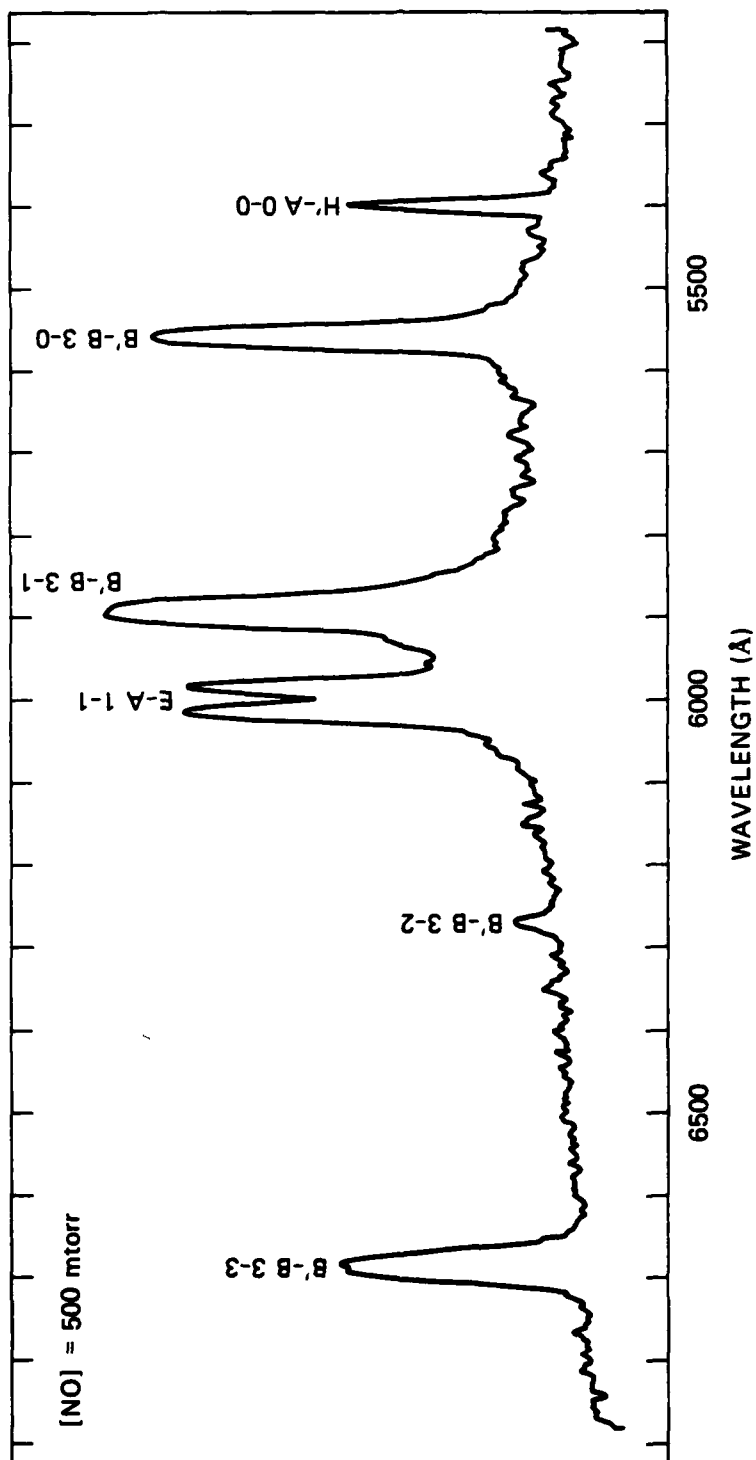
where $h\nu_1$ is a wavelength coincident with a transition from vibrationally excited ground state NO to some level in the NO A or B electronic states. For example, $h\nu_1$ can correspond to lines in the 2-7 NO(A-X) band at 2760 Å, whereas $h\nu_2$ can (for convenience) be a line in the 2-6 band at 2635 Å.

Because such high vibrational levels of NO are formed, their detection is characteristic of the presence of NO₂; that is, such vibrationally hot NO is unlikely to be formed in any other manner. Thus, the process is the basis of an NO₂ detection scheme, which could be useful in both atmospheric monitoring and probing of flames. UV detection of NO₂ by this method has considerable advantages in several respects over the conventional direct LIF detection of NO₂ in the visible spectral region in terms of efficiency and improved signal-to-noise ratio and should be given serious consideration as an alternative technique. Furthermore, two-photon consecutive processes of this type can in principle, be used for other molecules, the requirement being that the parent molecule exhibit continuous absorption, while the daughter molecule should have strong line absorption (and emission). Conceivable candidates include NH₂ and HNO₂.

Photoexcitation of NO at 1576 Å

Before investigating NO₂ photodissociation at the F₂ laser lines (1575.233, 1576.299 Å), we realized that it was important to see what would happen to the NO produced in this system. There are two questions here. The NO produced by one laser pulse would still be present at the next laser pulse (10 Hz was a typical laser frequency), with a totally relaxed energy distribution (ground electronic state, $v = 0$, 300 K rotational temperature). Thus, LIF processes could be simulated simply by photoexciting NO. On the other hand, the analogy of the process described in the previous section, where NO produced in high vibrational levels is further excited within the 10-ns laser pulse to electronically excited states of NO, could possibly be observed. Thus, two NO excitation processes could be operating when NO₂ is photo-dissociated.

Figure 1 shows an NO fluorescence spectrum of the visible spectral region. The resolution is poor because this is a saturated photographic spectrum, designed to maximize weak features. The principal sequence is the NO(B'²Δ-B²Π) 3-v" progression, whereas the feature at 6000 Å is the NO(E²Σ⁺-A²Σ⁺) 1-1 band. At 5401 Å is the NO(H²Σ⁺-A²Σ⁺) 0-0 band, previously reported by us (along with the E-A system) in 1470-Å NO photoexcitation.³ Weak NO(B²Π-X²Π) bands at shorter wavelengths are a consequence of the B'²Δ → B²Π cascade. This latter point is substantiated by demonstrating that



JA-6274-1

FIGURE 1 NO FLUORESCENCE SPECTRUM, 5000-7000 Å
1576.299 Å EXCITATION

a lowering of the total pressure causes disappearance of the B-X 2-v" bands. Because the B'-B 3-2 band is very weak, if it is the source of B(v = 2), just such a change is expected.

Figures 2(a) and 2(b) show uv spectra, with and without 20 torr helium, of NO fluorescence. In the absence of helium, the only observed emission is the $B'^2\Delta \rightarrow X^2\Pi$ 3-v" progression, and it may be seen that there are six lines in each band, the transitions from a single rotational level in $B'^2\Delta(v = 3)$ to the two ground state components of $X^2\Pi$. On addition of He, rotational thermalization occurs, and the individual lines merge into two bands.

As shown in Figure 2(b), He addition has a large effect on the overall spectrum, and other states and levels appear. The $C^2\Pi$ and $D^2\Sigma^+$ states are particularly prominent, and it is remarkable how effective He is in causing collisional cascading, considering that all the states have strong transitions to the ground state. For example, the time between NO-He collisions is about 5 ns, whereas the NO($B'^2\Delta$) radiative lifetime is about 118 ns. Helium must therefore be effective at moving the NO population between states [not between vibrational levels because there is no evidence for $B'^2\Delta(v = 2)$]. Similar behavior is seen in electronically excited CO.⁴

Actually, it is probable that the $C^2\Pi$ and $D^2\Sigma^+$ states are produced by a combination of collisional and radiative cascades. Although $B'^2\Delta \rightarrow C^2\Pi$ radiation does not occur, it is likely that collision of $B'^2\Delta$ with He will populate the nearby $E^2\Sigma^+$ or $H^2\Sigma^+$ states, which will radiate to $C^2\Pi$ and $D^2\Sigma^+$ in the infrared. This is a more likely way of generating $C^2\Pi$ and $D^2\Sigma^+$ than by removing 1.3 eV with He when all the intermediate states are efficient radiators. The presence of the NO($A^2\Sigma^+ \rightarrow X^2\Pi$) system in Figure 2(b) is probably a consequence of radiative cascading from the $C^2\Pi$ and $D^2\Sigma^+$ states.

The appearance of the $B'^2\Delta-X^2\Pi$ 3-6 band at 1900 Å presents an interesting problem because it looks different from the other B'-X bands. This difference occurs because all the lines of the long wavelength triplet have been suppressed, in particular the two longest wavelength lines. We have yet to identify the relevant rotational levels, but it seems most likely that the reason for this anomaly is that the suppressed lines, which are at 1905, 1906, and 1907 Å, lie within the envelope of the C-X 0-0 band, the short wavelength component of which has a head at 1910 Å and is degraded to shorter wave-

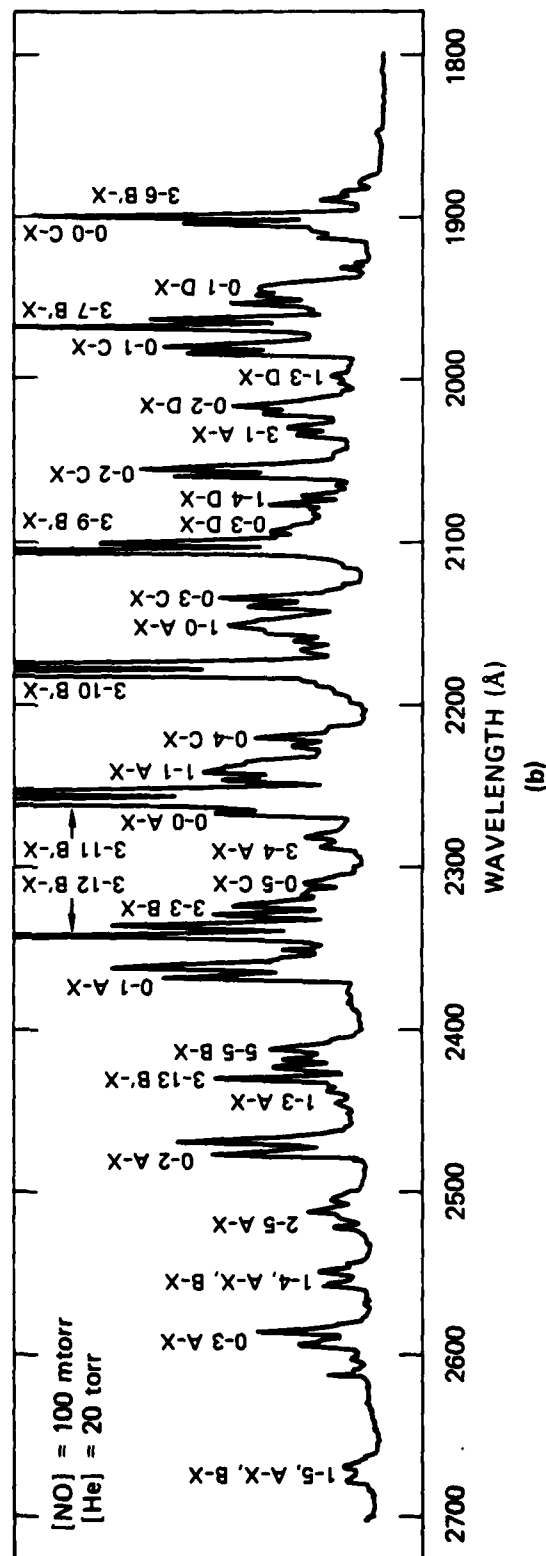
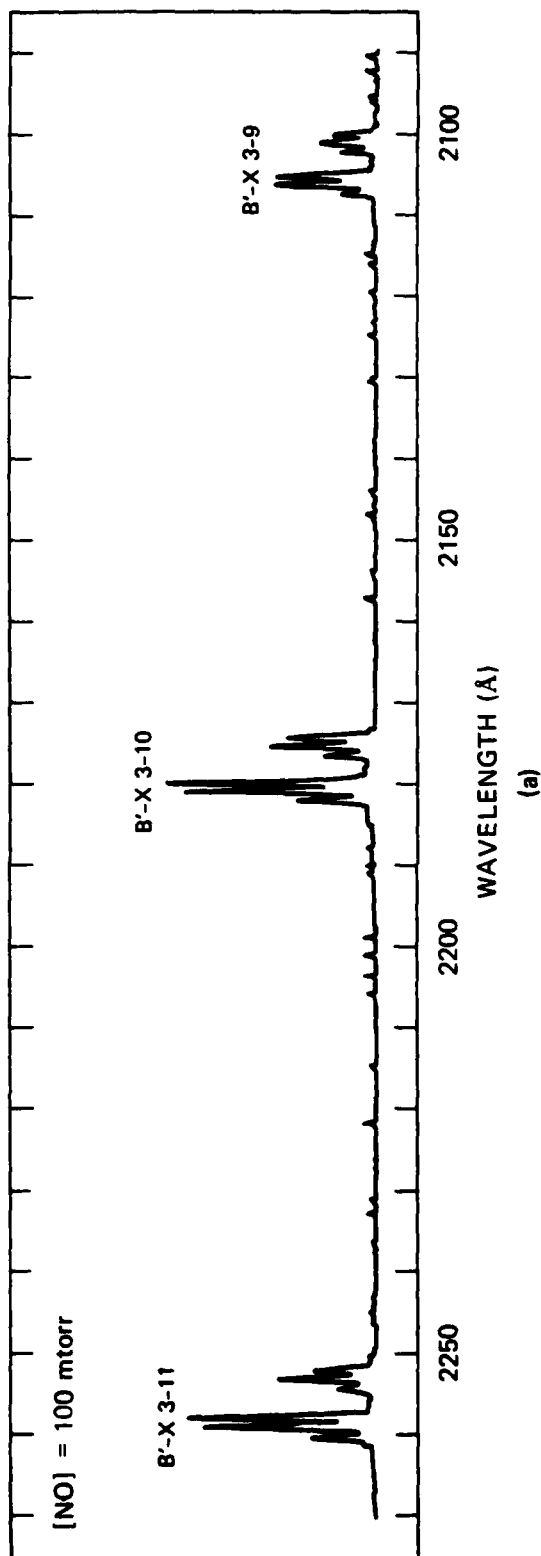


FIGURE 2 NO FLUORESCENCE SPECTRUM, 1900-2700 Å
1576.299 Å EXCITATION, He EFFECT

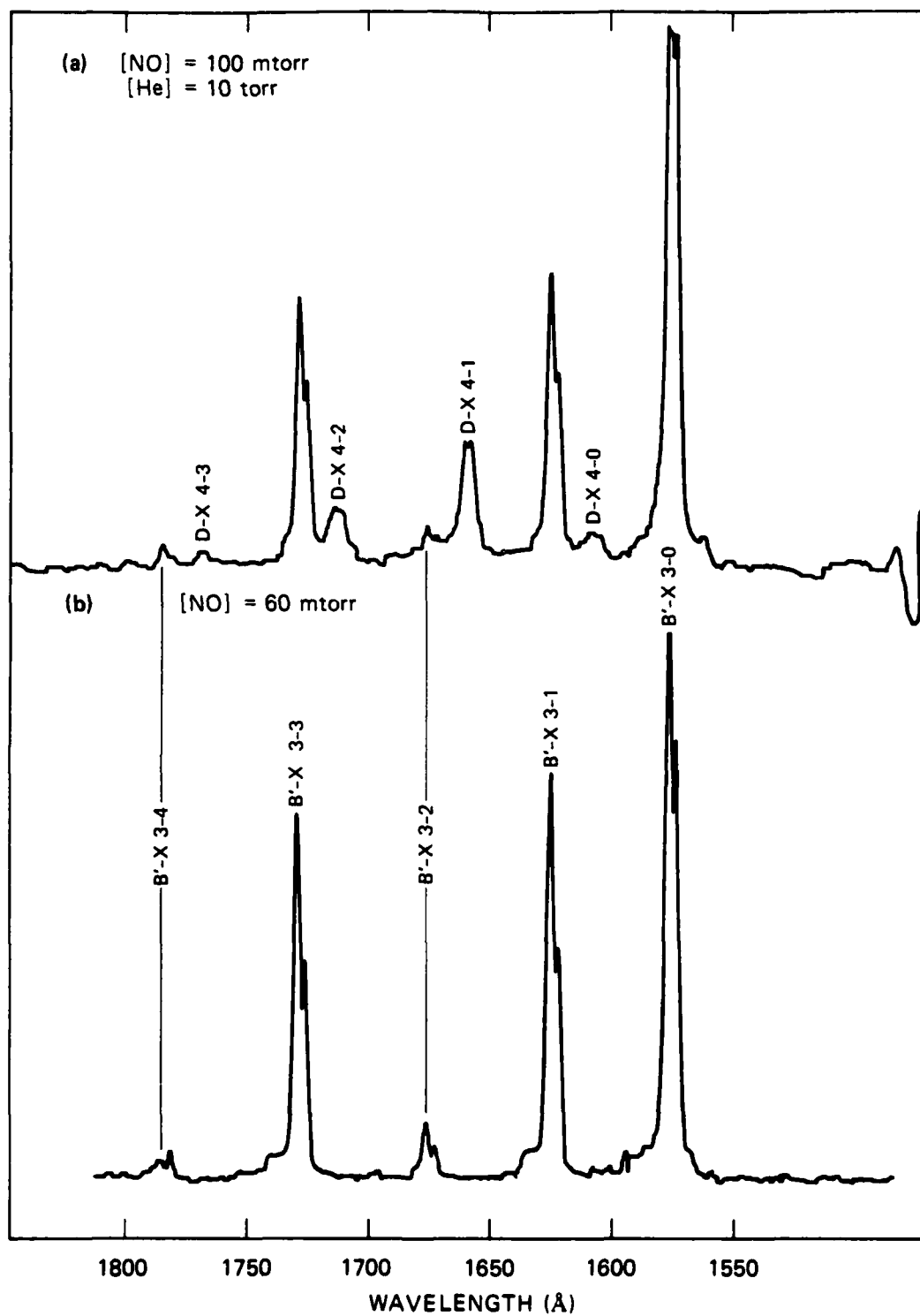
JA-6274-2

lengths. Therefore, it seems that accidental resonances occur between $B'^2\Delta-X^2\Pi$ 3-6 lines and $C^2\Pi-X^2\Pi$ 0-0 lines, that cause scattering of the former.

Figures 3(a) and 3(b) show spectra of the vuv emission, dominated by the $B'-X$ 3-v" bands. However, on He addition, the $D-X$ 4-v" progression is apparent. The $D(4)$ level lies 1380 cm^{-1} below $B'(3)$, so here is an example of rapid cross-relaxation between different states. It is fascinating to note that relaxation of $B'(3)$ to $B'(2)$ only involves removal of 1120 cm^{-1} , yet there is no evidence of $B'(2)$ production; collisional conversion of a Δ state to a Σ state is the preferred pathway. A further point is that neither the $E^2\Sigma^+(1)$ nor the $F^2\Delta(0)$ levels, lying 280 and 1430 cm^{-1} below $B'(3)$, respectively, are produced. The explanation for these effects lies in the Franck-Condon overlaps between $B'(3)$ and $D(4)$, compared with $B'(3)-B'(2)$, $B'(3)-E(1)$, and $B'(3)-F(0)$. Table 1 shows that, in fact, the $B'(3)-D(4)$ pair has the largest overlap, and thus this requirement is much more important than energy resonance, a conclusion previously discussed by Katayama, et al. with reference to such interactions in CN.⁵

On the other hand, from Figure 1 it is clear that there is intense emission from $E^2\Sigma^+$. The probable explanation for this apparent inconsistency is that the $E^2\Sigma^+$ state is strongly predissociated, so that even if a significant portion of the $B'^2\Delta$ population is moved to $E^2\Sigma^+(1)$, its $E \rightarrow X$ emission intensity would be very low. Why then is not the $E \rightarrow A$ intensity very low compared with $B' \rightarrow B$? The answer to that depends on the $E-A/E-X$ branching ratio compared with the $B'-B/B-X$ ratio. Below we show that the $B'-B/B-X$ ratio is 1/150. If the $E-A/E-X$ ratio is much larger than this, then the observation would be explained. In support of such a conclusion is the fact that the $C-A/C-X$ branching ratio is surprisingly large,⁶ approximately 0.65, and the C and E states are both Rydberg in character and may thus behave in a similar manner.

From the data of Figures 1 and 2, there is no evidence of any two-photon process of the type seen with NO_2 ; that is, the vibrationally excited NO produced during $B'-X$ emission is not excited by a subsequent 1576-Å photon to another emitting state. The spectroscopy of NO that is accessed by this accidental resonance with the F_2 laser line is very interesting, and energy migration between the various states and vibrational levels could easily be followed as a function of added quencher. An important point is that this



JA-6274-3

FIGURE 3 NO FLUORESCENCE SPECTRUM, 1550-1800 Å
1576.299 Å EXCITATION, He EFFECT

Table 1

Overlap Integrals for $B'^2\Delta(v=3)$ with Other States

<u>State</u>	<u>Overlap Integral</u>	<u>$\Delta E(\text{cm}^{-1})$</u>
$F^2\Delta(v = 0)$	2.1×10^{-3}	1435
$E^2\Sigma^+(v = 1)$	1.4×10^{-2}	281
$B'^2\Delta(v = 2)$	3.2×10^{-31}	1119
$D^2\Sigma^+(v = 4)$	6.8×10^{-2}	1379

fixed frequency source is a useful probe for NO. Rather than monitoring laser power with a power meter in the vacuum-uv, with its attendant problems, it is much easier to add a few millitorr of NO and monitor the yellow emission in the visible or the considerably more intense uv emission. Once the laser power is calibrated at a given set of pressure conditions, this emission is an absolute standard.

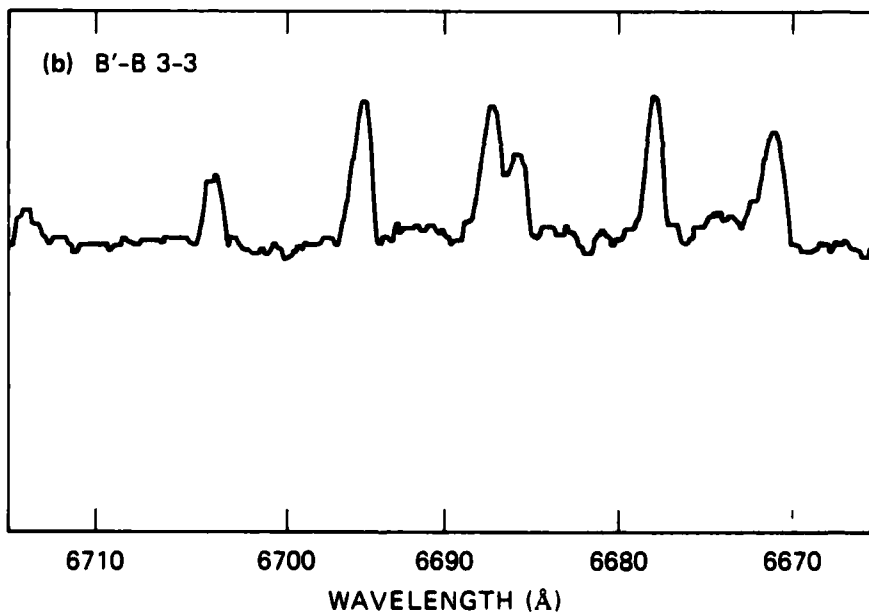
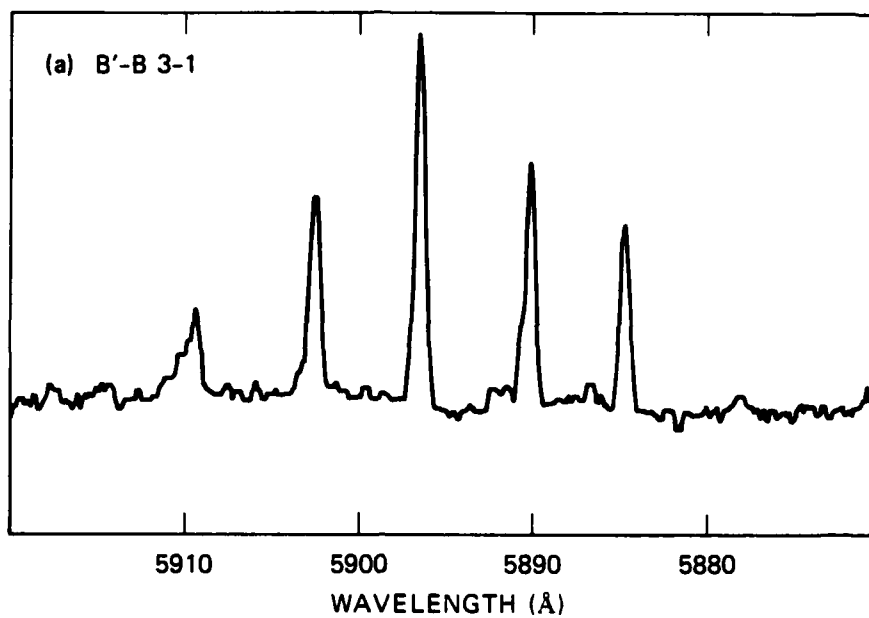
The rotational levels involved in these transitions can be identified on the basis of the resolved B'-B lines that appear in the visible spectral region and the tabulation of the B'-X 2-0 line positions given by Miescher.⁷ Figure 4 shows two of the B'-B bands observed. Five lines are apparent in the 3-1 band at the best obtainable resolution, although two pairs of triplets are expected, as in the uv. In the 3-3 band, the central one of the five lines is split into two, showing that there are in fact six lines, and the five lines in the 3-1 band are only due to coincidence, between an R line of one triplet and a P line of the other.

From this coincidence in the 3-1 band, one may easily set up an equation to identify the rotational levels involved. Because the separation of the pairs of triplets is just the spin-orbit splitting in the B²Π state, which is known as a function of vibrational level, one may write

$$B_v(1/2)(J'' + 2)(J'' + 3) = A + B_v(3/2)J''(J'' + 1) - \delta \quad (2)$$

which expresses the fact that from the initial rotational level in the B'²Δ state, the P line to the B²Π_(1/2) component is coincidental with the R line to the B²Π_(3/2) component. Values for the parameters A, B_{v(1/2)}, and B_{v(3/2)} are found in the literature, and δ is merely the energy difference between the R and P lines in question, zero (for our resolution) for the 3-1 band and -4 cm⁻¹ for the 3-3 band. Solving equation (2) then gives J'' = 6.67 for the 3-3 band and J'' = 6.75 for the 3-1 band. Considering the spectral resolution we have, we conclude that J'' = 6.5 must be the lower rotational level of the B²Π_(3/2) component. As it is an R line, the initial rotational level in B'²Δ(v = 3) must be J' = 7.5.

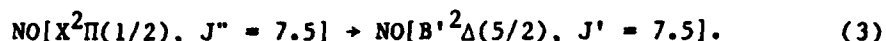
The remaining question is then the identity of the rotational level in the NO ground state responsible for the transition at the laser wavelength, 1576.299 Å.



JA-6274-4

FIGURE 4 RESOLVED NO (B'-B) BANDS
[NO] = 100 mtorr

Because the B'-X 2-0 line positions are tabulated and the rotational constants for B'²Δ(v = 2,3) are known, with the v = 2 → 3 rotationless spacing one may calculate line positions for the B'-X 3-0 band, with the expectation that the best fit to the F₂ laser photon energy will be found for a line with an upper state J' = 7.5, i.e., a P(8.5), Q(7.5), or R(6.5) line. In fact, the result is that Q₁₁(7.5) lies at 63439.49 cm⁻¹, only 0.25 cm⁻¹ from the laser line, which should give enough overlap to provide reasonable absorption. Thus, the absorption process is



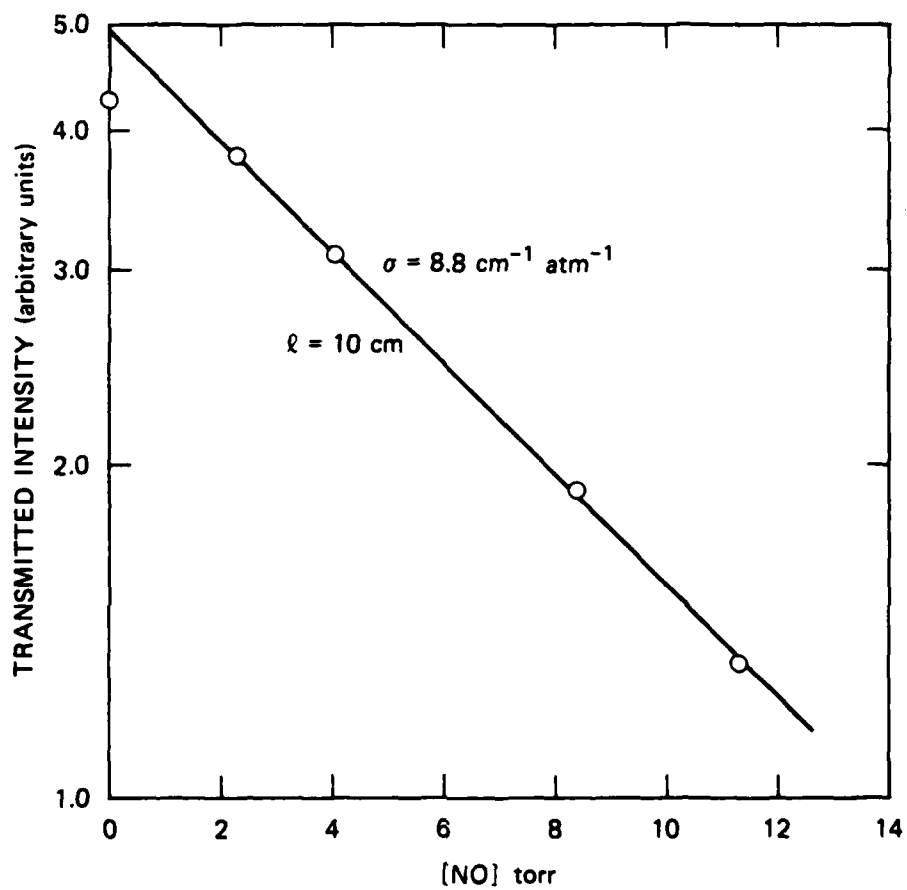
The cross section for absorption of the laser line by NO has been measured, as shown in Figure 5. The value of 8.8 cm⁻¹ atm⁻¹ indicates that the match is not ideal and may well exceed 0.25 cm⁻¹. We are in the process of calculating the mismatch from assumptions about the line shapes and knowledge of the absorption oscillator strengths.

Because we observed a strong emission in both the B'-B and B'-X systems, we measured the branching ratio for these two transitions. With use of a deuterium lamp for the uv spectral region and a tungsten lamp for the visible, we calibrated the monochromator-phototube combination to obtain absolute intensities for the B'-B 3-1 band at 5900 Å and the B'-X 3-12 band at 2335 Å. Using Franck-Condon factors given by Nicholls⁸ and an assumption of constant transition moments for the two band systems, we determined that the branching ratio for emission from B'²Δ(v = 3) to the X²Π and B'²Π states is 150.

C₂N₂ Photodissociation

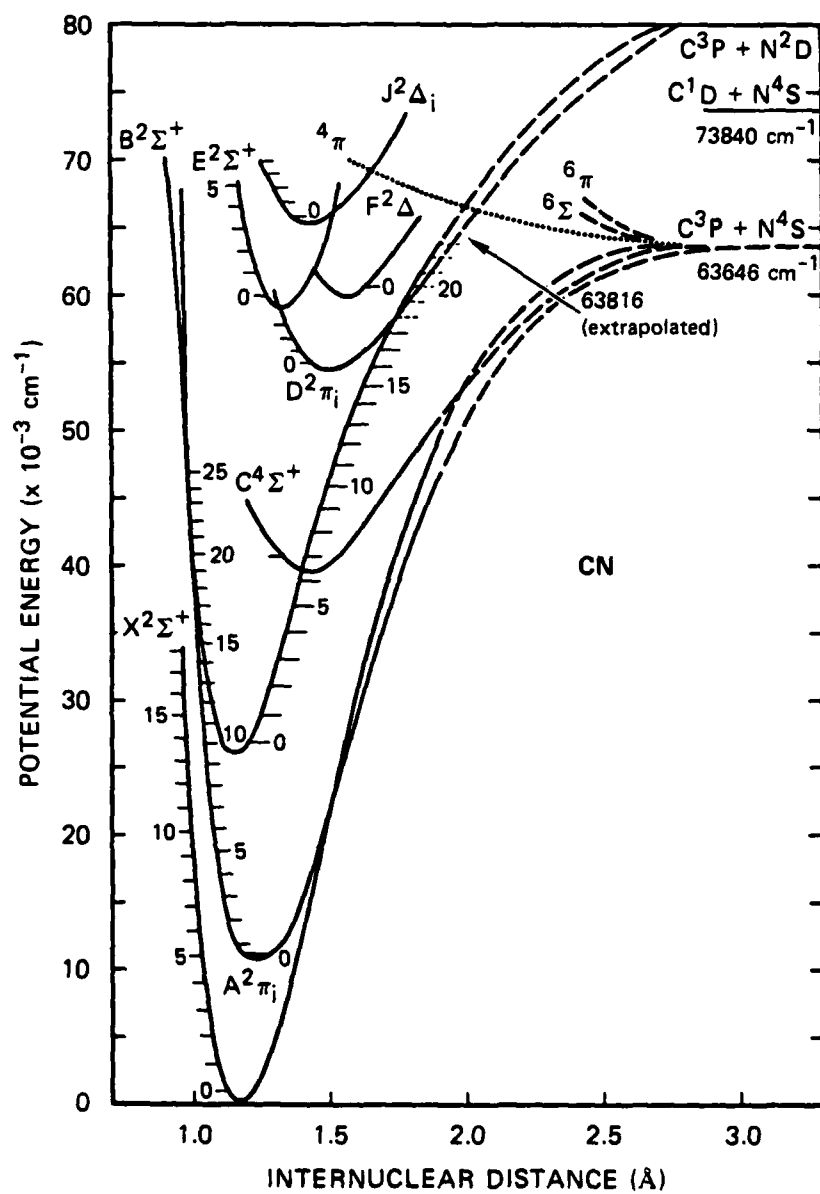
Our most extensive studies to date have involved photodissociation of cyanogen and its interaction with oxygen. These investigations have included spectroscopy, kinetics, energy transfer, multiphoton processes, and chemical generation of various excited states of diatomic and triatomic molecules.

The NC-CN bond strength is 5.58 eV, so with the 1576-Å F₂ laser that we used in all these studies, 2.3 eV excess energy is available to excite the CN fragments in a one-photon process. Figure 6 shows the CN potential curves, and Table 2 gives the maximum vibrational energies attainable, determined by



JA-6274-34

FIGURE 5 NO ABSORPTION CROSS SECTION AT 1576.299 Å



JA-6274-5

FIGURE 6 CN POTENTIAL CURVES

Table 2

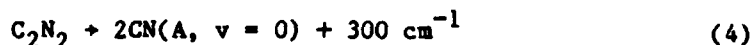
VIBRATION LEVEL LIMITS FOR C_2N_2
PHOTODISSOCIATION AT 1576 Å

<u>Photodissociation</u>	<u>Vibrational Level</u>
$C_2N_2 \rightarrow CN(X) + CN(X)$	$v = 9$
$C_2N_2 \rightarrow CN(A) + CN(X)$	$v = 5 (A)$
	$v = 4 (X)$
$C_2N_2 \rightarrow CN(A) + CN(A)$	$v = 0$

the assumption used for the CN product electronic state. Thus, if the products are CN(A) + CN(X), as determined by Cody et al.⁹ at 1600 Å, then the maximum CN(A) vibrational level is $v = 5$, and the maximum CN(X) level is $v = 4$.

Although the radiation from the 12-mJ F₂ laser is unfocused, we find that levels up to $v = 15$, and possibly $v = 16$ in the A state are produced, as well as intense emission from the B state. Figure 7, a spectrum of the visible radiation from this system, shows that the A levels above $v = 5$ do contribute to the spectrum. Thus, we tentatively conclude that multiphoton excitation is a major process in this system. "Multiphoton" is a loose description of processes that require either (1) a molecule to absorb more than one photon, (2) a molecule that is a photodissociation product to absorb during the laser pulse that produced it, or (3) the interaction of product molecules, each of which requires photoabsorption to generate. In the present case, we find that the emitting states are at much higher energy than can be achieved by single photon absorption, so we must ultimately determine the nature of the multiphoton process.

Before discussing the multiphoton effects, it is important to understand the single-photon process. For example, what CN(A) vibrational distribution is attributable to normal C₂N₂ photodissociation at 1576 Å? We have determined this distribution from CN(A, $v = 0-5$) by measuring emission intensities, using interference filters, for the 0-0, 1-0, 2-0, 3-1, 4-0, and 5-3 CN(A-X) bands. By taking into account filter transmission, phototube sensitivities, Franck-Condon factors, and frequency factors, we were able to establish the populations of these six CN(A) levels, as shown in Figure 8. There is a strong inversion with more than half of the CN(A) formed being in the $v=2$ level. It is likely that the photodissociative channel represented by



is not important. Given this distribution, it is apparent that the CN(A) levels shown in Figure 7, all for $v > 3$, represent only a few percent of the total excitation. The dynamics of the dissociation that produces such a distribution is of great interest for further study. Furthermore, it is

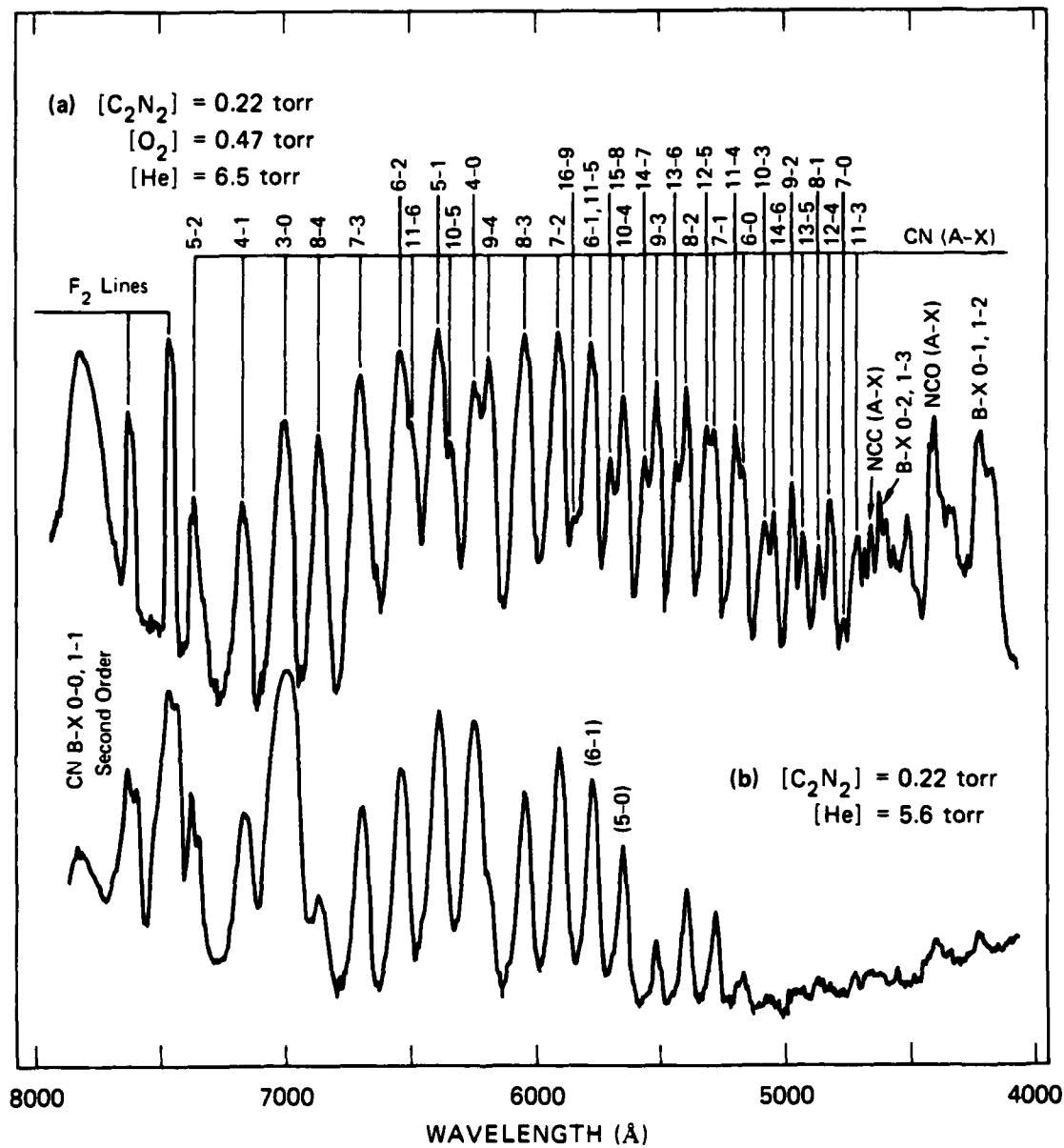
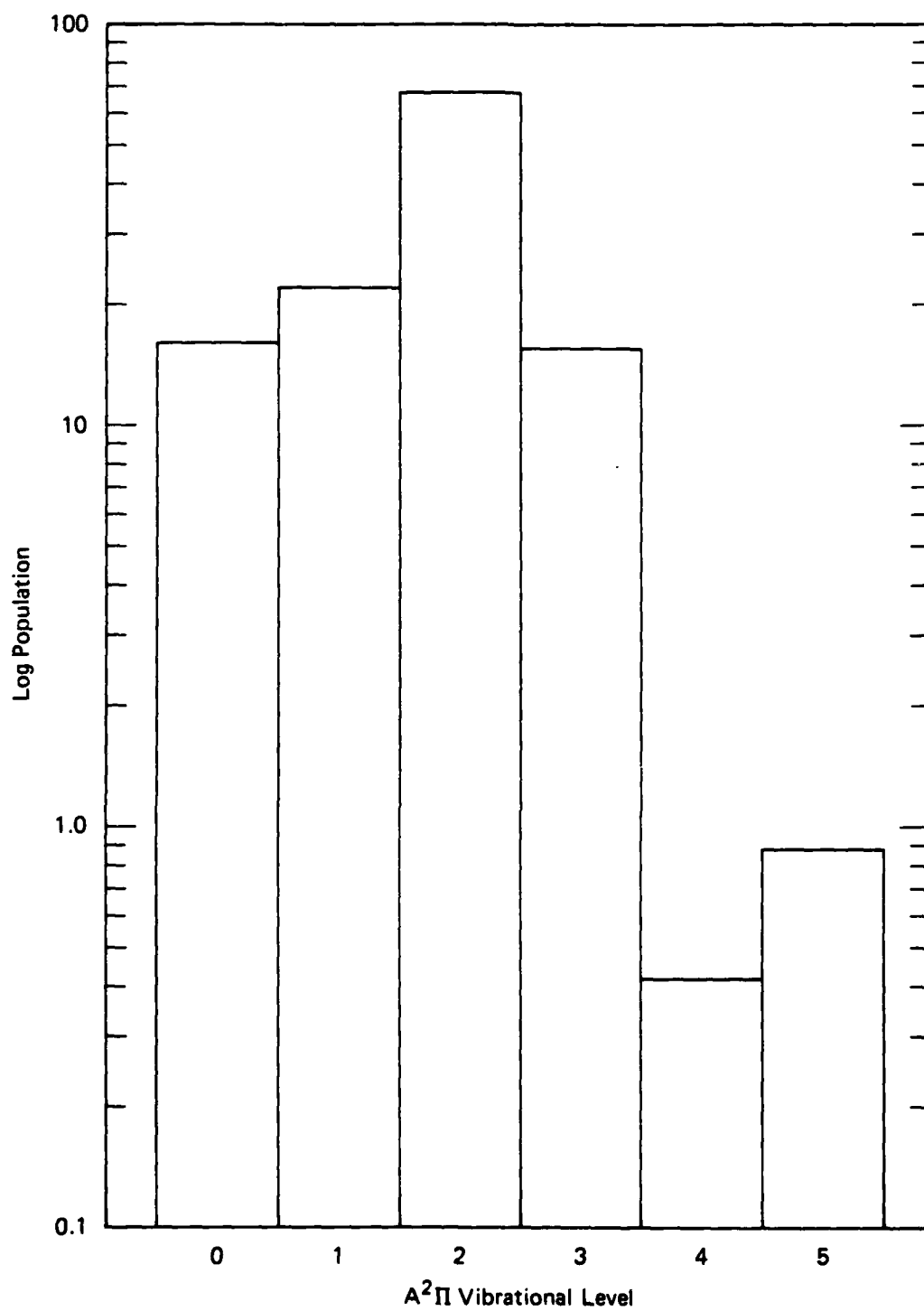


FIGURE 7 CN FLUORESCENCE SPECTRA 4000-8000 Å
 1576 Å EXCITATION



JA-6274-36

FIGURE 8 CN(A²Π) NASCENT VIBRATIONAL DISTRIBUTION
FROM 1576 Å C₂N₂ PHOTODISSOCIATION

important to study the vibrational levels individually, above and below the one-photon limit of $v = 5$.

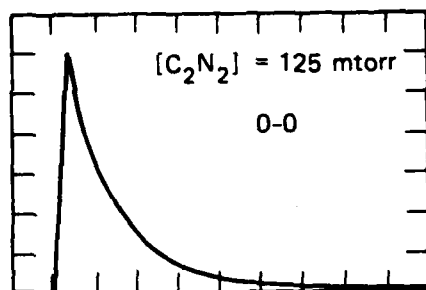
Insight into the mode of population is best obtained by observing the time-resolved emission of various bands. The traces in Figure 9 show the temporal behavior of $v = 0-5$ levels in the A-X system. For $v = 1-4$ the traces are similar, with no build-up time and with a decay in the 5- μ s region, close to the A state radiative lifetime. However, slower components are also evident and the 4-0 band is shown on a different time scale in Figure 10, demonstrating that the slow component represents about half the total integrated emission. This fraction is smaller for lower CN(A) levels.

Figures 11 and 12 show traces for bands from A levels with $v > 5$. The 5-3 band shows a fast component, just as for the lower levels, but now the slow component is dominant. For levels above $v = 5$ there is no fast component, so it is clear that the direct dissociation

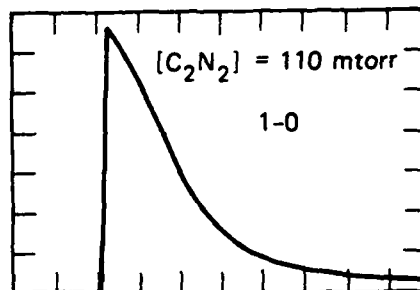


populates CN(A) levels all the way to the thermodynamic limit of $v = 5$, and higher vibrational levels are populated by another mechanism, one involving collisional effects, as demonstrated by the intensity buildups shown in Figure 12. Of course, there is no reason why this mechanism should become inoperative below $v = 5$. Thus, these levels show a slow component that becomes less important as v decreases, although the reason for this decreasing fraction is almost certainly because of the rapidly increasing population in the lower levels; that is, the amount of the slow component in all levels may be constant.

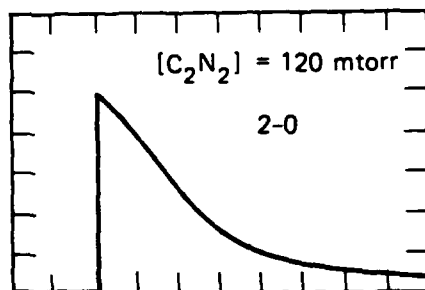
Emission of the CN(B-X) bands near 3885 Å is considerably more intense than that for any individual A-X band. The temporal behavior of this emission, principally the 0-0 and 1-1 bands, is shown in Figure 13a. The intensity maximizes within the laser pulse, and the decay lifetime is close to the 65 ns radiative lifetime of the B state. Thus, the B state is a primary product even though a 1576-Å photon falls 7300 cm^{-1} short of being able to generate CN(B) directly from C_2N_2 . It is thus apparent that a two-photon process in C_2N_2 is responsible for CN(B) state production,



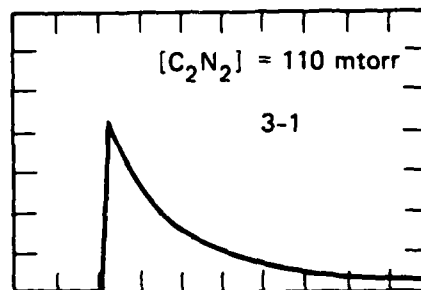
5 $\mu\text{s/div}$
TIME



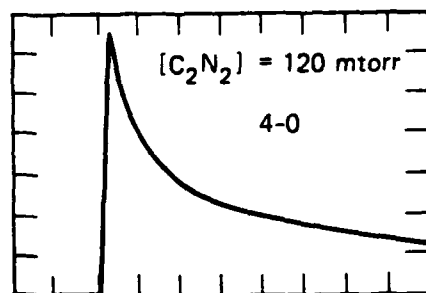
2 $\mu\text{s/div}$
TIME



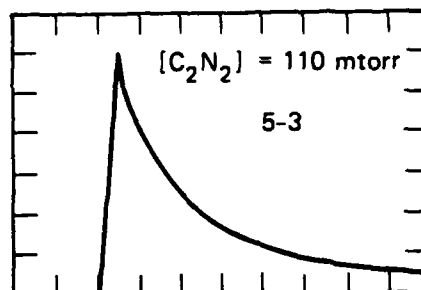
1 $\mu\text{s/div}$
TIME



1 $\mu\text{s/div}$
TIME



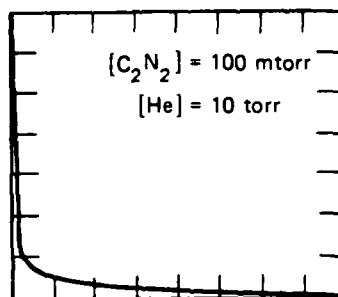
2 $\mu\text{s/div}$
TIME



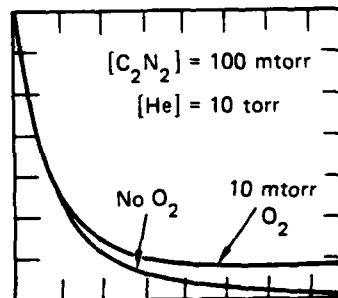
500 ns/div
TIME

JP-8274-8

FIGURE 9 CN (A-X) EMISSION FROM $V' = 0-5$



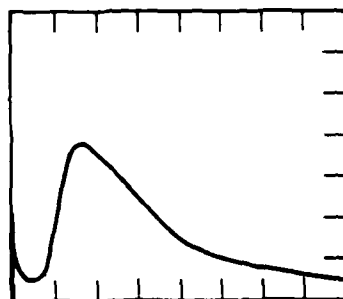
100 μ s/div.
 TIME



10 μ s/div.
 TIME

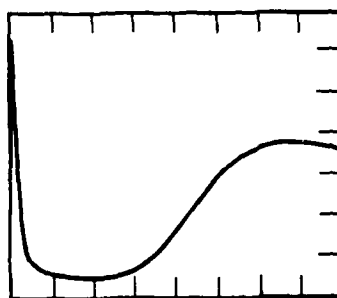
JA-6274-32

FIGURE 10 CN (A-X) 4-0 BAND EMISSION TIME PROFILES
 $[C_2N_2] = 100 \text{ mtorr}$, $[He] = 10 \text{ torr}$



20 μ s/div

TIME

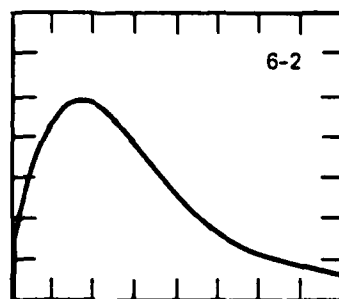


5 μ s/div

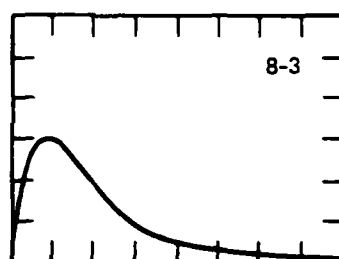
TIME

JP-6274-9

FIGURE 11 CN(A-X) 5-3 BAND EMISSION TIME PROFILES
 $[C_2N_2] = 100$ mtorr, $[He] = 10$ torr



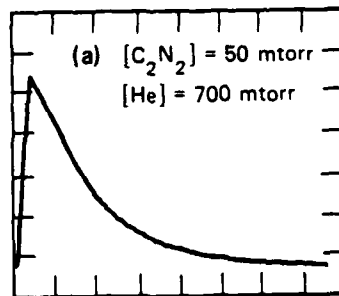
5 μ s/div.
TIME



5 μ s/div.
TIME

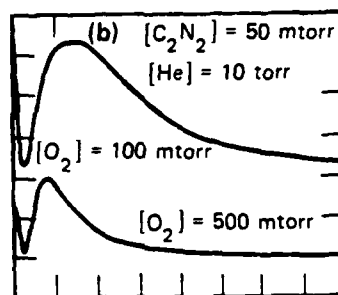
JP-6274-10

FIGURE 12 CN (A-X) 6-2 AND 8-3 BAND EMISSION TIME PROFILES
[C₂N₂] = 100 mtorr, [He] = 10 torr



50 ns/div

TIME

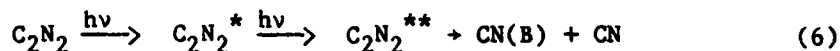


20 $\mu\text{s}/\text{div}$

TIME

JP-6274-16

FIGURE 13 CN (B-X) 3800 Å EMISSION TIME PROFILES

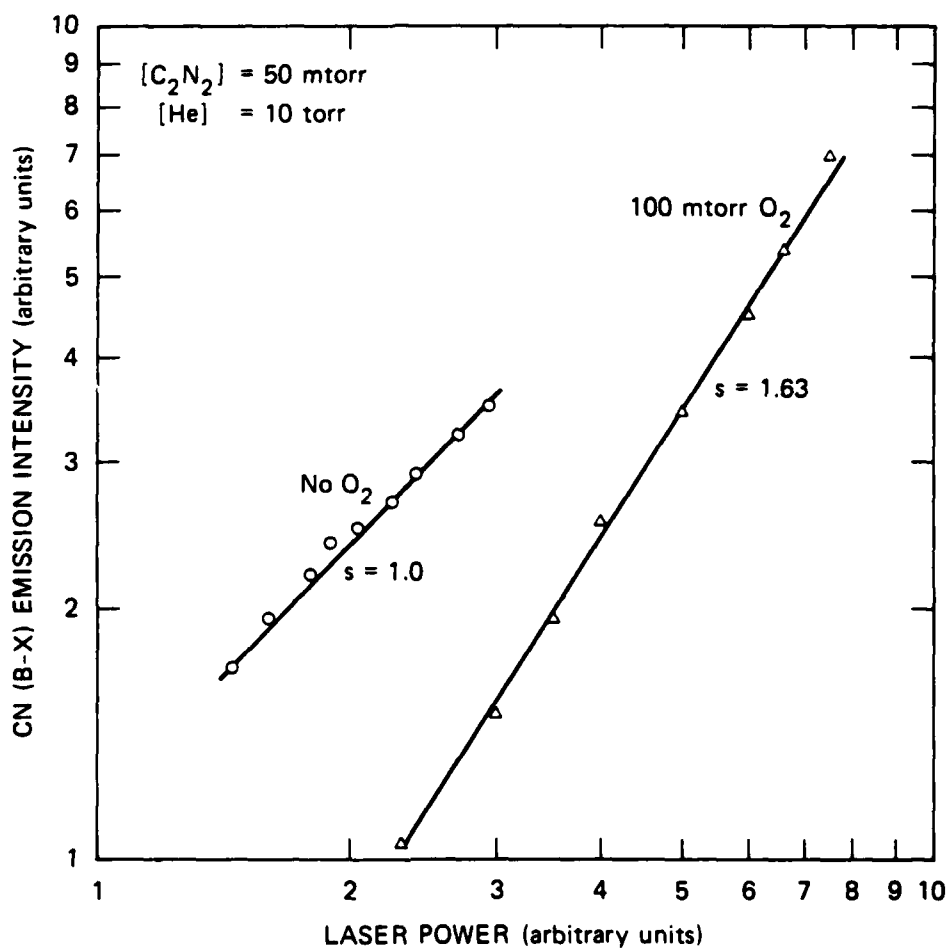


where the second CN can be in the X, A, or B states. Interestingly, two 7.9-eV photons into C_2N_2 leave the molecule 2 eV above the ionization limit, so generation of CN(B) must be a very inefficient process. Jackson and Halpern¹⁰ have reported CN(B) production from 1930 Å photodissociation of C_2N_2 and concluded that this observation could only be explained by true two-photon absorption in C_2N_2 , with an efficiency of 10^{-3} . Our efficiency is also of this order, perhaps slightly less, and probably the ionization loss channel is in part responsible for this low efficiency.

Because the CN(B) production must be due to a multiphoton process, it is of interest to confirm this by measuring the power dependence of the emission intensity. We do this by using NO(B'-B) 3-1 fluorescence, clearly a linear process, as a relative power monitor, and we found, as shown in Figure 14, that the CN(B-X) emission intensity is first-order in laser power. This is an unexpected result, and its explanation is not obvious. The usual rationale for a linear power dependence in a multiphoton process is that the higher transitions are saturated; that is, all molecules reaching the level A^* are then further excited to A^{**} because the $\text{A}^* \rightarrow \text{A}^{**}$ absorption cross section is much higher than that for $\text{A} \rightarrow \text{A}^*$. However, we know here that CN(B) is a minor product compared with CN(A, $v = 0-5$) one-photon generation, so that the first excited state, C_2N_2^* , dissociates rather than being further pumped to $\text{C}_2\text{N}_2^{**}$. Thus, the $\text{C}_2\text{N}_2^* \rightarrow \text{C}_2\text{N}_2^{**}$ process should have a linear power dependence, and the overall power dependence ought to be quadratic. Further research is required to resolve this problem.

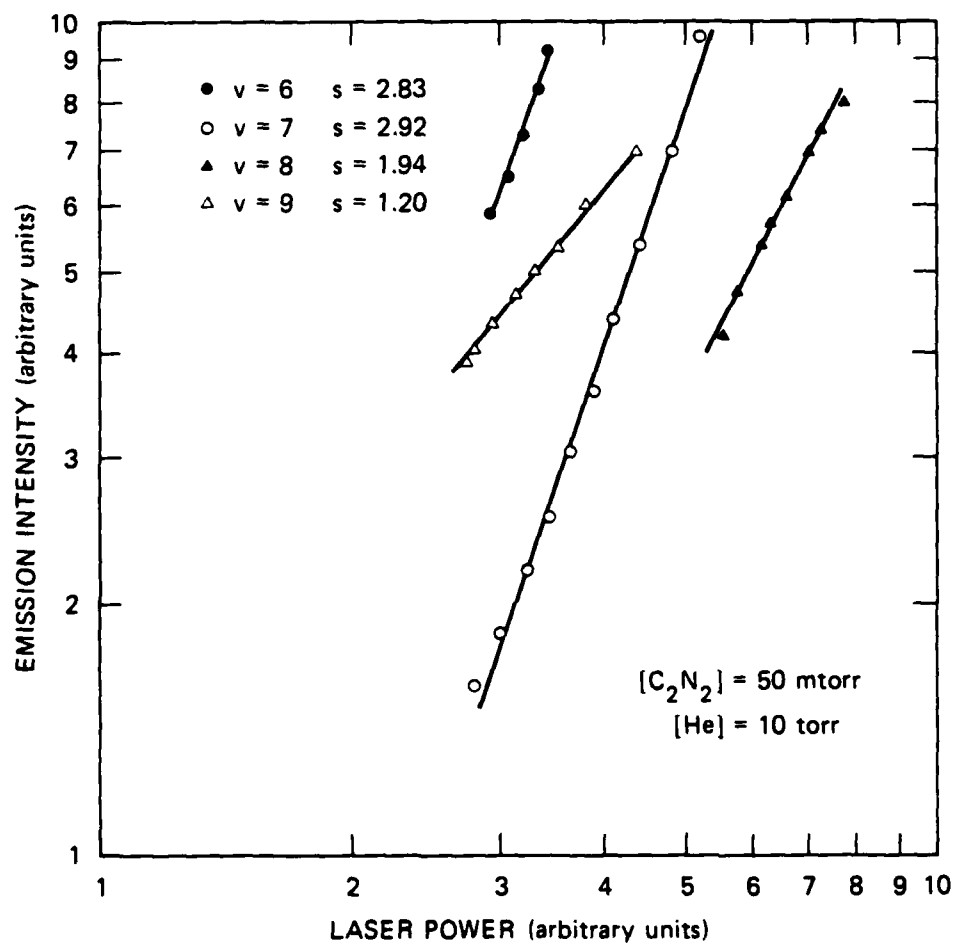
Shifting our attention to the CN(A) power dependence, we find that this is also a complicated matter. Figure 15 shows the power dependence of the CN(A-X) 5-3, 6-2, 7-2, 8-2, and 9-3 bands, and it may be seen that their integrated intensities have differing relationships to the laser power. For $v = 4$ and below, we have not performed such measurements systematically, because we know that the decays for $v = 3$, and 4, are multi-component. From Figure 16, in which the exponent of the expression

$$\text{emission intensity} \propto (\text{laser power})^n \quad (7)$$



JA-6274-11

FIGURE 14 POWER DEPENDENCE OF CN (B-X) 0-0, 1-1 BANDS WITH AND WITHOUT O₂



JA-6274-12

FIGURE 15 POWER DEPENDENCE OF CN ($A^2\Pi$, v)

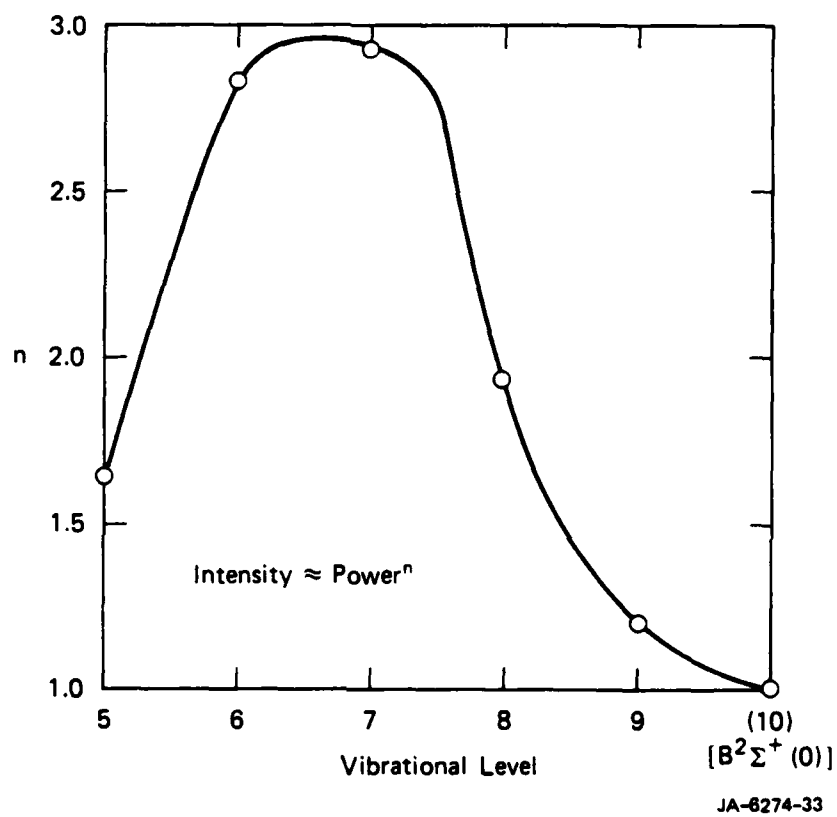


FIGURE 16 POWER DEPENDENCE OF CN(A) EMISSION

is plotted against vibrational level, we must conclude that different CN(A) levels have different mixes of sources. The $v = 7$ level is produced by (at least) three photons, and higher levels incorporate this source together with an additional source that appears, interestingly, to require fewer photons. The B(0) level is isoenergetic with A(10), and the data seem to indicate that for this energy region, the power dependence is first order. That is, for CN* generated at $\sim 26,000 \text{ cm}^{-1}$, both the A and B states are produced from a single source, presumably a sequential two-photon process in C_2N_2 .

For CN(A, $v = 6,7$), which appears to involve a clean three-photon process, we may be able to deduce the source. If, as we hypothesize, the principal photodissociative mode of C_2N_2 is to give one CN(A) and one CN(X) and because the CN(A) vibrational levels are populated in the one-photon case to the thermodynamic limit of $v = 5$, we should expect that the same is true for CN(X). That is, when the CN(A) is produced in $v = 0$, CN(X) can be produced up to $v = 4$. It is reasonable to suppose that the source of levels of CN(A) above $v = 5$ is the vibrational energy of ground state CN. The other alternative, that there is a radiative cascade from some high CN state into CN(A), is not substantiated because no unidentified emission is observed at wavelengths longer than 1600 \AA and the buildup in the time-resolved plots is more compatible with a collisional than a radiative source.

If high levels of CN(A) are produced by energy pooling between CN(X) molecules with $v < 4$, how many CN(X) molecules are needed? To make CN(A, $v = 7$), which has an internal energy of $21,000 \text{ cm}^{-1}$, from CN(X, $v = 4$), with an internal energy of 8000 cm^{-1} , two CN(X, $v = 4$) molecules are insufficient; nine CN(X) vibrational quanta are needed, which can be supplied in various three-molecule combinations (e.g., 4-4-1, 4-3-2, 3-3-3). At present, this is the most reasonable explanation for the cubic dependence shown in Figure 15, and confirmation will require knowledge of the kinetic behavior of the vibrationally excited ground state population.

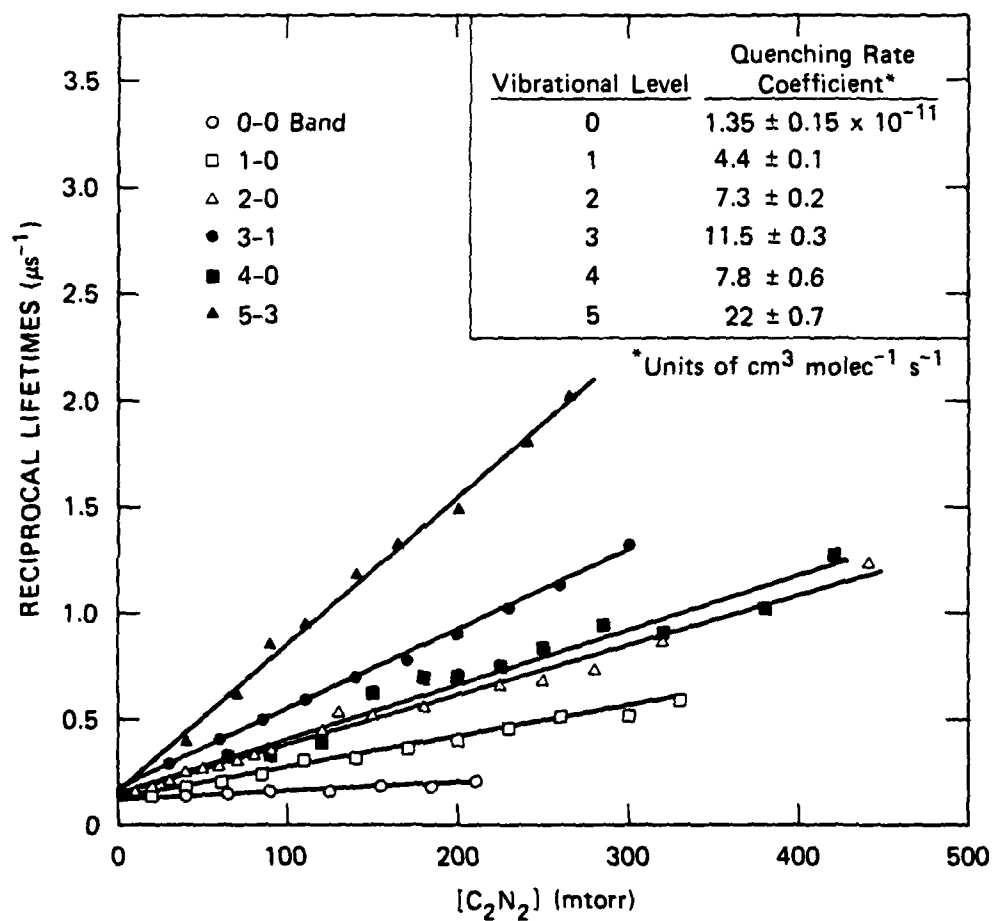
C_2N_2 Quenching and Radiative Lifetimes of CN($A^2\Pi$)

With the ability to generate six levels of the CN(A) state in a primary process, we can easily determine quenching rate coefficients, and by using C_2N_2 as the quenching gas, we are able by extrapolating the data to zero pressure to obtain the radiative lifetimes of the individual levels.

Although many workers have measured the lifetimes, there is a surprising lack of consensus not only of the absolute values, but also of the variation of lifetime with vibrational level. These issues have recently been addressed in two theoretical papers by Cartwright and Hay¹¹ and by Larsson et al.,¹² who have concluded that at the minimum, the relationship between radiative lifetime and vibrational level should be such that for the lowest levels, radiative lifetime should significantly decrease with increasing v . However, this behavior has not been observed experimentally. The data of Jeunehomme¹³ show a relatively constant radiative lifetime for $v = 1-9$, those of Duric et al.¹⁴ show a similarly constant but shorter value for the radiative lifetime, whereas those of Katayama et al.⁵ show values comparable to those of Duric et al. although the lifetimes appear to increase with vibrational level. Each of these studies has experimental problems, as described in the paper by Larsson et al., and it appears that definitive data have been lacking. Our study is the most direct experimental determination to date, involving as it does photodissociation of C_2N_2 to give $CN(A)$ in six vibrational levels as primary products. Figure 17 shows the data for quenching of the individual levels by C_2N_2 , the intercepts giving the radiative lifetimes. Although the $CN(A-X)$ 0-0 band is at 1.1μ , a spectral region difficult to study with a phototube, we were able to obtain data for comparison with the only other lifetime determinations for the $v = 0$ level, those presented by Jackson et al.¹⁵ and Conley et al.¹⁶

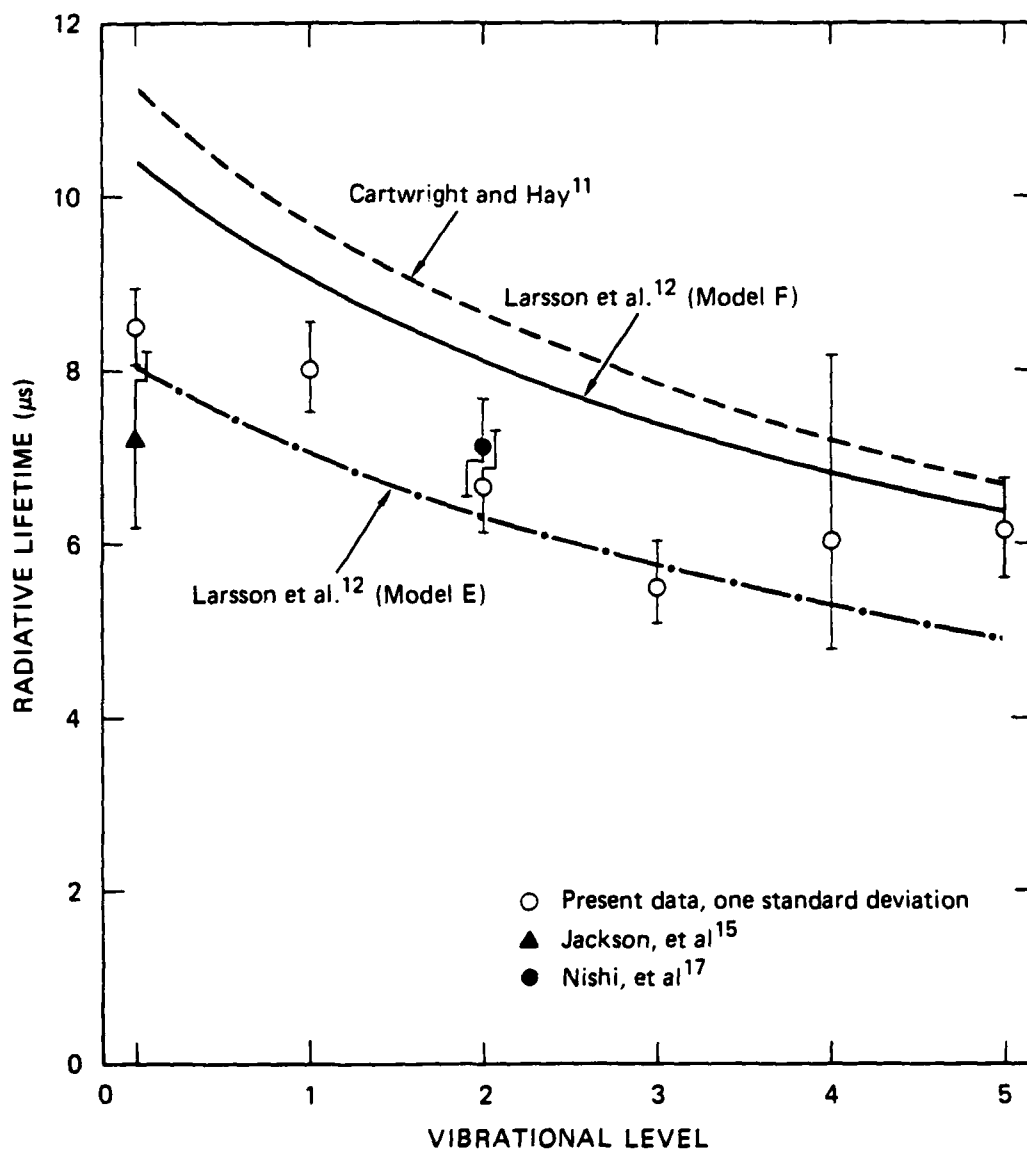
Figure 18 compares the lifetime measurements with those of the two theoretical models given by Larsson et al.¹² and the model presented by Cartwright and Hay.¹¹ Although the quenching data show very good precision, the intercepts are very sensitive where the C_2N_2 quenching rate coefficients are large, as for $v = 5$ in particular. The $v = 4$ data present the greatest problem for computer analysis because there is a slow component under the primary decay, seen in Figures 9 and 10, and the shape of this component is not known (it may start at $t = 0$ with zero intensity). Thus, the $v = 4$ data has the greatest error bars.

It is evident that the lifetimes follow the trend predicted by the three theories, falling from $8.5 \mu s$ to $6.2 \mu s$ as v increases from 0 to 5. Although the $v = 3$ value of $5.50 \mu s$ is somewhat low, there is no indication that the



JA-6274-13

FIGURE 17 CN ($\text{A}^2\Pi$, $v = 0-5$) QUENCHING BY C_2N_2



JA-8274-15

FIGURE 18 RADIATIVE LIFETIMES OF CN ($A^2\Pi$) VIBRATIONAL LEVELS COMPARED TO THEORY AND TWO RECENT EXPERIMENTAL DETERMINATIONS

data are at fault -- for example, the quenching line in Figure 17 is particularly precise and reproducible. It is possible that some specific interaction may occur between the $v = 3$ level and a neighboring ground-state level. The $v = 0$ lifetimes measured by Conley et al.¹⁶ are $8.4 \pm 2.1 \mu\text{s}$ and $6.2 \pm 0.9 \mu\text{s}$, whereas that recently reported by Jackson et al.¹⁵ is $7.2 \pm 1.0 \mu\text{s}$. Nishi et al.¹⁷ have recently reported a value for $v = 2$, shown in Figure 18.

The quenching data, summarized in Table 3, show an interesting trend, in that although the quenching rate coefficient increases with increasing vibrational level, the data for $v = 4$ alone show an unexpected drop. An attempt to correlate the coefficients to vibrational frequencies or overtones of C_2N_2 , was not particularly successful; therefore, it is not evident why $v = 4$ should be unique. However, because the observed rate coefficients are extremely large, particularly for $v = 5$, it is unlikely that the interaction involves V-V transfer. Instead, our expectation is that collisions with C_2N_2 cause intersystem crossing between $\text{CN}(\text{A})$ and $\text{CN}(\text{X})$,^{18,19} and thus very small amounts of energy may be involved in the exchange. Thus, lack of correlation with C_2N_2 vibrational modes is probably not surprising. It is not thermodynamically possible for the interaction between $\text{CN}(\text{A})$ and C_2N_2 to be reactive for the lower vibrational levels of $\text{CN}(\text{A})$. There is no obvious evidence for cascading of energy, which would in any case not affect the zero pressure lifetimes. If $\text{A} \rightarrow \text{X} \rightarrow \text{A}$ processes occur, they might be evident as an increasing lifetime with increasing C_2N_2 , causing the lines in Figure 17 to be nonlinear; however, this is not seen.

$\text{CN}(\text{A}^2\Pi, v=1)$ Quenching

Rate coefficients were determined for quenching by CO_2 , O_2 , NO , H_2 , and N_2 of the $v = 1$ level of $\text{CN}(\text{A}^2\Pi)$. The data are shown in Figure 19, in which the slopes give the rate coefficients. These values are tabulated in Table 4 along with the coefficients determined by Jackson et al.¹⁵ for the $v = 0$ level; the data for C_2N_2 as a quencher are also included.

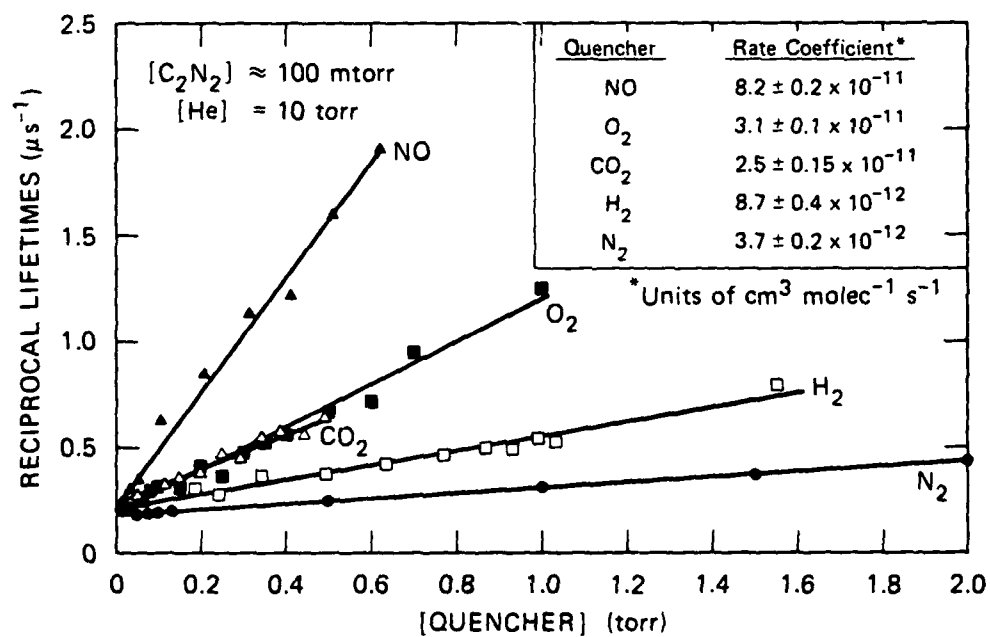
For the only point of direct comparison, the data for C_2N_2 , our value is 50% higher than that of Jackson et al.¹⁵ Consideration of their precision suggests that our value is preferred. For N_2 , there is an order of magnitude increase in rate coefficient in going from $v = 0$ to $v = 1$. Because N_2 is obviously not a reactant, it is likely that the cross-relaxation to the ground

Table 3

RATE COEFFICIENTS FOR QUENCHING
CN(A²Π) IN v = 0-5 BY C₂N₂

<u>Vibrational Level</u>	<u>Quenching Rate Coefficient</u> <u>(cm³ molec⁻¹ s⁻¹ x 10¹¹)</u>
0	*1.35 ± 0.15
1	4.4 ± 0.1
2	7.3 ± 0.2
3	11.5 ± 0.3
4	7.8 ± 0.6
5	22 ± 0.7

*Jackson et al.¹⁵ report a value of 0.9 ± 0.1 x 10⁻¹¹.



JA-6274-14

FIGURE 19 QUENCHING OF CN ($A^2\Pi$, $v = 1$)

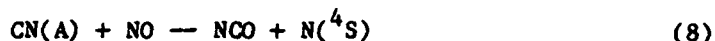
Table 4

RATE COEFFICIENTS FOR QUENCHING $CN(A^2\Pi, v=1)$

<u>Quenching</u>	<u>Quenching Rate Coefficient</u> <u>($\text{cm}^3 \text{ molec}^{-1} \text{ s}^{-1} \times 10^{11}$)</u>
O_2	3.1 ± 0.1
NO	8.2 ± 0.2
CO_2	2.5 ± 0.15
H_2	0.87 ± 0.04
N_2	0.24 ± 0.015
	$*(0.044 \pm 0.005, v = 0)$
C_2N_2	4.4 ± 0.1

*Jackson et al.¹⁵

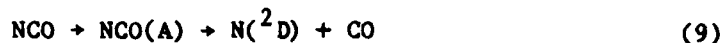
state is facilitated for the higher level. It is important to determine if a relationship exists between the A to X level spacings and the rate coefficients, for which we need to investigate higher A levels. Our C_2N_2 quenching data show a general increase of rate coefficient with v , although no reactive pathway is evident for $v = 0-5$. The large rate coefficients for CO_2 , NO , and O_2 for the $v = 1$ level should also be compared with $v = 0$. In either case, there are exothermic chemical pathways for each quencher, with NCO being produced from both O_2 and CO_2 . For NO , a four-center reaction making N_2 and CO is highly exothermic, whereas the reaction



is thermoneutral for $v = 0$, so there may be a large difference in rate for $v = 0$ and $v = 1$. Further v -dependent studies should be pursued.

The Heat of Formation of NCO

During our investigation of $CN + O_2$ interactions, our observations on NCO led us to consider the thermodynamics of this system. The most recent spectroscopic measurements on NCO have been performed by Sullivan et al.²⁰ and from observations of decreasing lifetimes of rotational levels in the $NCO(A)$ state, they deduced an upper limit in energy for the dissociative process



From this, they calculated the first dissociation limit



and were thus able to obtain a lower limit for the heat of formation of NCO of $\Delta H_f(298\text{ K}) > 48\text{ kcal/mole}$, which compares to the previously accepted value of Okabe²¹ of $\Delta H_f(298\text{ K}) > 39\text{ kcal/mole}$. The problem with this new value is that it is demonstrably too high, because if a value of 48 kcal/mole is used, the important reaction



is 6 kcal/mole endothermic. Schmatjko and Wolfrum²² report a rate coefficient of $3 \times 10^{-11} \text{ cm}^3 \text{ molec}^{-1} \text{ s}^{-1}$ for this reaction, which basically precludes any activation energy, while Wittig et al.²³ have shown that excess energy is available in the reaction, because NCO is formed with some vibrational excitation, with the reactant CN in its lowest vibrational level.

Thus, the lower limit to the NCO heat of formation reported by Sullivan et al.²⁰ must be too high by significantly more than 6 kcal/mole, and it appears that the lower limit of 39 kcal/mole reported by Okabe is close to the true value. If this is the case, the shortened lifetimes observed by Sullivan et al. for the NCO(A) state are not a consequence of approach to the $\text{N}(^2\text{D}) + \text{CO}$ second dissociation limit, and must have another explanation, one possibility being a curve-crossing involving a state going to the $\text{N}(^4\text{S}) + \text{CO}$ first dissociation limit.

The $\text{C}_2\text{N}_2\text{-O}_2$ System

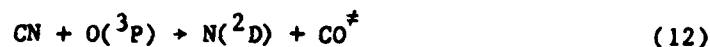
Diatomic Radiators

The interactions taking place in the $\text{C}_2\text{N}_2\text{-O}_2$ system are the most relevant to combustion processes. In the following discussion of our spectroscopic observations, we focus first on the diatomic emitters, then on the triatomic emitters.

A good deal is known about the initial reactions in a photolyzed $\text{C}_2\text{N}_2 + \text{O}_2$ mixture. Schmatjko and Wolfrum²² have investigated the fate of CN and have found that two important reactions are



and



The reactive pathways available to NCO are not known, but $\text{N}(^2\text{D})$ is known to react with O_2 ,



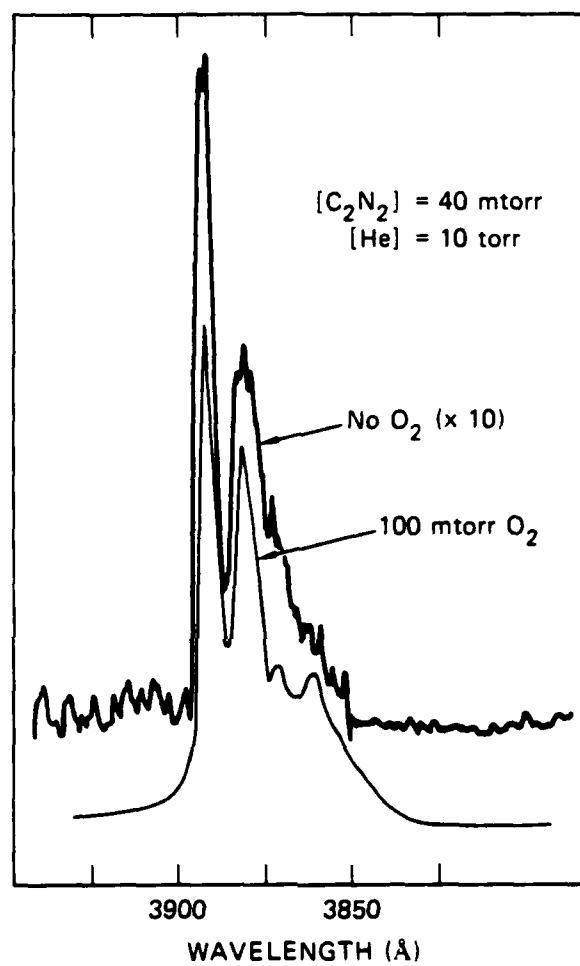
$\text{O}(^1\text{D})$ is also a possible product of this reaction.

Our observations focus on two diatomic emitters, CN(A) and CN(B), and in addition, we have detected emission from $\text{CO}(A^1\Pi)$ and from $\text{NO}(A^2\Sigma^+)$. The CN emissions in the absence of O_2 were discussed earlier; the basic effects observed on O_2 addition are that the emissions become much stronger, that the temporal behavior changes, and that the vibrational distribution in the CN(A) system shifts to higher "temperature".

In Figure 7 the spectra obtained with and without O_2 , show that the distribution of populations is markedly different, even at low levels. For instance, the 4-0 band is weaker than the 3-0 band without O_2 , but stronger with O_2 . The 9-4 band, adjoining 4-0, is hardly discernible in the absence of O_2 , but stronger than 4-0 after O_2 is added.

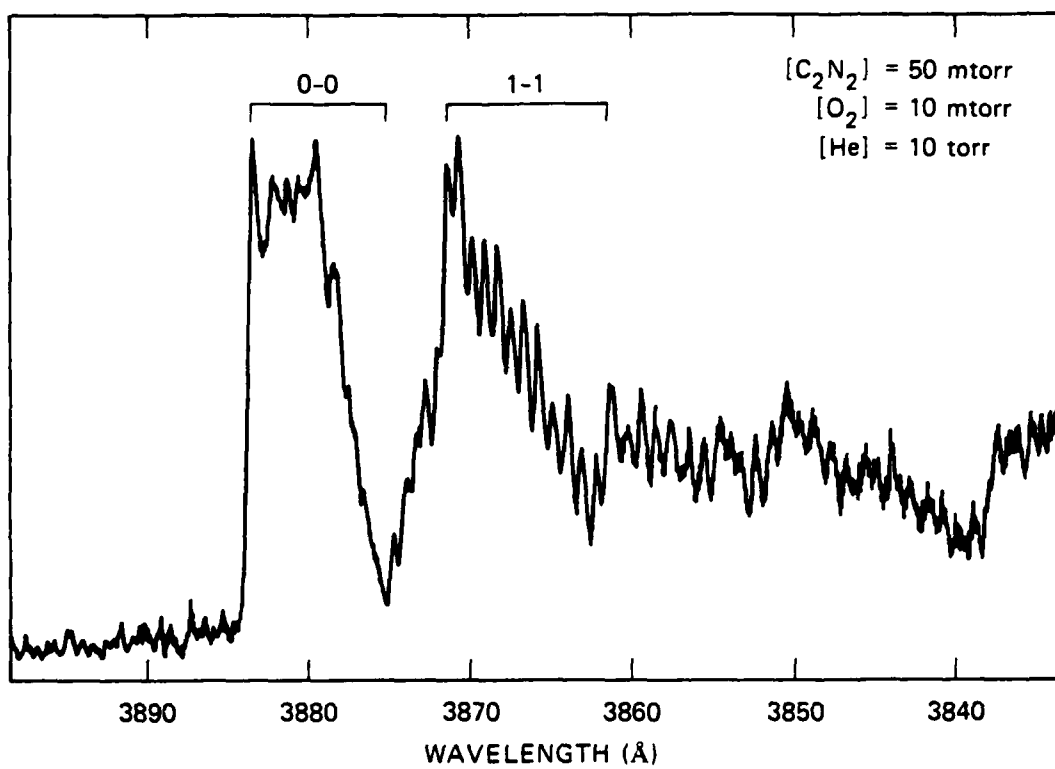
Although the spectra do not go below 4000 Å, the arrangement of the optical system passes radiation in the second order of the grating. Thus, the feature at ~ 7800 Å is in fact the CN(B-X) bands at 3885 Å. Comparison of the spectra in Figure 7 shows enhancement of the B-X system relative to A-X on O_2 addition, that is, that the processes populating the excited CN states in the presence of O_2 preferentially produce the $\text{CN}(B^2\Sigma^+)$ state. Nevertheless, as seen in Figure 20, the $\text{CN}(B^2\Sigma^+)$ vibrational distribution changes very little on O_2 addition, in spite of an order of magnitude intensity increase. Figure 21 shows a relatively high resolution CN(B-X) spectrum, with O_2 addition, demonstrating that there is very little population above $v = 1$.

An idea of the change in time behavior of the emissions on O_2 addition is shown in Figures 13 and 22, which compare the B-X 0-0 band in the absence and presence of O_2 . In the former case, one sees little but a single exponential, with a lifetime corresponding to the known radiative lifetime of $\text{CN}(B^2\Sigma^+)$, 65 ns. Thus, CN(B) is produced within the 10-ns laser pulse although, in fact, such a process requires 9 eV into C_2N_2 , 1.2 eV more than is available. Therefore, it seems that a rapid two-photon process occurs in C_2N_2 , during which an intermediate excited C_2N_2 state is further excited to a super-excited state, which then dissociates to CN(B). Such an effect has been previously proposed by Jackson and Halpern¹⁰ from their observations on 1930 Å C_2N_2 .



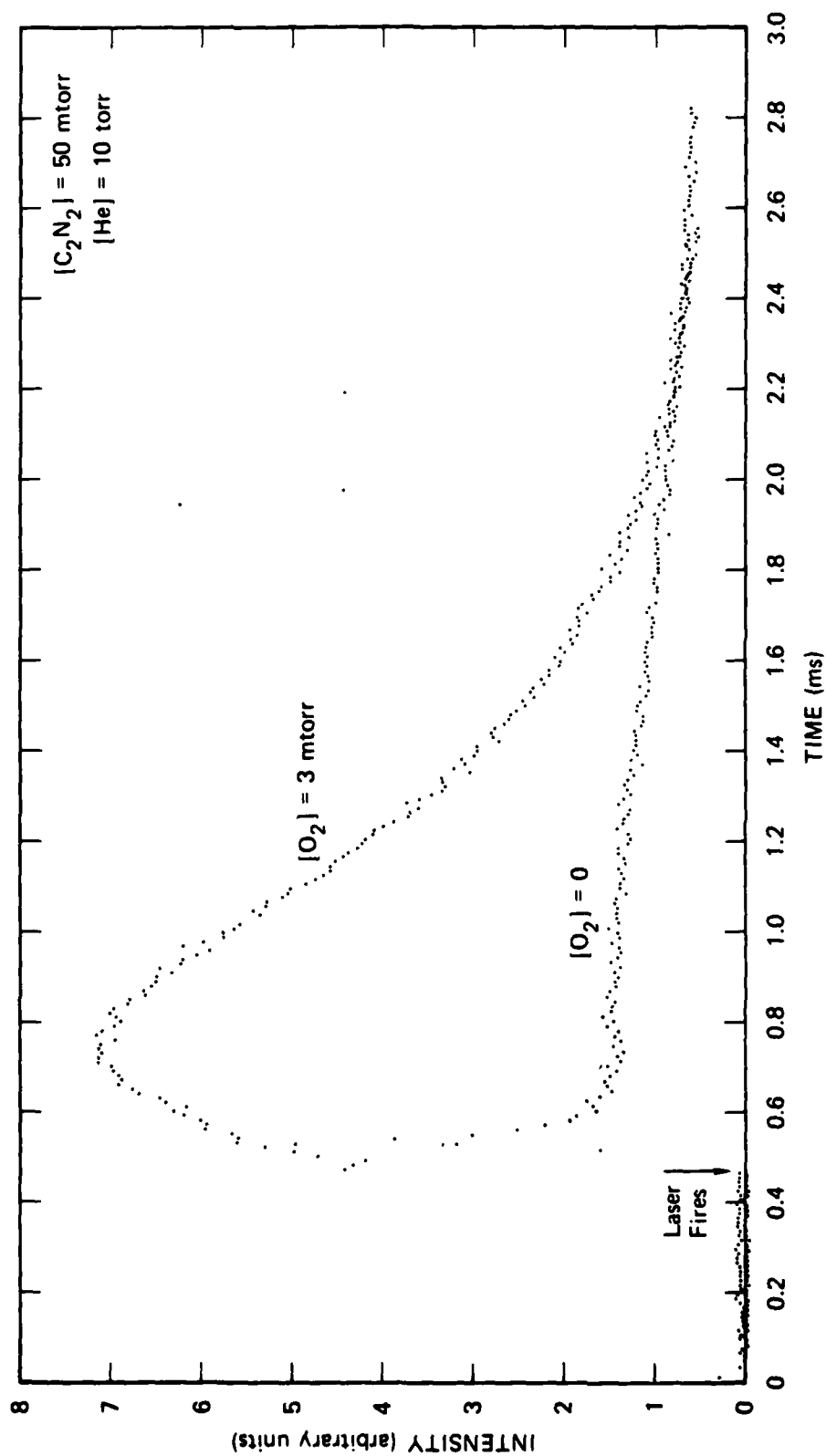
JA-6274-19

FIGURE 20 CN (B-X) 3880 Å BANDS, O₂ EFFECT



JA-6274-18

FIGURE 21 CN (B-X) 3880 Å BANDS



JA-6274-17

FIGURE 22 CN (B-X) 3880 Å BAND EMISSION TIME PROFILE, O_2 EFFECT

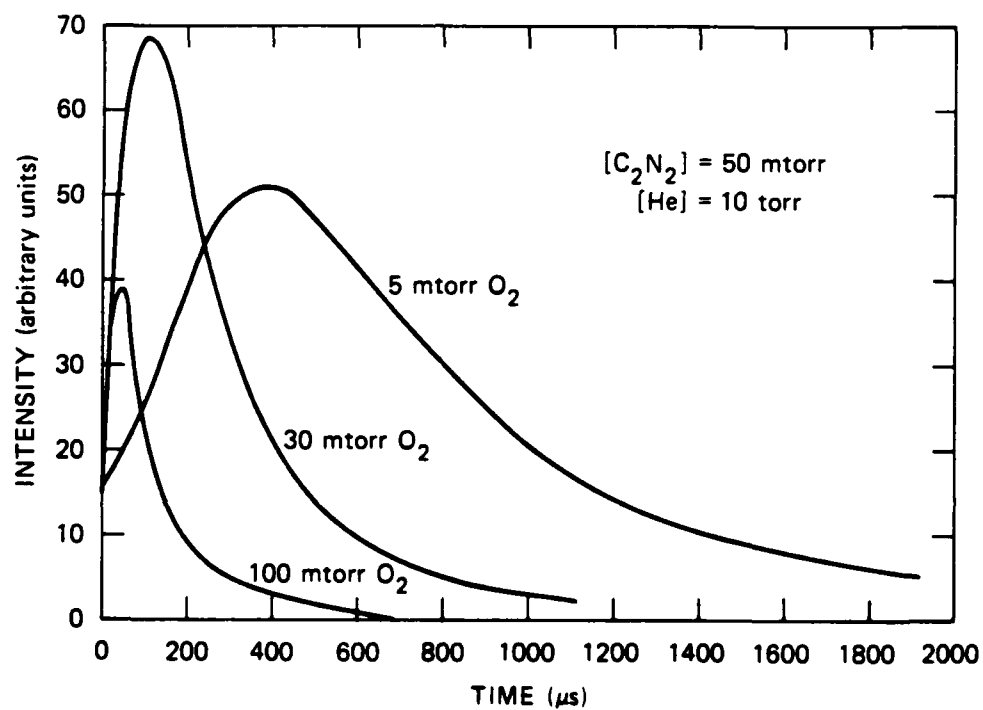
photodissociation. However, the possibility should not be excluded that trace quantities of ClCN in the C_2N_2 are responsible for the CN(B) production in the absence of O_2 , since the CN(B) threshold from ClCN is 1645 Å.²⁴

In the presence of O_2 , there is a large increase in integrated intensity, all at long times, as Figure 22 shows. Although there is still a fast 65 ns component (not apparent with the time resolution used), the principal emission now has a substantial build-up time of 20-200 μ s and a decay time of 100-600 μ s. The decay therefore represents not the loss of CN(B), but the decay of its source. Varying the O_2 concentration has a substantial effect on the time profiles, as shown in Figure 23.

The change in the mode of production of CN(B) on O_2 addition is reflected not only in its temporal behavior, but also in its power dependence (although not in its spectrum). Figure 14 shows a linear dependence of integrated CN(B-X) intensity on laser power, whereas upon O_2 addition, the intensity goes as the 1.6 power of the laser power, providing further evidence for the collisional nature of the CN(B) production process.

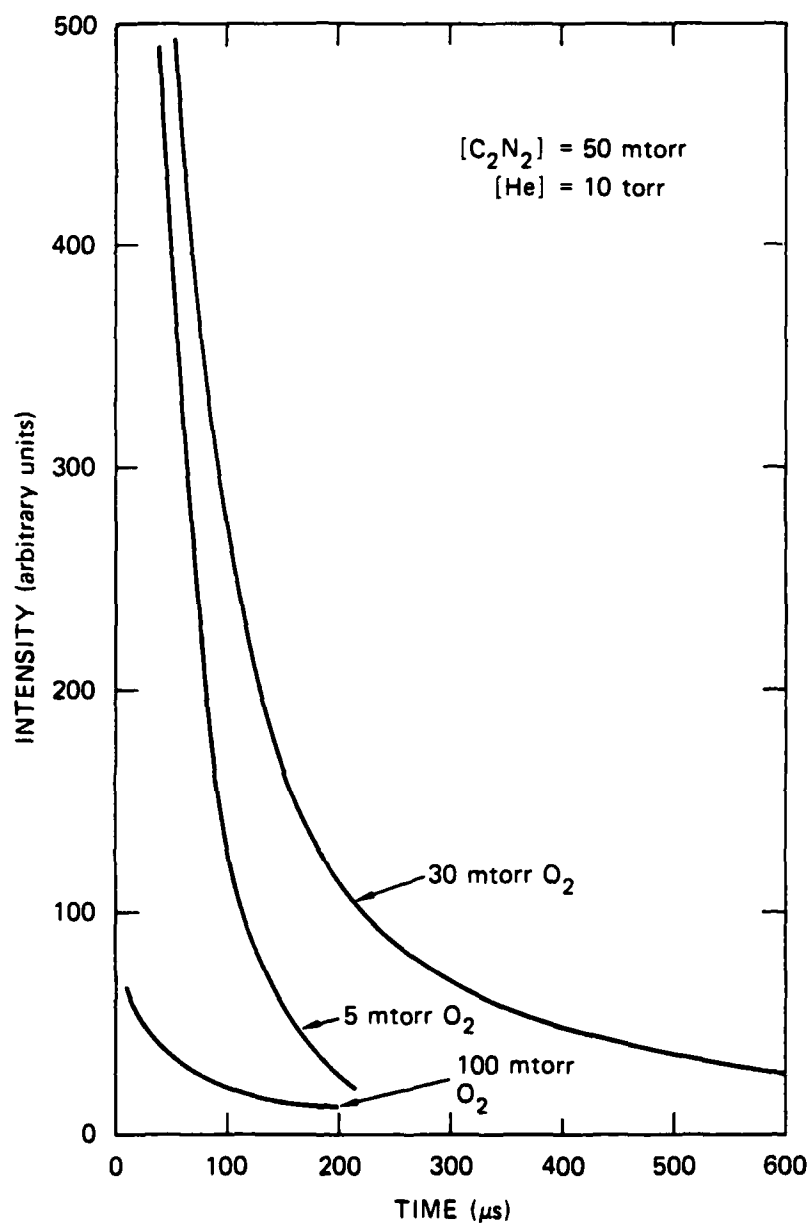
The effect on CN(A) of adding O_2 is to introduce a long-lived component to the emission. This is seen in Figures 10 and 24, which show the time behavior of the A-X 4-0 and 6-2 bands. In the case of the 4-0 band, the prompt radiation is unaffected by O_2 addition, as expected, and the additional intensity caused by O_2 comes at long times. Although the traces shown in Figure 10 are not dramatically different, the integrated intensities, which are measured by the photographic spectra, are greatly increased by the presence of the long-lived component. Figure 24, showing the temporal behavior of the A-X 6-2 band, demonstrates the chemical production of the $v = 6$ level; the integrated intensity of the long-lived component is an extremely sensitive function of the amount of O_2 present. Note that the buildup of the long-lived component is far more rapid for the A state than for the B state (Figure 22 and 23).

As mentioned earlier, the high vibrational levels of the CN(A) state are much more sensitive to O_2 than are the low levels; in fact, the 2-0 band is unaffected by O_2 addition. Thus, the CN(A)-producing reaction that is induced by O_2 preferentially populates high levels of the A state.



JA-6274-27

FIGURE 23 CN (B-X) 0-0, 1-1 EMISSION TIME PROFILES FOR VARIOUS $[\text{O}_2]$



JA-6274-28

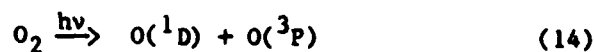
FIGURE 24 CN (A-X) 6-2 BAND INTENSITY FOR VARIOUS $[O_2]$

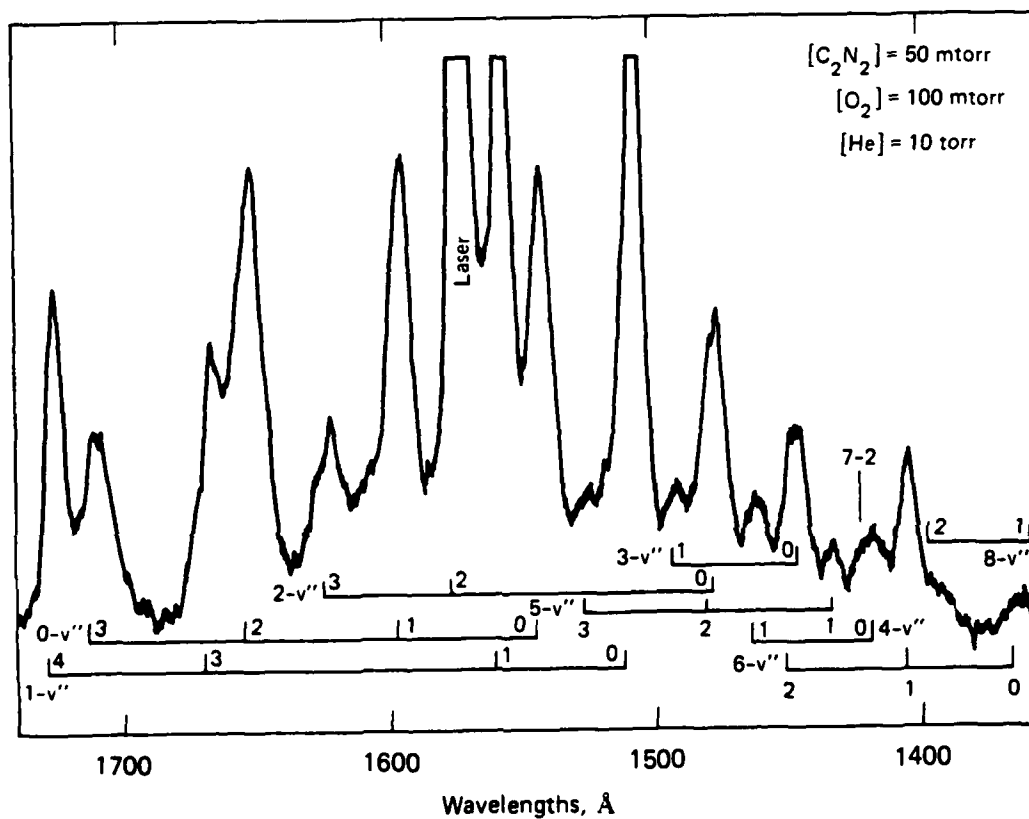
The spectrum of the CO(A-X) system that appears on photolysis of $C_2N_2-O_2$ is shown in Figure 25. Although bands from $v' = 1$ and 0 are the most intense, CO(A) levels up to $v = 8$ are discernible, the 6-1 band being particularly prominent. As $v = 8$ in the CO(A) state lies 9 eV above the ground state, a highly exothermic reaction is needed to generate such a high degree of excitation. The facts that CO itself does not absorb 1576-Å radiation and that various vibrational levels are populated indicate that excitation occurs through a chemical process, which is borne out by the observations, shown in Figure 26, that the emission builds up and decays relatively slowly; the CO(A¹Π) radiative lifetime is 10 ns. The temporal behavior of this emission looks neither like that of the CN(A-X) nor the CN(B-X) system; the emission is strongest at the highest O₂ density used.

The observed NO(A-X) emission in the 2000-3000 Å region is characterized by a vibrational distribution in which only the $v = 0$ and 1 levels of NO(A²Σ⁺) are populated, as shown in Figure 27. The temporal behavior of this emission is shown in Figure 28, the profile looking somewhat like CN(B-X) emission.

The four emitters discussed in this section, CN(A), CN(B), CO(A), and NO(A), all exhibit slow decays, suggesting long-lived sources, the characteristics of which must be that the reactants either have a long lifetime or are continually generated, and that oxygen must be involved. The long-lived components of the system are the ground state particles, O(³P), CN(X), and the ground state triatomics, NCO being the only one of whose presence we can be certain.

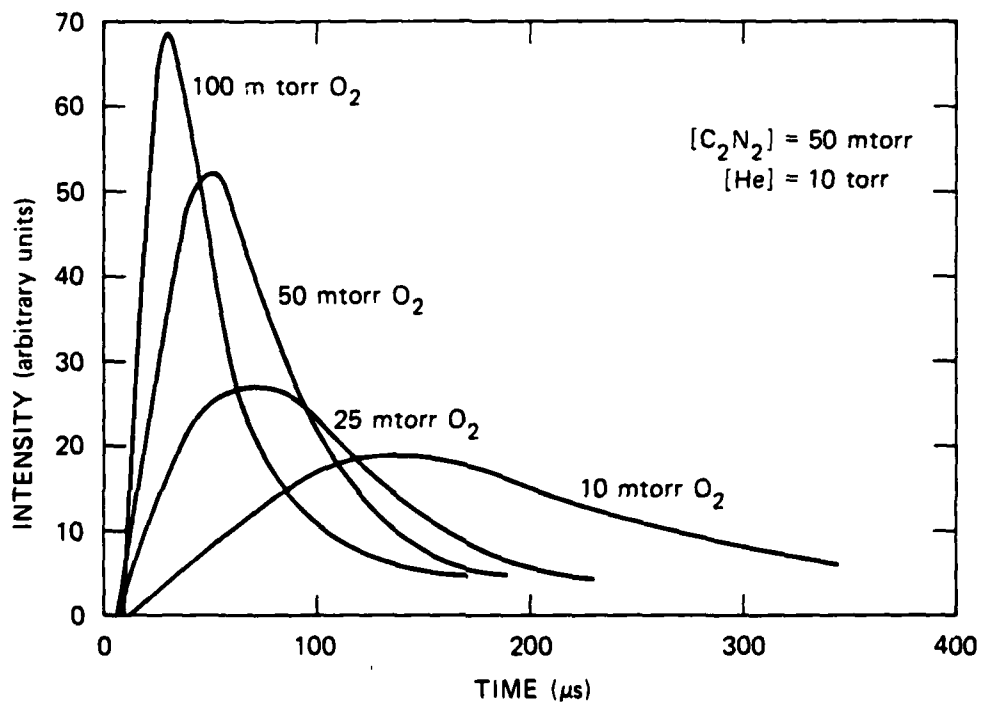
Perhaps the most diagnostic observation is that CO(A) is formed, with vibrational excitation giving a total energy of 9 eV. Such a reaction must involve both a highly reactive reactant and a very stable product. Of the various possibilities considered, the interaction between N(²D) and NCO seems to be the best candidate. The following sequence of reactions indicates how CO(A¹Π) might be formed:





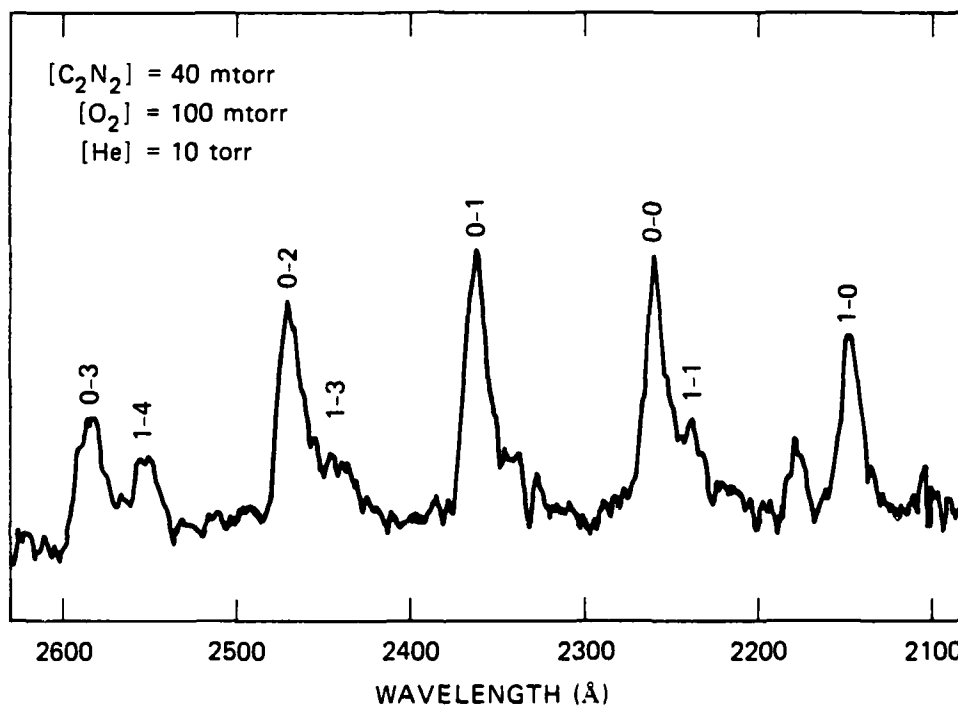
JA-6274-20

FIGURE 25 CO (A-X) EMISSION SPECTRUM



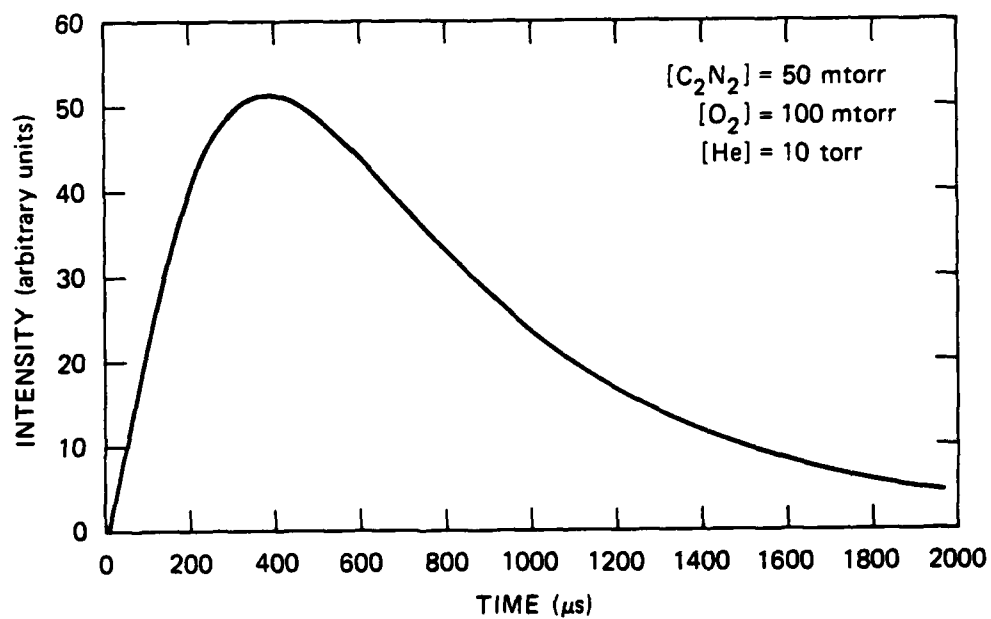
JA-6274-29

FIGURE 26 EFFECT OF O_2 ON CO (A-X) 1-0 EMISSION TIME PROFILE



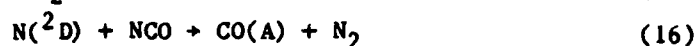
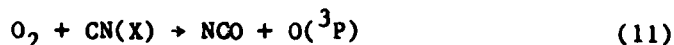
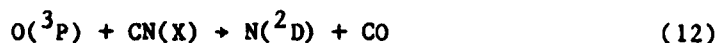
JA-6274-22

FIGURE 27 NO (A-X) EMISSION SPECTRUM



JA-6323-30

FIGURE 28 NO (A-X) 0-2 EMISSION TIME PROFILE



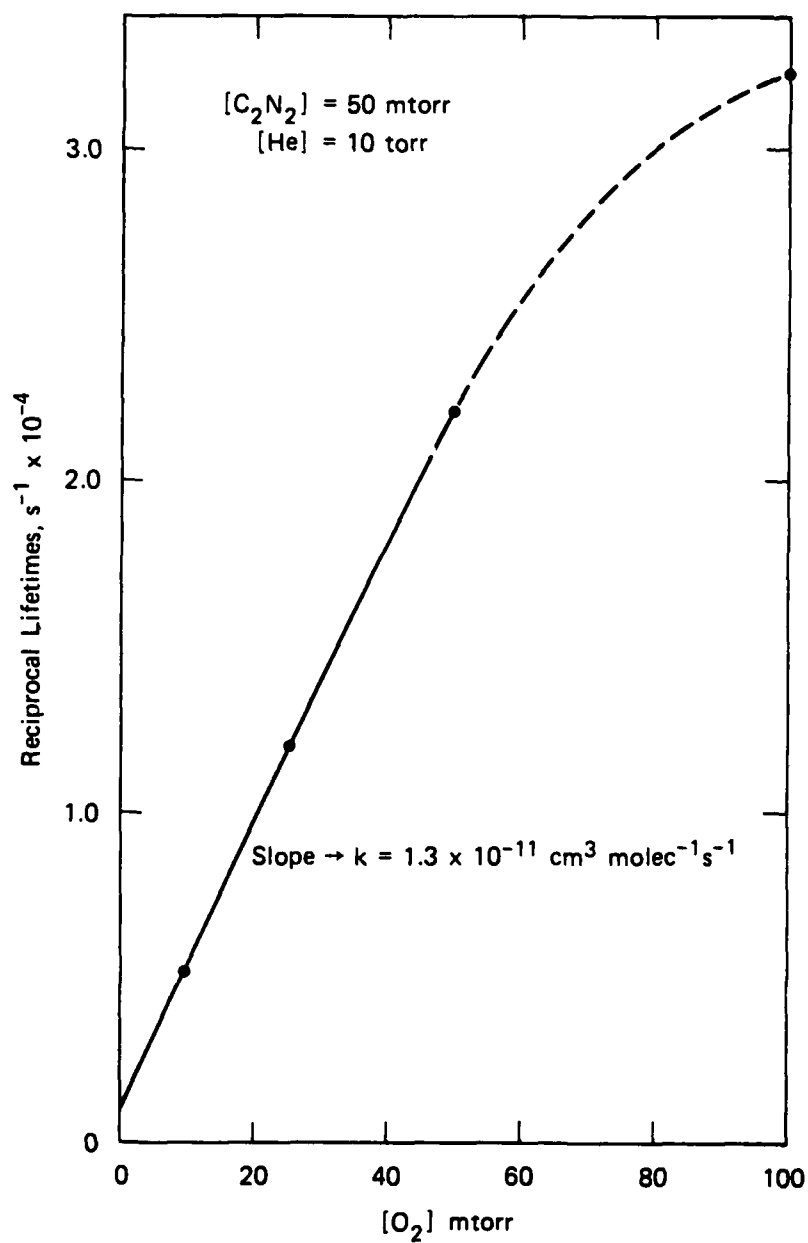
If $\text{CO}(\text{A}^1\Pi)$ were formed in this manner, then the apparent decay of the emission, shown to be a function of O_2 in Figure 26, might reflect the quenching of $\text{N}(^2\text{D})$ by O_2 . Figure 29 shows such a plot, the linear section corresponding to a rate coefficient just twice the accepted value for the $\text{N}(^2\text{D}) + \text{O}_2$ reaction.²⁵ Considering the uncertainties in such an approximate treatment, this agreement may not be inconsistent with the suggested process.

Because the $\text{CN}(\text{B-X})$ time behavior (Figure 22) is rather similar to that of $\text{CO}(\text{A-X})$, one may propose a second branch for reaction (16)



The exothermicity of reaction (16) to make ground state CO is 233 kcal/mole, more than enough to give $\text{CO}(\text{A}^1\Pi)$ in $v = 8$. It is extremely difficult to find a similarly exothermic pathway. As a $\text{CN}(\text{B})$ source, reaction (17) has the interesting property that the excitation limit for the B state is $v = 1$; experimentally, we find most of the population in $v = 0$ and 1. Nevertheless, although a common source for these two emissions would be attractive, the time profiles as a function of O_2 are sufficiently different to preclude a single source.

The very distinct $\text{CO}(\text{A-X})$ 6-1 band that appears in the spectrum of Figure 25 offers a clue to the source of the excitation. Just such a unique signature has been reported by Golde and Thrush²⁶ in the $\text{N}_2^+ - \text{CO}$ system, and they contend that the $\text{N}_2(\text{a}^1\Pi_g)$ state generates the $\text{CO}(\text{I}^1\Sigma^-)$ state by energy transfer and that the $\text{CO}(\text{I}^1\Sigma^-)$ state then preferentially crosses to the $\text{A}^1\Pi$ state at $v = 1$ and 6, due to localized perturbations. Fontijn et al.²⁷ have presented a spectrum of vuv radiation from a $\text{CF}_4 - \text{O}_2$ afterglow, in which the observed CO emission looks very similar to the emission that we observed in that the 6-1 band is strongly enhanced. Thus, it may be that metastable $\text{CO}(\text{I}^1\Sigma^-)$ plays a central role in all these systems; it would not be the first



JA-6274-21

FIGURE 29 EFFECT OF O_2 ON DECAY OF CO (A-X) EMISSION

time that a state that is difficult to detect spectroscopically has turned out to be chemically important.

Measurements of the power dependence of the CN(B-X) emission indicate a dependence between linear and quadratic, whereas the $N(^2D) + NCO$ mechanism suggests that a cubic dependence ought to be expected. Such determinations often give values smaller than the true power dependence; thus, this observation is not inconsistent with the reaction sequence discussed above.

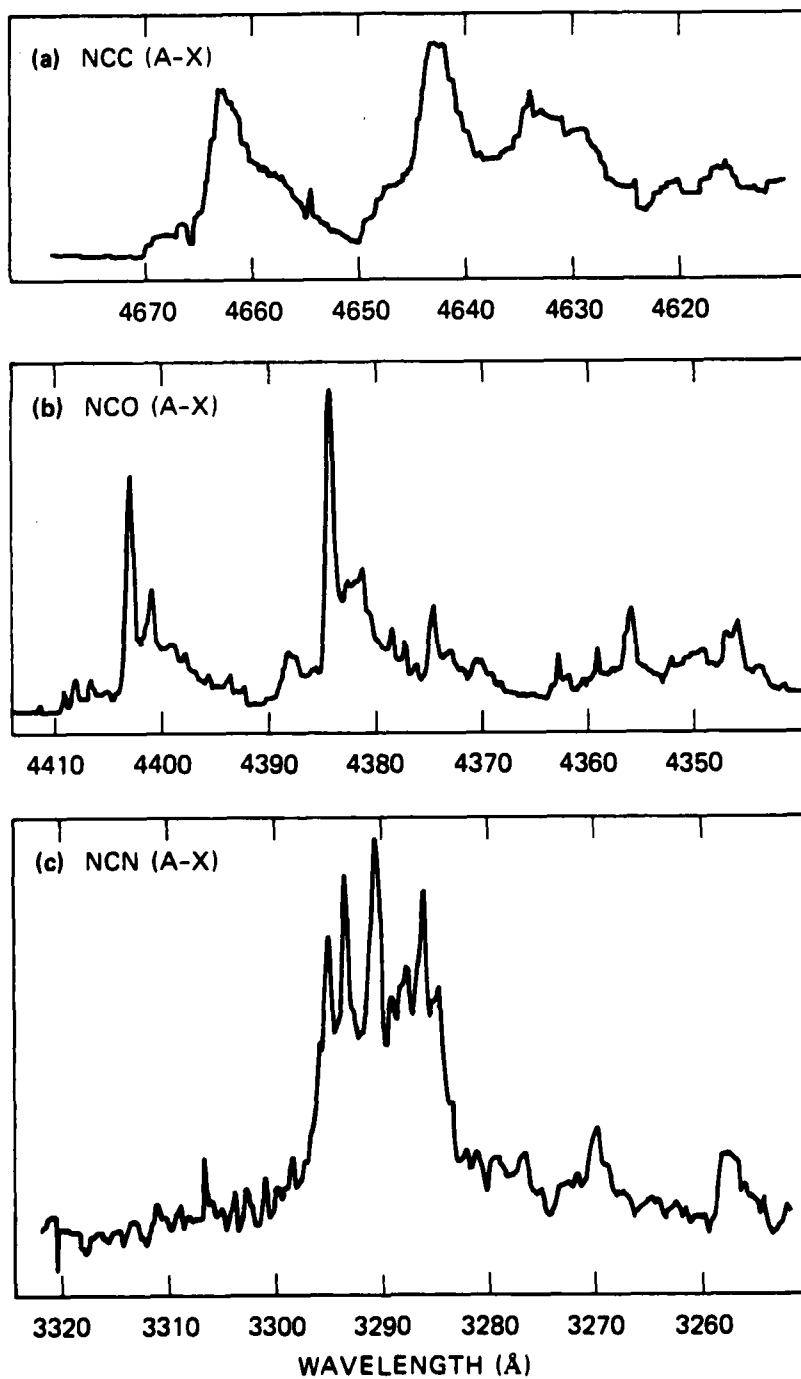
Triatomic Radiators

Three triatomic molecules are produced in the $C_2N_2-O_2$ system in their first electronically excited states: NCN, CCN, and OCN. The first of these can also be discerned in the absence of O_2 , but its intensity becomes very much stronger on O_2 addition. Just as with the CN(A) and CN(B) states, the effect of added O_2 is very strong.

The spectra of these A-X transitions are shown in Figure 30, and in Figure 31 is a lower resolution spectrum of the 4200-4400 Å region, showing both the extensive development of the NCO bands, and the CN(B-X) $v'-(v'+2)$ region. Although a strong feature occurs at the position of the B-X 5-6 band, this identification cannot be correct because the spectrum in Figure 21 shows no evidence for the 5-5 band, which would be equally prominent if the $v = 5$ level were populated.

The temporal behavior of the triatomics is shown in Figure 32 for a fixed C_2N_2 and O_2 pressure. They behave in a remarkably similar manner, although the precision of the data is sufficiently good that the slight differences are certainly real. Nevertheless, it is tempting to try to explain these profiles by a single-source reaction. Because the radiative lifetimes of these excited states are less than a microsecond, the profiles reflect collisional, and not radiative, processes, and because in each case O_2 is a critical component of the system, it seems that a reaction involving either atomic or molecular oxygen is required, even when the product contains no oxygen.

The temporal profiles of the triatomics are again a strong function of the O_2 density. Figure 33 shows this relationship for NCO(A), where the decay rates are in the millisecond range.



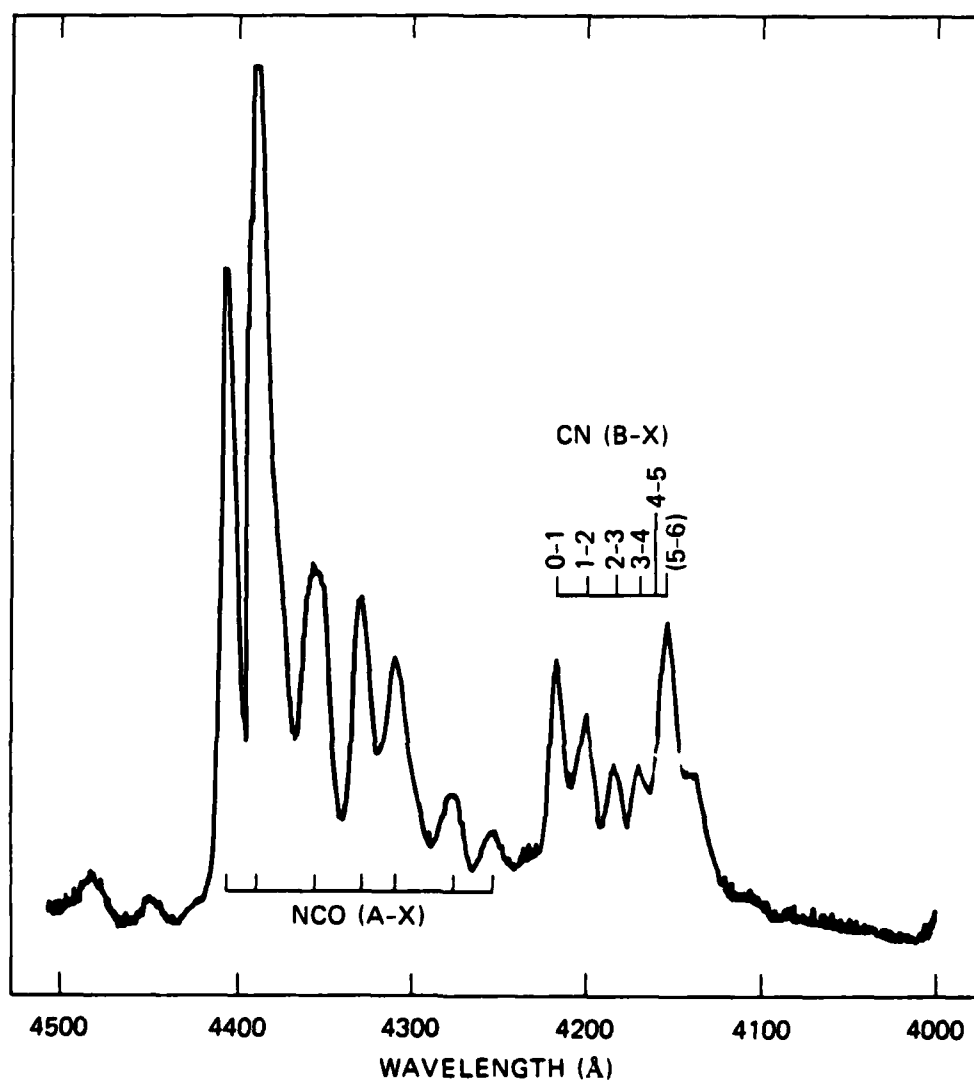
JA-6274-23

FIGURE 30 TRIATOMIC SPECTRA

$[C_2N_2] = 50$ mtorr

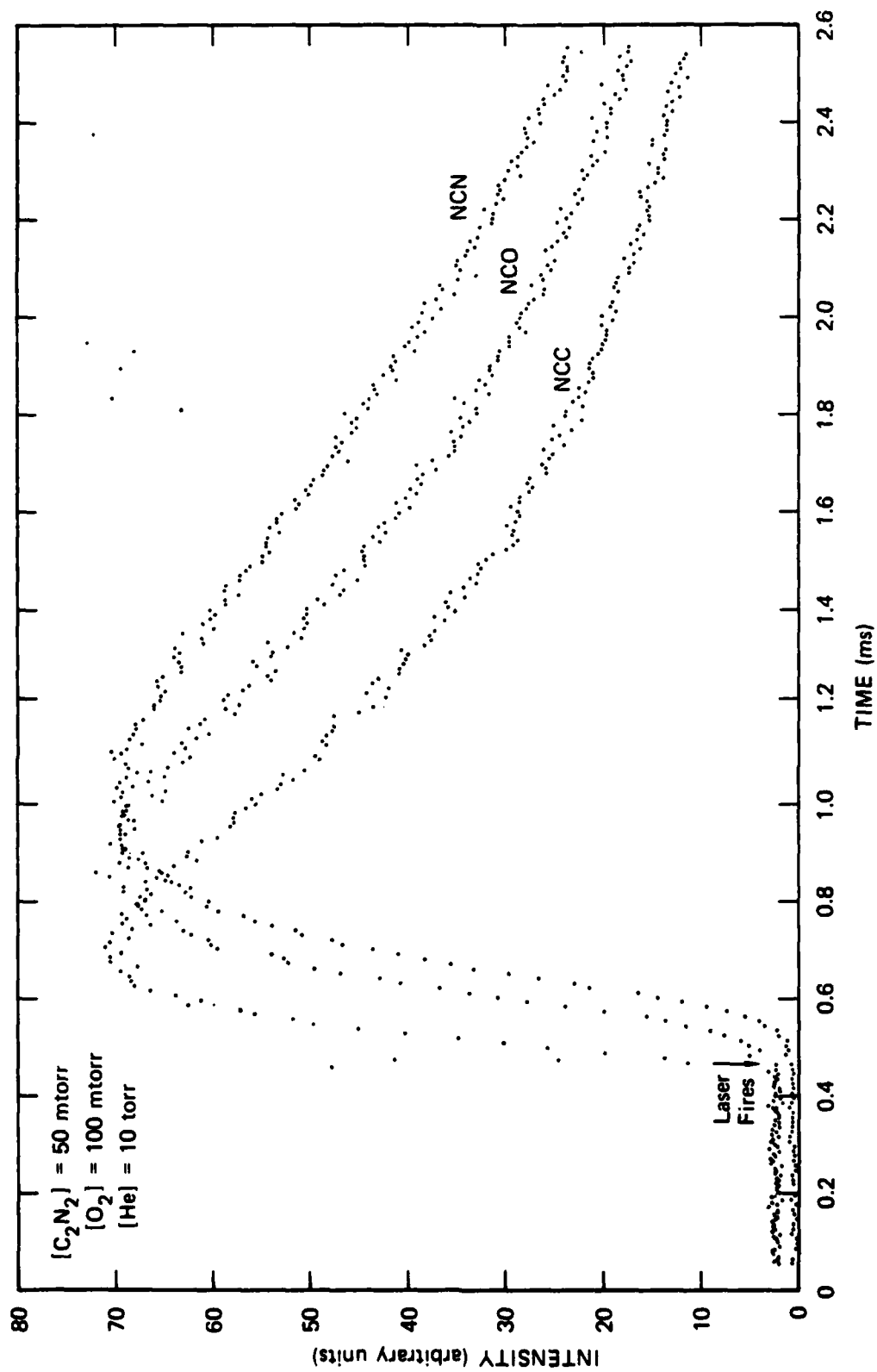
$[O_2] = 100$ mtorr

$[He] = 10$ torr



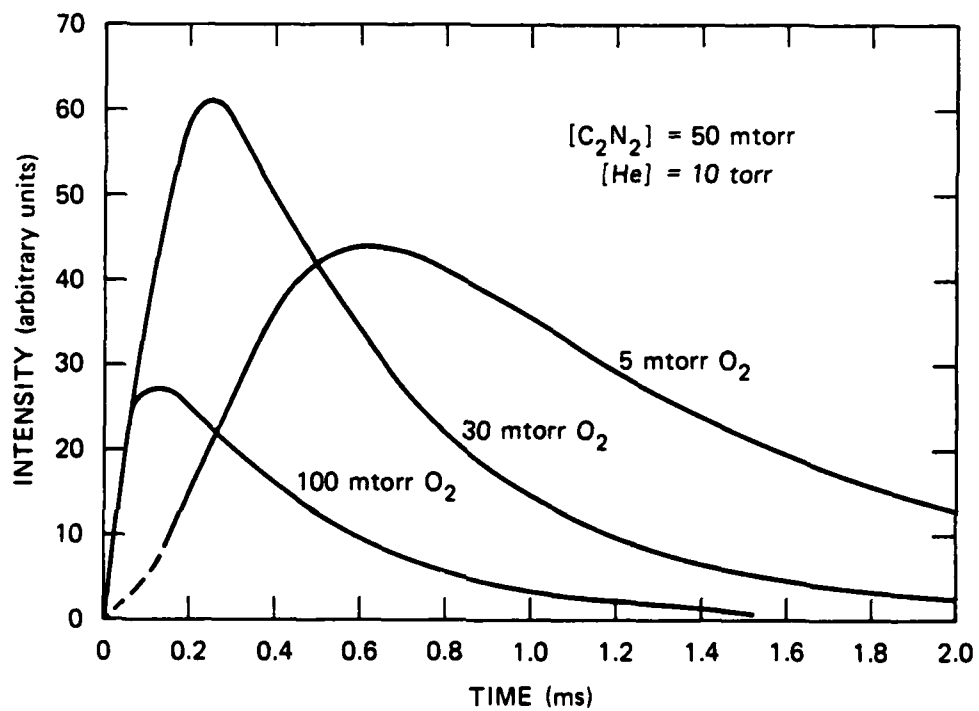
JA-6274-24

FIGURE 31 NCO (A-X) AND CN [B-X, $v' - (v' + 1)$] EMISSION SPECTRUM



JA-6274-25

FIGURE 32 TRIATOMIC TIME PROFILES



JA-6274-31

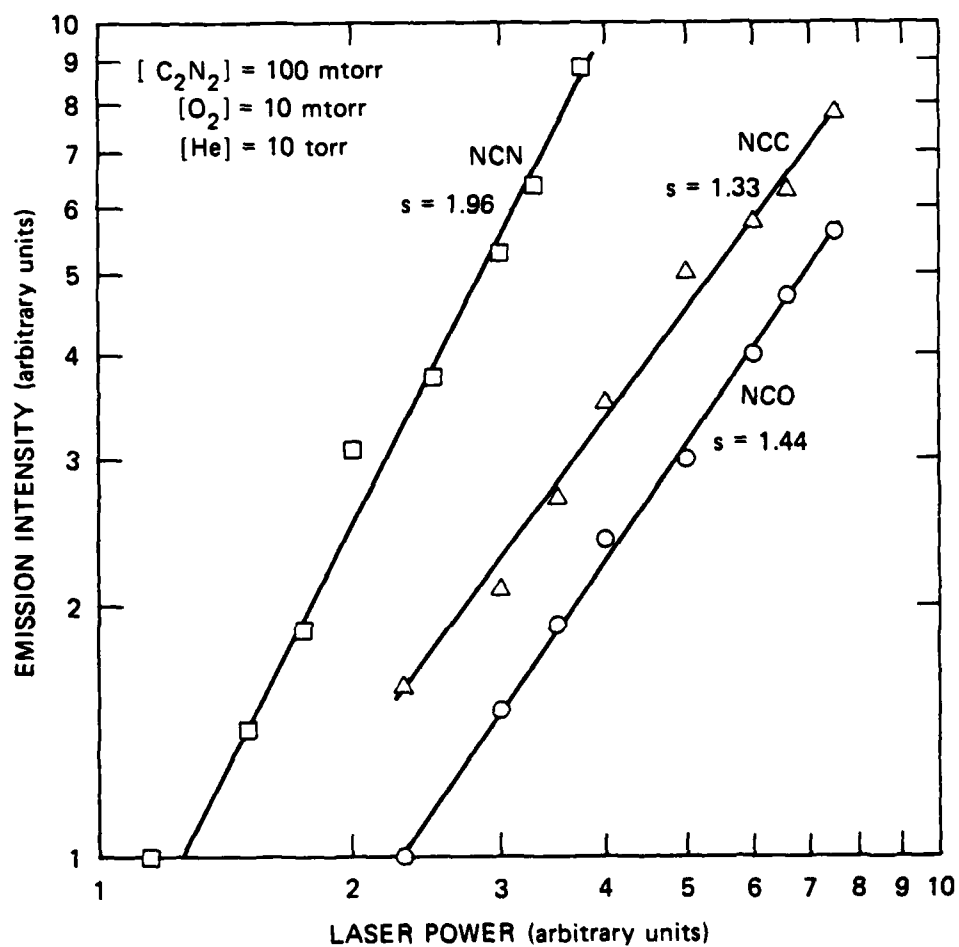
FIGURE 33 NCO(A-X) EMISSION (4400 Å) TIME PROFILES
FOR VARIOUS [O₂]

A restriction placed on reactions that occur over such a long time is that the known components of the system become limited. For example, the lifetime of CN is controlled by its reaction with O_2 . At 30 mtorr O_2 , the CN lifetime is 100 μs . Thus, CN cannot be involved in the chemistry that makes the triatomic excited states because their decay times are much longer. Similarly, because $N(^2D)$ is made from CN [reaction 13] and has a lifetime in 30 mtorr O_2 of 180 μs , it also seems to be too short-lived to account for the decays of the triatomics, which are about three times longer. Since these products are both highly excited and unstable [the heat of formation of $NCN(A)$ is approximately 210 kcal/mole, or 9 eV], it is not at all evident what reactants can produce them.

However, if the source is not chemistry, but energy transfer, then there is a long-lived species that could be responsible: vibrationally excited CO. This is generated in the reaction between $O(^3P)$ and CN, reaction 12, and for the channel giving $N(^4S)$ as a product, excitation up to $CO(v = 17)$ is possible. Schmatjko and Wolfrum²² measured up to $v = 12$ and observed that for C_2N_2 densities comparable to ours, there was no apparent loss of $CO(v = 12)$ even at 250 μs after initiation. Thus, here is a species that is long-lived and is certainly energetic enough to generate the excited triatomics: $CCN(A)$ and $NCO(A)$ require $CO(v = 11)$, whereas $NCN(A)$ requires $v = 16$. How efficient such $V \rightarrow E$ processes might be is unknown, but this explanation for the excited triatomic production gets around the severe energy requirements for chemical production, and is consistent with the $CO(v)$ lifetimes in C_2N_2 .

Because vibrationally excited CO is formed through reaction 12, the power dependence of the triatomic emissions might be expected to be at least quadratic. Again, this does not appear to be the case, as shown in Figure 34, where for both NCO and CCN the dependence is between linear and quadratic. NCN, however, does exhibit quadratic behavior, which could correlate with the fact that the most energy is required for its excitation.

Apparently, CCN and NCN are formed in their ground states during the early part of the reaction. It is possible, in fact, that CCN is a photodissociation product. If this could be substantiated by LIF probing on the A-X band at 4600 Å, then the heat of formation of CCN could be specified much more precisely than the value of 133 ± 30 kcal/mole given in the JANAF

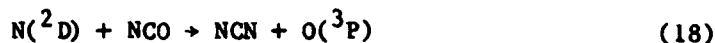


JA-6274-26

FIGURE 34 POWER DEPENDENCE OF TRIATOMIC EMISSIONS

tables. For instance, if CCN is produced at 1576 Å, then $\Delta H_f(\text{CCN}) < 143$ kcal/mole. Such information is extremely important in determining possible reactive pathways in combustion processes.

For NCN formation, there is the possibility of various switching reactions involving NCO; that is,



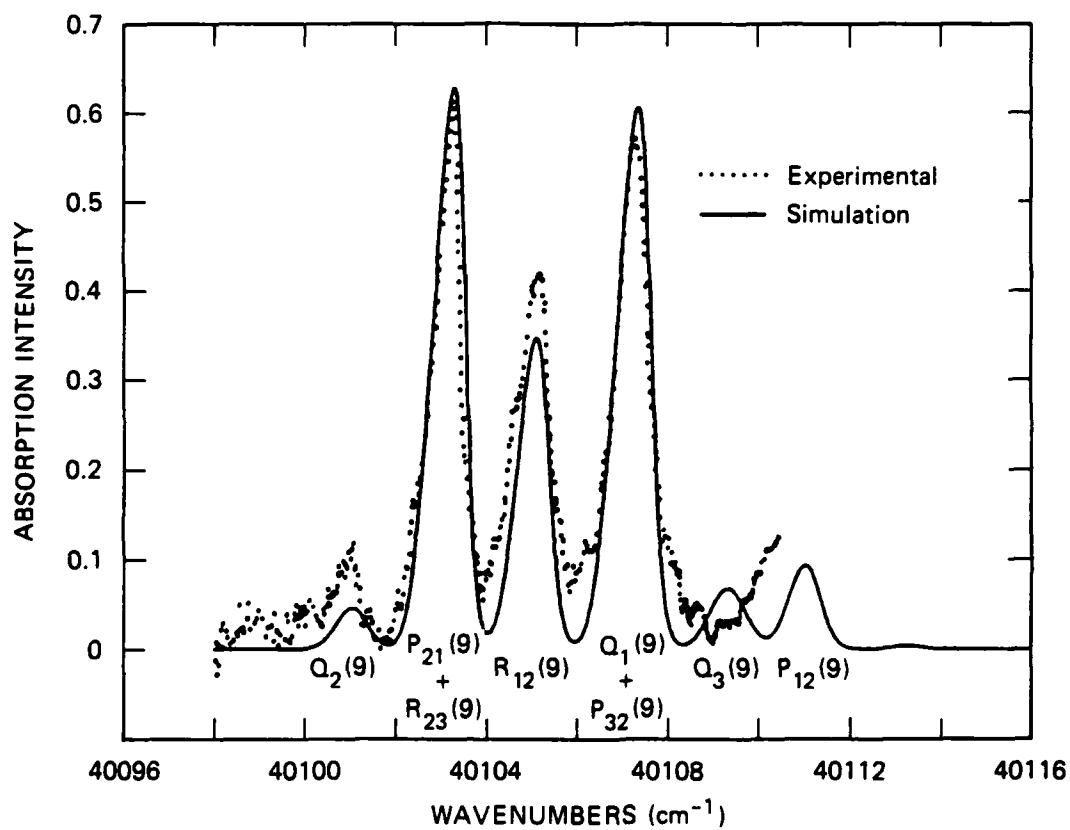
and demonstrations of such reactions would also be useful in understanding the overall chemistry of the system.

The Herzberg I System of O_2

A concerted effort was made to develop an LIF technique to study the $\text{O}_2(\text{A}^3\Sigma_u^+)$ state, using injection-locking of 2485-Å radiation to give a narrow high-intensity line. We were not successful, and it is important to try to understand the reason, because in principle, it was a reasonable experiment. Also, we hoped that the idea could be extended to generating the $\text{NO}(\text{a}^4\Pi)$ state.

Using the same arrangement that was used for the NO_2 photodissociation study, we tried to directly excite O_2 to the $v = 8$ level of the $\text{A}^3\Sigma_u^+$ state. This A-X transition is the Herzberg I system of O_2 and is an important component of the terrestrial airglow. Calculations show that the radiative lifetime for this transition is about 100 ms,²⁸ a value that suggests that it should not be excessively difficult to see emission from the A state. For instance, we are able to see radiation from the $\text{O}(^1\text{D})$ state, which has a 150-s lifetime.

The problem of instrumental wavelength calibration was overcome by making an absorption measurement of O_2 in the same spectral region in order to precisely locate the positions of the lines that we wished to pump. Figure 35 shows an absorption spectrum obtained with a pathlength of 4 meters and a pressure of two atmospheres. This is the K = 9 set of lines, tabulated by



JA-6274-35

FIGURE 35 O₂ (A³Σ_u⁺ ← X³Σ_g⁻) 8-0 BAND ABSORPTION

Herzberg,²⁹ and the data give us a narrow tuning range over which to look for emission. The reason to search for radiation is that it is not the spectroscopy that is of interest here, but the kinetics. Detection of radiation would enable us to determine rate coefficients for quenching the $O_2(A)$ state, the most important quenchers being O_2 and N_2 .

Others have attempted this experiment before,^{30,31} but with little chance of success because the radiation source was not tunable to the absorption line. It is of no value to use large photon fluxes if they are not within the bandpass of the absorption. In this experiment, the laser line width was 0.6 cm^{-1} , whereas the absorption line width is 0.1 cm^{-1} . Thus, approximately 15% of the radiation is absorbable by O_2 . The success of the experiment depends on the ratio of absorption oscillator strength to quenching rate coefficient, and the signal level (total photons counted) is basically independent of O_2 pressure.

The number of photons emitted in such a system is the product of the number absorbed and the fraction of those that radiate. Over a 1-cm path, this number is given by

$$\text{photons emitted} = (\sigma \tau_R^{-1} f/k) I_0 \quad (20)$$

where σ is $1 \times 10^{-23}\text{ cm}^2$, for the strongest line in the absorption spectrum of Figure 34, τ_R^{-1} is 6 s^{-1} , f is the overlap between the laser line and the absorption line (15%), and k is the $O_2(A, v = 8)$ quenching rate coefficient by O_2 . This can have a maximum value of $3 \times 10^{-10}\text{ cm}^3\text{ molec}^{-1}\text{ s}^{-1}$, and therefore the smallest photon emission rate, for all $v = 8$ bands, is 3×10^{-14} times the incoming photon flux, I_0 . This latter is 6 mJ/pulse , or 7×10^{15} photons/pulse; thus we have a minimum of 200 photons emitted over all bands for each laser pulse.

The strongest band from $v = 8$ is the 8-2 band at 2700 Å , from which 23% of the radiation emanates. Thus, the minimum number of photons emitted in this band is 45/pulse. Finally, we needed to know the system collection efficiency. This was obtained by calibration against radiation from the H_2 anti-Stokes Raman line, a process for which a precise cross section is known. This resulted in a value of 1×10^{-4} for the system detection efficiency. Thus, the minimum photon count rate becomes 0.0045 photon/pulse.

The viability of the experiment then depends on the ratio of this signal level to the noise. Of course, if quenching by O_2 has a rate coefficient such as that measured by Kenner and Ogryzlo³² for the $v = 0$ level of the $O_2(A)$ state, $3 \times 10^{-13} \text{ cm}^3 \text{ molec}^{-1} \text{ s}^{-1}$, then the signal rate will be 1000 times higher, 4.5 photons/pulse.

It was experimentally determined that the signal-to-noise was such that we could reliably detect 0.3 hv/pulse, leading to the conclusion that we would obtain no signal unless the $O_2(A, v = 8)$ quenching rate by O_2 is less than $0.0045/0.3 = 0.015$ times the collision frequency. Therefore, the lower limit we can set on the O_2 quenching rate coefficient is $5 \times 10^{-12} \text{ cm}^3 \text{ molec}^{-1} \text{ s}^{-1}$.

CONCLUSIONS

NO₂ Photodissociation

The work on NO₂ photodissociation carried out at 2485 Å has established that there is a complete population inversion of the vibrationally excited NO product. Most of the population is found close to the thermodynamic limit of $v = 8$, a fact that suggests some interesting consequences. One obvious conclusion is that it should be possible to make an ir laser operating on, for example the $v = 7 \rightarrow 6$ NO band at 5.9 μ . Another point is that excitation of the high vibrational levels of NO is characteristic of NO₂ photodissociation in the 2400-3000 Å region, so that detection of these levels following a laser pulse of the right frequency is diagnostic for the presence of NO₂. There are a variety of advantages of detecting NO₂ in this manner over the more conventional visible LIF technique. A considerable enhancement in signal levels is possible if the 2491 Å NO₂ band is utilized, but we have not yet been able to carry out the necessary measurements to completely quantify this conclusion.

NO Photoexcitation

We have established that the 1576 Å F₂ laser line excites a particular rotational level in the B'² Δ state of NO. This makes possible state-to-state studies that involve NO(B'² Δ) as the initial level, and permits an experimenter to access a variety of NO states that have been little studied. Furthermore, this observation provides an excellent method for monitoring the laser intensity, in a manner much more specific than is attainable with a power meter.

O₂(A³ Σ_u^+) Photoexcitation

Our attempt to generate the $v = 8$ level of the O₂(A³ Σ_u^+) state by LIF techniques proved to be unsuccessful, the principal difficulties being the small absorption cross section, and the rapid quenching by O₂. Nevertheless, we were able to set a lower limit on the quenching rate coefficient, and provide guidelines to others who wish to carry out a similar study, on O₂ or

on other molecules with strongly forbidden transition. Ours was the most recent and sophisticated attempt to carry out this experiment on O_2 , and it is clear what will be required for success. We are presumably within an order of magnitude of detecting an emission signal, that is, given a laser with ten times the power we could have seen a signal. The most obvious improvement would be to match the laser line width to the absorption line width; this would give a factor of six improvement in the light absorbed by the O_2 , which could well be sufficient to make the experiment work. We estimate that the generation of the $NO(a^4\Pi)$ state in the same manner, and at the same wavelength, is of no greater difficulty.

C_2N_2 Photodissociation

New information has been obtained in a variety of areas that involve the 1576 Å photodissociation of C_2N_2 . The products of this process include $CN(A^2\Pi)$ in its first six vibrational levels, and we have been able to carry out a new determination of the radiative lifetimes for each level. We believe that these data are superior to any others currently in the literature, and are in fact the first that show the relationship between lifetime and vibrational level that is theoretically predicted.

We have investigated the quenching of the six levels by the parent molecule, and find a general increase in rate coefficient with increasing vibrational level. This process, which proceeds at collisional frequency for $v = 5$, is believed to involve intersystem crossing to the CN ground state. Other quenchers have also been investigated, for the $v = 1$ level. They are less efficient than C_2N_2 , and may involve reactive channels. Further work should be performed to elucidate the products, particularly with O_2 and H_2 .

Although the one-photon limit for the production of $CN(A)$ is $v = 5$, excitation up to at least $v = 9$ is observed, and strong emission from the $v = 0$ and 1 levels of the $CN(B)$ state is also seen. In the former case, the high levels are probably generated by energy pooling involving vibrationally excited ground state CN molecules, since the temporal behavior of the emission shows a relatively slow build-up. However, the $CN(B)$ emission temporal behavior suggests that it is made in a two-photon process, in agreement with other studies at 1930 Å. The power dependence of the emission from the high $CN(A)$ levels indicates that some of these are produced in processes requiring

three photons, and it is important to study the behavior of the presumed energy carrier, vibrationally excited ground state CN, to observe the process in more detail.

Upon addition of O_2 , the system gets considerably more complex. We find greatly enhanced emission intensities from CN(A) and CN(B), as well as generation of much higher vibrational levels of CN(A). These are clearly chemical effects, taking place in the 0.1-1 ms time domain, and more work is needed to achieve a full understanding of the system. It is probable that $N(^2D)$ and NCO are important reactants. These are two particles that are produced in copious quantities in a hot $C_2N_2-O_2$ system, and they are expected to have a large part in determining the overall chemistry. Correlations between the concentrations of these species and the CN(A) and CN(B) emitters should provide useful indications as to the course of the reactions.

Other strong emissions in the $C_2N_2-O_2$ system are seen from electronically excited NCO, NCN, and NCC, as well as from the CO(A) and NO(A) states. Each has its characteristic time profile, and we believe that the triatomics are excited after being generated in the ground state, the agent for their excitation most probably being vibrationally excited CO; again, an energy pooling process is required.

We feel that there is every reason to believe that the key to understanding the overall chemistry of this system lies with the vibrationally excited diatomics, CN and CO, and with the two species generated early in the evolution of the system, $N(^2D)$ and NCO. CN and NCO can be monitored by LIF techniques, using a dye laser operating in the 3800-4000 Å region. CO and $N(^2D)$ are most easily detected by means of resonance lamps in the vacuum uv region. Subsequent investigations are likely to be most profitable when the strong visible and uv emissions in the $C_2N_2-O_2$ system are correlated with the above-mentioned four species. From the point of view of improving our understanding of combustion and propellant chemistry we feel that further work along these lines is urgently needed.

PUBLICATIONS

Articles in Print

T. G. Slanger, W. K. Bischel, and M. J. Dyer, "Nascent NO Vibrational Distribution from 2485 Å Photodissociation of NO₂" J. Chem. Phys. 79, 2231 (1983).

Articles in Preparation (all with M. R. Taherian)

"Photoexcitation of NO at the 1576 Å F₂ Laser Line"

"Radiative Lifetimes and C₂N₂ Quenching Rate Coefficients for CN(A²Π, v = 0-5)"

"Quenching of CN(A²Π, v=0,1) by CO₂, O₂, NO, H₂, and N₂"

"C₂N₂ Photodissociation at the 1576 Å F₂ Laser Line"

"Photochemistry of the C₂N₂-O₂ System"

Note in preparation

"Studies on Direct Excitation of the O₂(A³Σ_u⁺) 8-0 band at 2489 Å"

The following individuals have contributed to the work in this report:

M. R. Taherian

W. B. Bischel

M. J. Dyer

M. J. Rossi

D. L. Huestis

L. E. Jusinski

REFERENCES

1. G. E. Busch and K. R. Wilson, J. Chem. Phys. 56, 3626 (1972).
2. H. Zacharias, M. Geilhaupt, and K. H. Welge, J. Chem. Phys. 74, 218 (1981).
3. R. A. Young, G. Black, and T. G. Slanger, J. Chem. Phys. 48, 2067 (1968).
4. T. G. Slanger and G. Black, J. Chem. Phys. 58, 194 (1973).
5. D. H. Katayama, T. A. Miller, and V. E. Bondybey, J. Chem. Phys. 71, 1662 (1979).
6. W. Groth, D. Kley, and U. Schurath, JQSRT 11, 1475 (1971).
7. E. Miescher, Helvetica Physica Acta 29, 401 (1956).
8. R. W. Nicholls, J. Res. National Bureau of Standards, 68A, 535 (1964).
9. R. J. Cody, M. J. Sabety-Dzvonik, and W. M. Jackson, J. Chem. Phys. 66, 2145 (1977).
10. W. M. Jackson and J. B. Halpern, J. Chem. Phys. 70, 2373 (1979).
11. D. C. Cartwright and P. J. Hay, Astrophys. J. 257, 383 (1982).
12. M. Larsson, P.E.M. Siegbahn, and H. Ågren, Astrophys. J. 272, 369 (1983).
13. M. Jeunehomme, J. Chem. Phys. 42, 4086 (1965).
14. D. L. Durić, R. Erman, and M. Larsson, Phys. Scripta 18, 39 (1978).
15. W. M. Jackson, W. Payne, J. B. Halpern, and X. Tang, Proc. International Conference on Lasers '82, Dec. 13-17, 1982.
16. C. Conley, J. B. Halpern, J. Woods, C. Vaughn, and W. M. Jackson, Chem. Phys. Lett. 73, 224 (1980).
17. N. Nishi, H. Shimohara, and I. Hanazaki, J. Chem. Phys. 77, 246 (1982).
18. V. E. Bondybey, J. Chem. Phys. 66, 995 (1977).
19. W. M. Jackson and R. J. Cody, J. Chem. Phys. 61, 4183 (1974).
20. B. J. Sullivan, G. P. Smith, and D. R. Crosley, Chem. Phys. Lett. 96, 307 (1983).
21. H. Okabe, J. Chem. Phys. 53, 3507 (1970).
22. K. J. Schmatjko and J. Wolfrum, 16th International Symposium on Combustion, M.I.T. Cambridge, MA (1976).
23. H. Reisler, M. Mangir, and C. Wittig, Chem. Phys. 47, 49 (1980).
24. D. D. Davis and H. Okabe, J. Chem. Phys. 49, 5526 (1968).

25. G. Black, T. G. Slinger, and G. A. St. John, J. Chem. Phys. 51, 116 (1969).
26. M. F. Golde and B. A. Thrush, Proc. Roy. Soc. (London) A330, 109 (1972).
27. A. Fontijn, R. Ellison, W. H. Smith, and J. E. Hesser, J. Chem. Phys. 53, 2680 (1970).
28. H. Lefebvre-Brion and F. Guerin, J. Chem. Phys. 49, 1446 (1968).
29. G. Herzberg, Can. J. Phys. 30, 185 (1952).
30. H. Broida (private communication, 1977).
31. E. A. Ogryzlo (private communication, 1982).
32. R. D. Kenner and E. A. Ogryzlo, International Journal of Chemical Kinetics, XII, 501 (1980).

Reprinted from

THE JOURNAL
OF
CHEMICAL PHYSICS

VOLUME 79

NUMBER 5

1 SEPTEMBER 1983

**Nascent NO vibrational distribution from 2485 Å NO₂
photodissociation**

T. G. Slanger, W. K. Bischel, and M. J. Dyer

Molecular Physics Laboratory, SRI International, Menlo Park, California 94025

pp. 2231-2240

Published by the
AMERICAN INSTITUTE OF PHYSICS

Nascent NO vibrational distribution from 2485 Å NO₂ photodissociation

T. G. Slanger, W. K. Bischel, and M. J. Dyer

Molecular Physics Laboratory, SRI International, Menlo Park, California 94025
(Received 8 April 1983; accepted 25 May 1983)

The initial NO vibrational level distribution has been determined for NO₂ photodissociation at 2485 Å. Excitation spectra of the NO vibrational levels were measured by using both the NO $A^2\Sigma^+ \leftarrow X^2\Pi$ and $B^2\Pi \leftarrow X^2\Pi$ transitions, the latter being somewhat stronger due to saturation effects. It was determined that the NO population was strongly inverted, with most of the nascent NO being in $v = 6-8$; the thermodynamic limit is $v = 8$. Injection locking of the KrF laser output permitted study of the 2491 Å NO₂ band, and it was evident that the increased absorption in this region gave greatly enhanced signal levels in the excitation spectra, at those wavelengths where NO₂ and NO absorption lines coincide. It was demonstrated that in the 2640-2830 Å wavelength region, NO₂ can be detected by use of a single dye laser, simultaneously dissociating NO₂ and electronically exciting the resultant vibrationally hot NO. Deactivation of NO($v = 8$) by NO₂ was found to proceed with a rate coefficient of 1.1×10^{-11} cm³ molecule⁻¹ s⁻¹, whereas the coefficient for quenching by N₂ and He was $\leq 2 \times 10^{-13}$ cm³ molecule⁻¹ s⁻¹. The peculiar NO rotational distributions noted by Zacharias *et al.* in their study of NO₂ dissociation at 3371 Å were also observed in the present work.

INTRODUCTION

The photochemistry of NO₂ has been a fertile field of study for many years, and as each new technological tool becomes available, it is applied to this interesting molecule. To a large extent, the long history of NO₂ research is directly related to the strength of the O-NO bond, and the fact that the molecule has low-lying electronic states; a whole gamut of physicochemical studies can be carried out with radiation at wavelengths above 2000 Å.

The technique of laser-induced fluorescence (LIF) has made it possible to study nascent product distributions in photodissociative processes. Although there have been a number of studies of NO₂ photodissociation in the VUV region, where electronically excited NO states have been identified, e.g., the work of Welge,² there has until now been only a single LIF determination of the distribution of NO ground state vibrational levels, reported by Zacharias *et al.*¹ for 3371 Å photodissociation. At that wavelength, only the first three NO levels are accessible, and the authors found an inverted distribution.

There have been other studies in which less direct determinations have been made of vibrational distributions, suggesting population inversions. Busch and Wilson³ made measurements at 3470 Å, at which photolysis wavelength only NO($v = 0, 1$) can be produced. McKendrick *et al.*⁴ showed that at 2485 Å there was at least some production of NO($v = 6$). Grant and co-workers^{5,6} carried out multiphoton studies on the system, and reached the conclusion that at input energies below the NO + O(¹D) threshold, vibrationally excited NO was produced, with no indication of NO($v = 0$) generation. In the present paper, we report the determination of relative NO vibrational populations from NO₂ photodissociation at 2485 Å and other wavelengths, where up to nine NO levels can be reached.

EXPERIMENTAL

A diagram of the apparatus is shown in Fig. 1. The essence of the experiment is that NO₂ was dissociated

by the KrF excimer laser, either with the normal ~5 Å bandwidth, or with its output narrowed by injection locking. To study the vibrational distribution of the resulting NO, the doubled dye laser output was scanned over the relevant NO($A-X$) and NO($B-X$) bands, thereby generating an excitation spectrum. The resulting fluorescence was detected with a monochromator-phototube combination at shorter wavelengths than the excitation wavelength.

For some of the experiments described below, it was necessary to narrow the bandwidth of the excimer laser. This was accomplished by injection locking the KrF laser using the technique of Bigio and Slatkine⁷. An unstable resonator with a magnification of 4 (mirror radii $R_1 = 75$ cm, $R_2 = 300$ cm, $L = 113$ cm) was set up as the basic laser cavity. The radiation used to injection lock the KrF laser was provided by a YAG pumped dye laser that had been doubled to the UV at 2780 Å and then Raman shifted⁸ one anti-Stokes order in H₂. The bandwidth of the UV dye laser radiation was approximately 0.5 cm⁻¹. The first anti-Stokes order was separated from the other orders using a Pellin-Broca prism and injected into the KrF unstable laser cavity through a 1 mm hole in the rear mirror (R_2). The timing between the YAG and excimer lasers had to be adjusted and maintained to 1-2 ns for good injection locking due to the fact that the dye laser pulse was much shorter than the excimer laser pulse (6-8 ns vs 13 ns). With this laser system, we were able to obtain more than 50 mJ output in a beam apertured to a circular beam diameter of 10 mm. We were able to tune this laser over the range 2478-2495 Å. At 2491 Å, we measured a suppression of the normal laser emission at 2483 Å of greater than a factor of 5, thus indicating that most of the energy was in the injected line. This was confirmed by the excitation scans of NO₂ with and without injection locking.

There was a constant flow of gas through the reaction cell—a 10 Torr He background with NO₂ introduced as a 0.7% mixture in He, used without further purification.

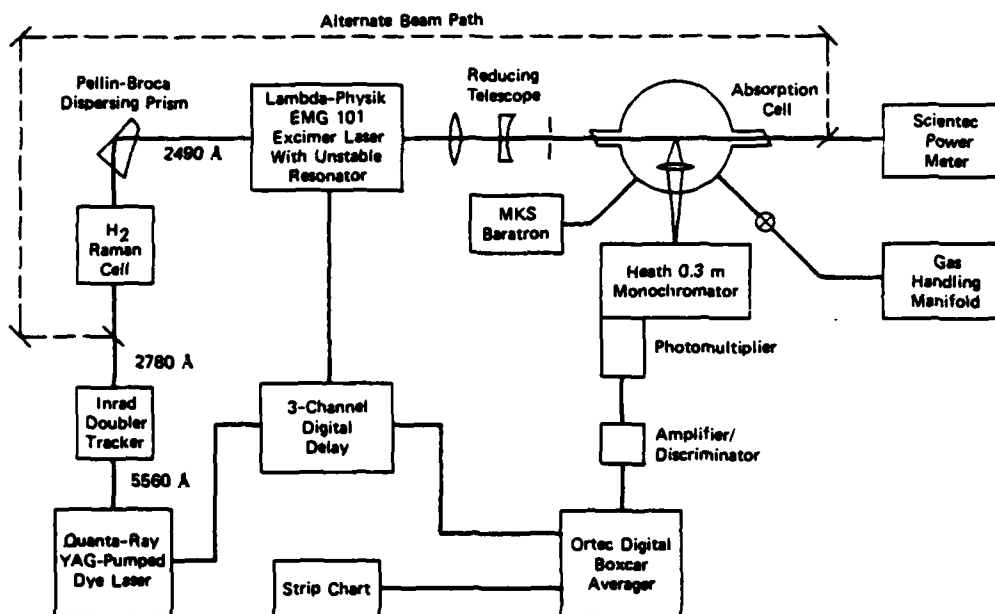


FIG. 1. Apparatus schematic.

Pressures were measured with an MKS Baratron.

Radiation from a small portion of the beam was focused onto the monochromator slit, and detected with a photomultiplier. The signal was amplified, fed into an Ortec digital boxcar averager, and then to a strip chart recorder. A delay of 100 ns was used between the excimer and dye laser pulses when they were operated independently. The system was operated at 10 Hz, and photons were accumulated with a 10 μ s gate.

RESULTS

The present results include fluorescence and excitation spectra of the NO *A-X* and *B-X* transitions, kinetic data on quenching of vibrationally excited NO, and comparison of relative NO(*v*) production from NO₂ photoexcitation to the two states in the 2480–2495 Å region. These are described in turn.

NO fluorescence spectra

In the work of McKendrick *et al.*,⁴ it has been shown that NO₂ photodissociation with KrF excimer laser light leads to production of NO(*A²Σ⁺*) in the *v*=3 level, attributed to two one-photon processes. The first photon dissociates NO₂, leaving some NO in the *v*=6 level of the ground state, and the second photon excites this NO in the NO(*A-X*) 3–6 band, the two heads of which are at 2482 and 2490 Å. McKendrick *et al.*⁴ presented a spectrum of the *A-X* 3–*v*'' progression, and we have also observed this spectrum [Fig. 2(a)], although it is somewhat weaker than others that we shall describe. This is so principally because the *A-X* 3–6 band has a very small oscillator strength, and has never been detected in the laboratory. The Franck-Condon factor given by

Ory *et al.*⁹ is 6×10^{-4} , and by Nicholls¹⁰ is 1×10^{-4} .

Since we have used a dye laser in conjunction with the excimer laser, we have had flexibility in choosing the NO transitions to be excited, and in Fig. 2(b) is presented a fluorescence spectrum of the NO(*B-X*) 2–*v*'' progression. This was obtained by injection locking the KrF output to the R1(12)–P1(8) transition pair of the *B-X* 2–4 band at 2492.2 Å. Under the conditions used, there is some relaxation of the *B*(*v*=2) level to *v*=1 and 0, since the *B²Π* lifetime is relatively long, 3 μ s. NO(*A²Σ⁺*) relaxation requires considerably greater pressures, due to the 200 ns lifetime, as shown by McKendrick *et al.*⁴ The nomenclature that we use for the *A-X* and *B-X* spectral lines is that given by Engleman *et al.*¹¹ It should be noted that there is little apparent overlap between the spectra in Fig. 2, i.e., the KrF laser bandwidth does not extend as far as the *B-X* 2–4 band, effectively 2490 Å (see Fig. 6). This is consistent with observations of Bigio and Slatkine.⁷

Excitation spectra

Excitation spectra are essentially absorption spectra, sampling the populations of the lower levels in a transition between two states. Thus, to investigate the population of vibrationally excited ground state NO molecules produced by NO₂ photodissociation, we wish to tune through NO *A-X* or *B-X* bands that terminate on the *X*(*v*) levels.

The *A-X* and *B-X* transitions that we consider here are often intermingled, particularly those whose upper levels are *v*=1. This is because the absolute energies of these two levels are quite close; *A*(1)=47 431 cm⁻¹, *B*_{1/2}(1)=47 438 cm⁻¹, *B*_{3/2}(1)=47 406 cm⁻¹. An example

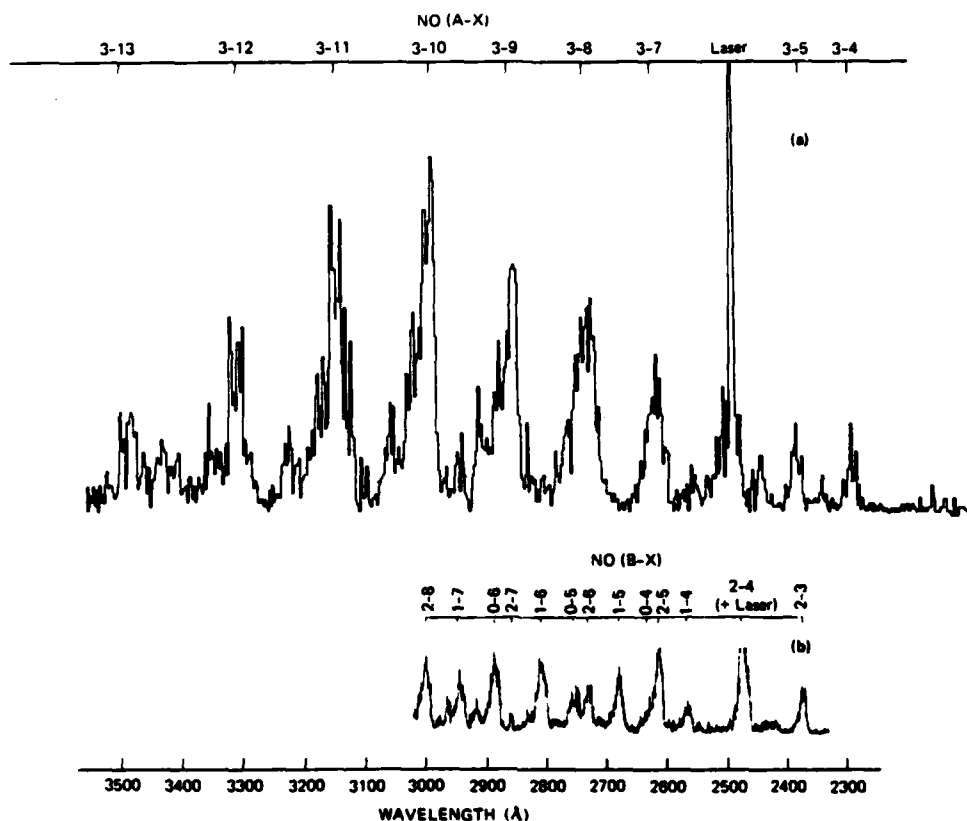


FIG. 2. Fluorescence spectra, 100 ns detection delay, 70 mTorr NO₂, 10 Torr He, (a) NO(A-X) 3-8 pumping (excimer laser only). (b) NO(B-X) 2-4 pumping (injection locking).

is given in Fig. 3, where an excitation spectrum is shown for the 1-7 bands in both the A-X and B-X systems. A particular point to be noted is that the B-X bands are about twice as intense as the A-X bands. Considering that the former is a much weaker transition than the latter in terms of oscillator strengths, we were initially surprised by this effect, which will be discussed in the next section.

In Table I we list the threshold wavelengths for producing NO in the indicated vibrational levels from NO₂ photodissociation. Thus, at 2485 Å NO excitation up to $v=8$ is thermodynamically possible, and this was the limit observed; no signal was seen from a scan of the A-X 3-9 band. Figure 4 shows a scan of the A-X 2-8 band, along with the B-X 0-6 band.

For technical reasons, we were unable to operate the dye laser below about 2750 Å, so that there was a lower limit on the NO vibrational level that could be sampled when the dye and excimer lasers were operating independently. This limit was $v=5$, since the longest wavelength $v'-4$ band is the A-X 0-4 band at 2720 Å. A scan of the A-X 0-5 band is shown in Fig. 5(a), but these data are different, because >90% of the signal originates with the dye laser; turning the excimer laser

off results in almost no change in signal, as seen in Fig. 5(b). Thus, the dye laser alone, operating on the A-X 0-5 band at 2860 Å, dissociates the NO₂ and then pumps the NO($v=5$) level. Table I shows that 2920 Å is the threshold for making NO($v=5$), so the process is plausible. However, the lack of effect of the excimer laser suggests a sharp fall-off in the production rate of $v=5$ compared to $v=6-8$ for 2485 Å dissociation, indicating a population inversion.

TABLE I. Wavelength thresholds for producing NO(v) from NO₂.

NO vibrational level	Threshold wavelength (Å)
0	3977
1	3701
2	3464
3	3161
4	3079
5	2920
6	2779
7	2653
8	2540
9	2437

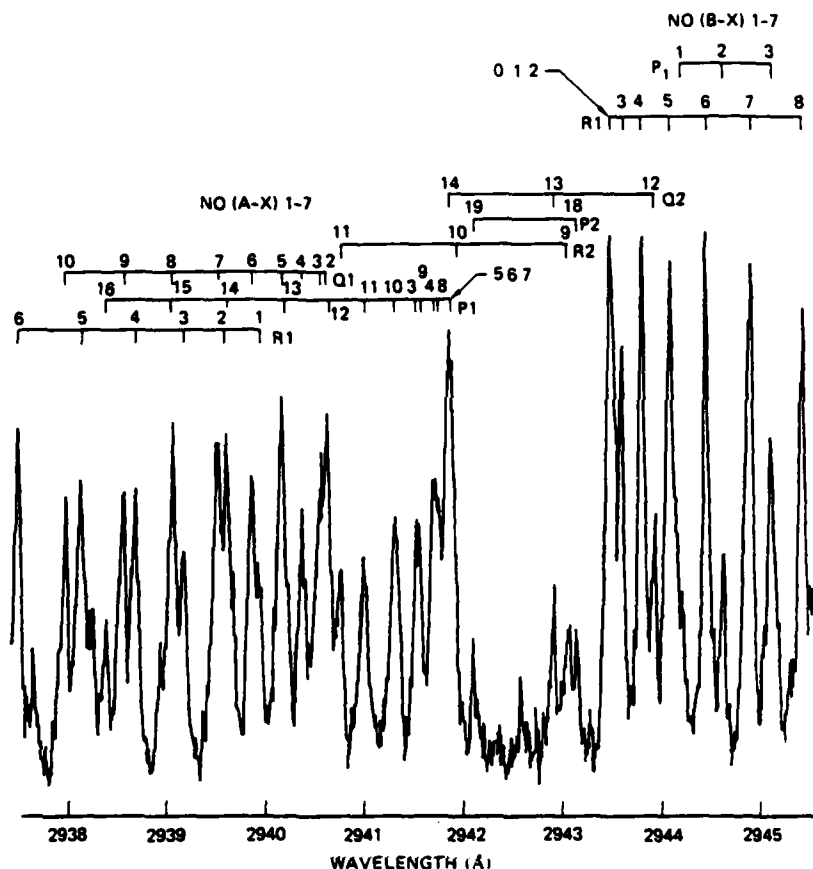


FIG. 3. NO(A-X) and (B-X) 1-7 excitation spectrum. 100 ns detection delay, 70 mTorr NO₂, 10 Torr He.

Having established this effect, we looked more closely at the data for $v=6$, because the 1-6 A-X and B-X bands at 2810 Å should not dissociate NO₂ to produce NO($v=6$), the threshold wavelength being 2779 Å. In this instance, the NO($v=6$) population drops by a factor

of 3.5 when the excimer laser is turned off, and it must be assumed that the residual signal involves some thermal excitation to overcome the 400 cm⁻¹ gap between 2779 and 2810 Å. As expected, there is no signal without the excimer laser when sampling $v=7$ and 8.

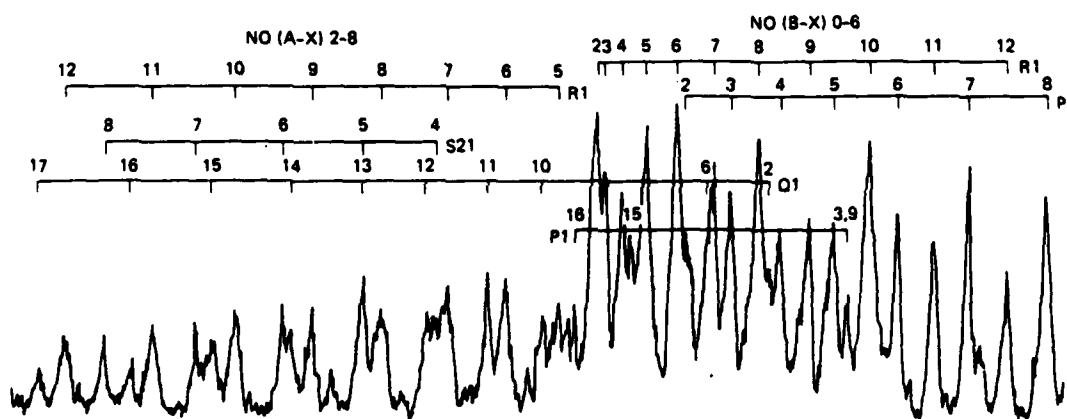


FIG. 4. NO(A-X) 2-8 and NO(B-X) 0-6 excitation spectrum. 100 ns detection delay, 70 mTorr NO₂, 10 Torr He.

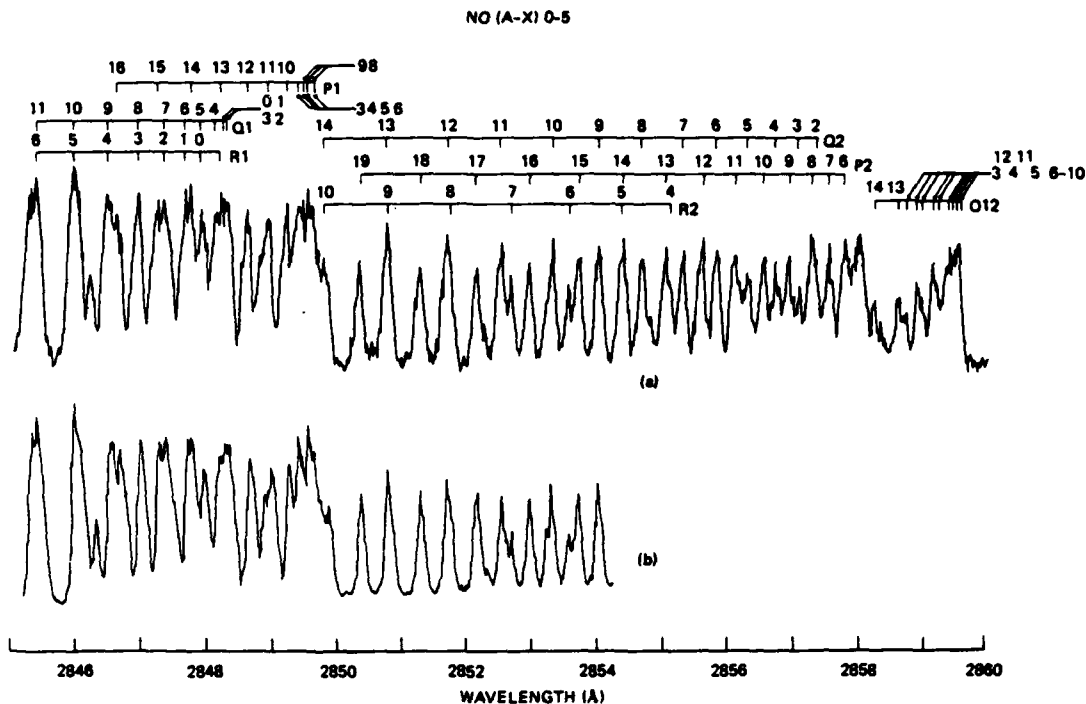


FIG. 5. NO(A-X) 0-5 excitation spectrum, 100 ns detection delay, 70 mTorr NO₂, 10 Torr He. (a) Excimer laser on. (b) Excimer laser off.

The NO₂ 2491 Å band

When the KrF laser is injection locked to the dye laser output, the tuning range permits study of NO₂ photodissociation in the 2491 Å band of NO₂, the 000-000 band of the $\tilde{B}^2B_2-\tilde{X}^2A_1$ transition. This feature has been carefully analyzed by Hallin and Merer,¹² and we can make comparisons between NO(ν) produced from dissociation within this band and in the underlying continuum.

However, we can not obtain a vibrational distribution, since a third laser would then be required in addition to the excimer-dye laser combination. What can be done is to sample the NO($\nu=4$) level, as lines of the B-X 2-4 band lie throughout the NO₂ 2491 Å band. One is then dependent on coincidences between lines in the two bands. Where there is no such coincidence, the excitation scan refers only to NO($\nu=4$) produced in NO₂ continuum absorption.

Such a scan is shown in Fig. 6 for the B-X 2-4 band, and underneath it is an absorption spectrum of the 2491 Å NO₂ band, taken with the dye laser at its 0.5 cm⁻¹ linewidth. It is evident that there are two strong resonances in the excitation scan, but also that outside the NO₂ band, where the NO₂ absorption cross section is about two orders-of-magnitude smaller, the signals are by no means negligible.

By continuing the injection locked scan to shorter wavelengths, we can scan the A-X 3-6 band, the fea-

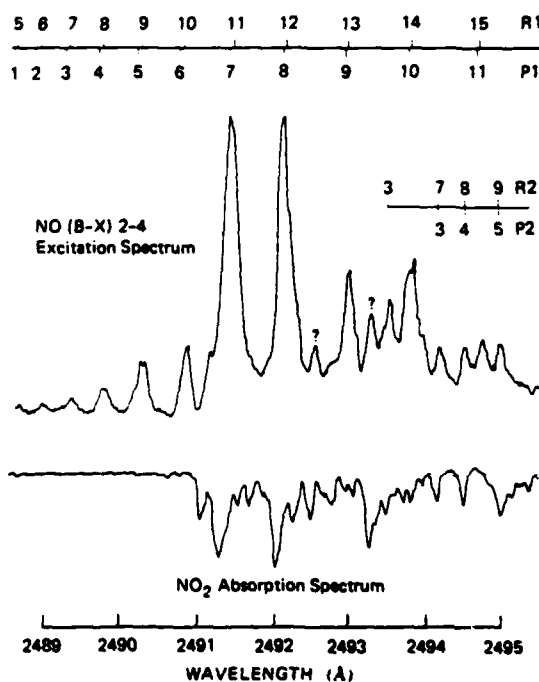


FIG. 6. NO(B-X)2-4 excitation spectrum, and NO₂ absorption spectrum. 100 ns detection delay, 70 mTorr He, 10 Torr He for excitation spectrum.

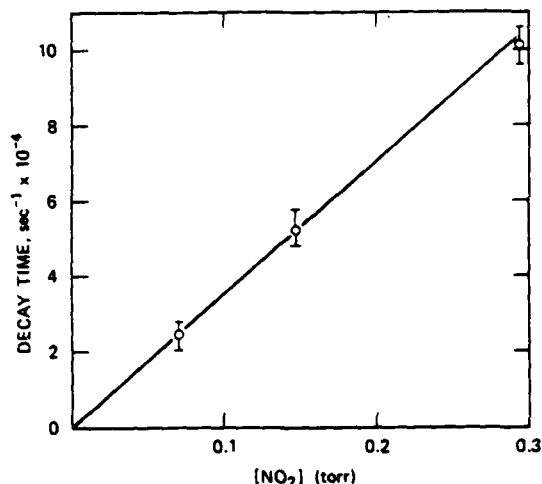


FIG. 7. NO(X, $v=8$) lifetime vs [NO₂], NO₂ added as 0.7% mix in He.

ture observed by McKendrick *et al.*⁴ The lines have similar intensities to the B-X 2-4 lines lying outside the NO₂ 2491 Å band, and we have followed the spectrum out to 2478 Å. Thus, the tuning range is at least 2478–2495 Å, considerably greater than the 10 Å reported by Bigio and Slatkine.⁷

Quenching of NO($v=8$)

As the NO($v=8$) level is the highest accessible with KrF excimer radiation, observations of its temporal behavior are not affected by cascading from higher levels. Thus, its decay can be unambiguously interpreted as NO($v=8$) quenching. By delaying the dye laser pulse with respect to the excimer laser, we can sample the NO($v=8$) population as it decays, using a boxcar averager, and this was done as a function of [NO₂]. The resulting NO($v=8$) lifetimes are plotted against [NO₂] in Fig. 7, and the loss rate coefficient is 1.1×10^{-11} cm³ molecule⁻¹ s⁻¹, considerably larger than the value of 2.1×10^{-12} cm³ molecule⁻¹ s⁻¹ obtained by Stephenson¹³ for quenching of the NO($v=1$) level by NO₂. This is presumably a consequence of the better match between the NO₂ ν_2 fundamental frequency, 1618 cm⁻¹, and an NO $v=8-7$ quantum (1680 cm⁻¹), compared to a $v=1-0$ quantum (1876 cm⁻¹).

He and N₂ were also evaluated as quenchers of NO($v=8$) and were found to be ineffective. The upper limit on the rate coefficient for both gases is 2×10^{-15} cm³ molecule⁻¹ s⁻¹.

DISCUSSION

The high flux density of lasers results in many effects not encountered with conventional light sources. One of these involves the saturation of optical transitions, which occurs when the stimulated emission rate exceeds the radiative rate. Under such circumstances, there is equilibration between the upper and lower lev-

els of a transition, and the population of the upper levels is no longer proportional to the oscillator strength of the transition.

The excitation spectra of Figs. 3 to 6 suggest that such is the case in the present system, since the A-X system is inherently much stronger than the B-X ($\tau_A = 200$ ns, $\tau_B = 3$ μ s), yet we see here that the B-X bands are approximately twice as strong as the A-X bands. In particular, in Fig. 3, in which the 1-7 bands in each transition are probed, detection being made on the 1-6 bands, not only are the lower levels the same, but the Franck-Condon factors show very little variation.⁹ For the 1-6 transitions they are 0.10 and 0.11 for the A-X and B-X bands, and for the 1-7 transitions, they are 0.061 and 0.064, respectively.

To determine if the similar A-X and B-X intensities are due to saturation, we need only calculate the actual laser flux Φ and compare it to Φ_s , the flux required for saturation. Φ is given by

$$\Phi = \frac{I}{A\tau_L} \cdot \frac{\nu_D}{\nu_L},$$

where I is the energy/pulse, A is the beam cross-sectional area, τ_L is the pulse width, ν_D is the absorber Doppler width, and ν_L is the laser linewidth. A 10 mJ pulse at 2500 Å consists of 1.2×10^{16} photons, the beam cross sectional area was 0.07 cm², the pulse width was 10 ns, the Doppler width of an NO line at 2500 Å and 300 K is 0.08 cm⁻¹, and the dye laser line width was 0.5 cm⁻¹, resulting in a value of $\Phi = 3 \times 10^{24}$ photons cm⁻² s⁻¹.

The saturation flux is given by¹⁴

$$\Phi_s = 4\pi \left(\frac{\pi}{\ln 2} \right)^{1/2} \cdot \frac{c\Delta\lambda}{\lambda^4} \cdot \frac{1}{\tau_R A_{v',v''}},$$

where c is the velocity of light, λ is the wavelength, $\Delta\lambda$ is the absorption (Doppler) linewidth, and $\tau_R A_{v',v''}$ is basically the Franck-Condon factor for the NO transition being pumped, which is typically 0.1. Thus, Φ_s has a value of 9×10^{20} $h\nu$ /cm² s, and Φ/Φ_s , the saturation factor, is 3300.

We therefore conclude that all the NO transitions are saturated, and the population of adjacent A and B rotational levels, excited from a single rotational lower level, will differ only by the upper state degeneracies, which will then favor emission from the B² Π state over the A² Σ^+ state by a factor of 2, essentially as observed.

In order to obtain a vibrational distribution from the data, the procedure is then straightforward. Since the signals in the excitation scans for either the B-X or A-X transitions will be proportional only to the NO(v) population and the Franck-Condon factor for emission, it is not necessary to consider the band oscillator strength, the absorption Franck-Condon factor, or the dye laser intensity, unless one or more of these becomes extremely small.

A possible instance of just such an occurrence is the situation with the A-X 3-6 band, where the Franck-Condon factor is some three orders-of-magnitude smaller than for the other A-X or B-X bands. Nevertheless, excitation scans comparing the A-X 3-6 and B-X 2-4

TABLE II. NO(A-X) parameters for obtaining NO(*v*) distribution from 2485 Å NO₂ photodissociation.

Excitation band	Detection band	Detection FC factor (Ref. 5)	Excimer intensity (mJ)	Average R1 peak height (arb. units)	Relative population
2-8	2-7	0.11	20	16	7.3 (<i>v</i> = 8)
1-7	1-6	0.10	15.0	15	10 (<i>v</i> = 7)
1-6	1-5	0.13	16.7	13	4.4 (<i>v</i> = 6)
1-6	1-5	0.13		3.5	
(dye laser alone)					
0-5	0-4	0.091	16.5	15	0.7 (<i>v</i> = 5)
0-5	0-4	0.091		14	
(dye laser alone)					
2-4	2-5	0.10	20	1	0.5 (<i>v</i> = 4)
(B-X)					

bands at ~2490 Å show the A-X lines only a factor of ~4 weaker than the B-X lines. It is probable that the reason that this ratio is not substantially larger is because the *v* = 6 population is considerably greater than that in *v* = 4.

An initial vibrational distribution in NO can be mapped out by using the signal levels from the A-X and B-X excitation scans, from the relationship

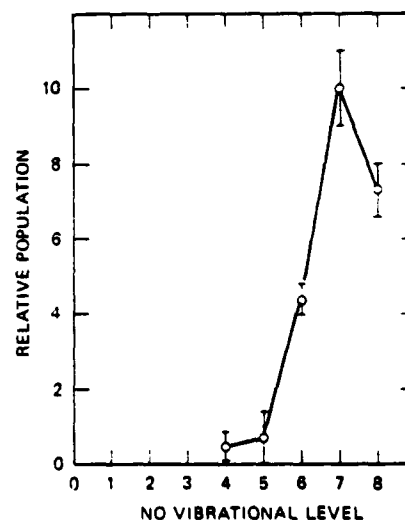
$$S \approx N_{v'} q_{v'v} I_p$$

where *S* is the observed signal, *N_{v'}* is the population in NO(*v'*), *q_{v'v}* is the Franck-Condon factor for the observed radiation, and *I_p* is the (relatively invariant) excimer laser power. For data on the *v* = 5 and 6 levels, the contribution to the NO(*v*) population from the dye laser must be subtracted, while the data on A-X 3-6 and B-X 2-4 must be treated somewhat differently, since the dye laser and broadband excimer laser powers are not independent in the injection locked mode.

Table II lists the parameters used in obtaining the vibrational distributions, and the last column gives a relative set of populations normalized to NO(*v* = 7). With one exception, only the A-X data are used, as levels 5 and 8 were not sampled in the B-X transition. For the *v* = 4 level, the B-X 2-4 band is the only relevant datum. Its excitation spectrum is shown in Fig. 6, but it is not immediately evident what intensity to take, as the *P*-*R* pair intensities fall off rapidly but not abruptly as the dye laser is tuned away from the NO₂ 2491 Å bandhead. The R1(10)-P1(6) intensity is seven times greater than that for R1(5)-P1(1), whereas in both the B-X 0-6 and 1-6 bands, for example, the sum of R1(10) and P1(6) is less than twice the sum of R1(5) and P1(1). The reason seems to be that there are weak S-form lines to the short wavelength side of the 2491 Å band,¹² which enhance the NO₂ dissociation in the region of the R1(10)-P1(6) and R1(9)-P1(5) pairs, so that only the first four *P*-*R* pairs should be considered in arriving at a signal strength to compare with the A-X data. The relative intensities given in Table II for the A-X bands are obtained from the average height of R1 lines from *J* = 1 to

10; for the B-X 2-4 band, the average height of the four *P*-*R* pairs is halved (to account for the degeneracy factor), and multiplied by 2/3, since the *R* lines have about twice the intensity of the *P* lines.¹¹

The distribution is plotted in Fig. 8, and shows very sharp peaking at *v* = 7; only two vibrational levels away, at *v* = 5, Fig. 5 shows that the 16.5 mJ excimer laser pulse makes virtually no contribution to the excitation spectrum, which is produced entirely by the 5.7 mJ 2850 Å dye laser pulse. The vibrational distribution produced in 2850 Å NO₂ photodissociation has of course not been determined, since we only have a datum point for *v* = 5, the maximum level. However, the fact that the level population per mJ of pumping energy is three times as great for the *v* = 5 level produced at 2850 Å as for the *v* = 7 level produced at 2485 Å bears a striking correlation with the fact that the NO₂ photoabsorption

FIG. 8. NO(*v*) distribution from 2485 Å NO₂ photodissociation.

cross section is three times greater at 2850 than at 2485 Å.¹⁸ Thus, it appears that at both wavelengths, the preferentially populated NO(*v*) levels are those at or close to the thermodynamic limit.

Since we have no absolute measurements of the fluorescence yields, we have no indication of the extent to which NO(*A*) may be depleted by multiphoton ionization. However, the cross section for the process NO(*A*, *v*'') → NO*(*v*') will be approximately *v* independent, so deduced vibrational distributions in the NO ground state should be unaffected.

The most relevant study in the literature is that of Zacharias *et al.*,¹ carried out at 3371 Å. In this case, NO(*v*=2) is the maximum level, and they showed that here too a vibrational population inversion is obtained; the *v*=2 population accounted for 51% of molecules in the ²Π_{1/2} sublevel, and 42% in the ²Π_{3/2} sublevel. An earlier study by Busch and Wilson,³ at 3470 Å, had established that the *v*=0 and 1 levels were equally populated, so it is evident that in all NO₂ studies to date in which vibrational populations have been determined, the distributions are nonstatistical and inverted.

Since we have not yet sampled levels in the range *v* = 0–3, we cannot say if our distribution is bimodal. If it is not, then Fig. 8 represents the total distribution, and we would conclude that > 85% of the excess energy is in NO vibrational modes, even on the assumption that the molecules are not rotationally hot. We intend to carry out measurements with dye lasers at shorter wavelengths, to sample the lower vibrational levels, using both continuum and 2491 Å dissociation of NO₂.

To obtain an idea of rotational temperatures, the data for the A²Σ⁺–X²Π_{3/2} 0–5 band (Fig. 5) were used. From the P2 lines, identified from *J* = 4 to 19, a plot of log [intensity/(2*J*' + 1)] vs *J*'(*J* + 1), is linear over most of the spectrum [P2(9) to P2(19)], the slope indicating a 750 K rotational temperature. Below P2(9), the change in slope suggests a much lower temperature, on the order of 130 K. Our initial impulse was to attribute this difference to a lesser reliability of the line intensities in the congested region close to the origin, but in fact Zacharias *et al.*¹ have seen just such behavior in their experiment. The data for their highest accessible level, *v*' = 2, are in a sense directly comparable to our *v*' = 5 data shown in Fig. 5, since this excitation spectrum is due almost entirely to the dye laser, for which the maximum accessible level is *v*' = 5.

Zacharias *et al.*¹ found that for *v*' = 2, the "rotational temperature" for the first few levels was 60 K, whereas for levels above *J* = 9, a 1600 K temperature fit the data. Similar observations were made on the *v*' = 1 level, so there seems to be no question about the validity of the data. They suggest that there are competing channels involved in the dissociation, to which we can only add that the same effect seems to occur when the dissociating photon has considerably more energy (0.65 eV). The fact that Zacharias *et al.*¹ observed a higher rota-

tional temperature than was measured in the present experiments is probably a consequence of relaxation caused by the 10 Torr He used here.

The question of the mechanism of the dissociative process was discussed by McKendrick *et al.*⁴ and in choosing between two-photon sequential excitation and one-photon dissociation followed by LIF of the NO product, they correctly chose the latter, although their only observable was the NO(*A*–X) 3–*v*' progression. The fact that the distribution that we have observed exhibits a sharp cutoff for *v* > 8, lends strong support to their conclusion. We can thus say that our observations are entirely consistent with one-photon dissociation, and with neither two-photon excitation of NO₂, nor three-photon ionization followed by dissociative recombination.

With reference to the 2491 Å NO₂ band, inspection of Fig. 6 indicates that although there is a large NO(*v*=4) population enhancement due to the increased NO₂ cross section on lines within this band, the signal would most likely be much greater if a higher NO vibrational level were sampled. We plan to examine this question by using a second dye laser at longer wavelengths; if the NO vibrational distribution is similar in the 2491 Å band as in the underlying continuum, then sampling the NO(*v*=7) level can be expected to give a much larger signal.

In recent work by Morrison and Grant⁵ and by Morrison *et al.*,⁶ NO₂ photodissociation has been studied by multiphoton ionization, using 4200–5200 Å radiation as a source. There is no indication from the MPI spectra of any signal enhancement at 4982 Å (twice the 2491 Å wavelength), but it is not necessarily valid to compare one- and two-photon processes in this manner. Nevertheless, they reach the interesting conclusion that below the threshold for the NO+O(¹D) dissociative channel at 2439 Å, the NO vibrational distribution contains no NO(*v*=0) (although when the threshold is exceeded, the excess internal energy decreases and *v*=0 is seen). To the extent that we can compare our experiment and theirs, their lack of detection of NO(*v*=0) suggests the absence of a bimodal NO(*v*) distribution, and implies that Fig. 8 represents the total distribution.

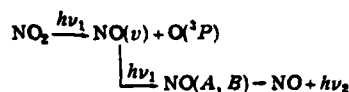
The most reasonable explanation for such a unique vibrational distribution is that a significant change in bond length occurs between the NO₂ ground state and the dissociating excited state, such that in a vertical transition, the excited molecule finds itself well up on a potential wall. Passage through the exit channel is then accompanied by transverse motion, and the molecule and atom may in principle separate with little translational energy, but with considerable vibrational energy in the molecular fragment. This is the model proposed by Mitchell and Simons,¹⁶ and considered by Zacharias *et al.*¹ to explain their *v*=0–2 distribution. Similar concepts have been used successfully by Moser *et al.*¹⁷ to explain the high degree of NO vibrational excitation observed in the 2480 and 1930 Å photodissociation of NOCl.

Our problem with this interpretation is that the NO₂ absorption cross section at ~2500 Å is at a minimum,

and the identity of the absorbing state is not entirely clear. The 2491 Å band is known to involve the \tilde{B}^3B_2 - \tilde{X}^3A_1 transition,¹² and at longer wavelengths (3700-4600 Å) Douglas and Huber¹³ claim that absorption is to the \tilde{A}'^3B_1 or \tilde{A}^3B_1 states. Zacharias *et al.*¹ have invoked the \tilde{A}^3B_1 and \tilde{B}^3B_1 states in 3371 Å photodissociation, and noted that their equilibrium bond lengths are substantially greater than in the ground state. A greater spectroscopic understanding of NO₂ at 2500 Å is necessary before we can claim that the high degree of vibrational excitation that we observe is a consequence of the same effect.

There are some interesting consequences of the observations we have made on NO₂, relating on the one hand to combustion diagnostics, and on the other hand to studies of vibrationally excited species.

In a fairly unique wavelength region, basically 2640-2860 Å, NO₂ can be detected with high sensitivity by a single laser, using sequential photons. The process



has a long wavelength limit of 2860 Å, which corresponds to the A-X 0-5 band. At this wavelength, $v=5$ is the highest accessible level in the NO product; any longer wavelength radiation can only pump NO levels in $v \geq 6$, which could not be formed, and thus the second photon cannot be absorbed.

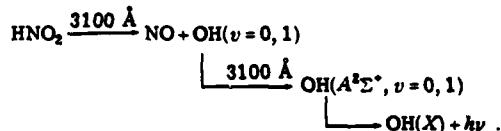
On the short wavelength side, the single wavelength process will become ineffective if the vibrational distribution in the NO product is strongly inverted, as we show is the case in Fig. 8 for 2485 Å NO₂ photodissociation. In this case, the B-X 2-4 band is a poor NO probe (except within the 2491 Å NO₂ band) because NO($v=4$) is so underpopulated. It is probably valid to say that the effective limits of the single wavelength process are the A-X 0-5 band at 2860 Å and the A-X 2-6 band at 2640 Å.

Detection of NO₂ by tuning through these bands, and sequentially dissociating the parent molecule and exciting the product NO($v=5, 6$) is then a very specific process. The resultant NO excitation spectrum will be unique, since such highly vibrationally excited molecules will not normally be found in a combustion system. Furthermore, detection can be made at much shorter wavelengths—the signal from a 2860 Å NO₂ probe can be monitored on the NO(A-X) 0-1 band at 2370 Å. This may be a very useful feature in avoiding contaminant emission, such as scattered laser light, and long wavelength emission from polyatomic molecules. Finally, detecting NO₂ with UV radiation rather than using LIF in the visible region presents certain advantages, for example, (a) the NO(A) radiative lifetime is some two orders-of-magnitude shorter than that of the NO₂ states excited in the visible, thus potentially decreasing quenching problems, (b) LIF of NO₂ is a very inefficient process, since the reradiation emerges over a large spectral region,¹⁴ whereas the NO radiation is concentrated in a few bands, and (c) in many

flames there will be much less extraneous optical emission in the UV than in the visible, making NO detection easier. For similar reasons, consideration should also be given to the relative merits of monitoring atmospheric NO₂ in the UV rather than the visible.

In terms of photochemical kinetics, the strong population inversion suggests that it is possible to prepare NO(v) in fairly specific levels. For instance, studies on NO($v=8$), to the exclusion of higher levels, are best carried out using a KrF laser on NO₂. If $v=6$ is to be studied, a dye laser operating at ~2700 Å would be the preferred source.

Finally, we would like to suggest that processes of the type described may be useful for detection of other polyatomic molecules, the requirement being that there is a photodissociative continuum for the first photon, and bands involving the ground state of the vibrationally excited diatomic product in the same spectral region. For example, it is probable that HNO₂ can be detected by the process



CONCLUSION

We have demonstrated that a strongly inverted NO vibrational distribution is produced from NO₂ photodissociation at 2485 Å, consistent with other studies at longer wavelength. In regions of the NO₂ absorption spectrum coincident with NO(A-X) and NO(B-X) line positions, radiation at a single wavelength both dissociates the NO₂ and gives an LIF NO spectrum, and since high NO vibrational levels are involved, the process is diagnostic of the presence of NO₂. Because the NO₂ 2491 Å band has a very large absorption cross section relative to other UV regions, NO₂ detection should be very sensitive at that wavelength.

We have shown that injection locking of the KrF excimer radiation can be carried out over at least a 17 Å range, thus giving a tunable source of 10-20 mJ pulses at the dye laser linewidth in the 2485 Å region.

As the highest thermodynamically permissible NO vibrational levels are strongly populated in this process, it is simple to measure relaxation of these levels without cascading effects from higher levels; we have measured NO($v=8$) quenching by NO₂, N₂, and He.

ACKNOWLEDGMENTS

This study was supported by Contract DAAG-29-81-K-0001 from the Army Research Office. We are grateful to J. A. Barker, D. R. Crosley, and P. W. Fairchild for useful discussions.

¹H. Zacharias, M. Geilhaupt, and K. H. Welge, *J. Chem. Phys.* 74, 219 (1981).

²K. H. Welge, *J. Chem. Phys.* 45, 1113 (1966).

- ³G. E. Busch and K. R. Wilson, *J. Chem. Phys.* **56**, 3626 (1972).
- ⁴G. B. McKendrick, C. Fotakis, and R. J. Donovan, *J. Photochem.* **20**, 175 (1982).
- ⁵R. J. S. Morrison and E. R. Grant, *J. Chem. Phys.* **77**, 5995 (1982).
- ⁶R. J. S. Morrison, B. H. Rockney, and E. R. Grant, *J. Chem. Phys.* **75**, 2643 (1981).
- ⁷I. J. Bigio and M. Slatkine, *Opt. Lett.* **6**, 336 (1981).
- ⁸W. K. Bischel, B. E. Perry, and D. R. Crosley, *Appl. Opt.* **21**, 1419 (1982).
- ⁹H. A. Ory, A. P. Gittleman, and J. P. Maddox, *Astrophys. J.* **139**, 346 (1964).
- ¹⁰R. W. Nicholls, *J. Res. Natl. Bur. Stand.* **68**, 535 (1964).
- ¹¹R. Engleman, P. E. Rouse, H. M. Peek, and V. D. Balamonte, Los Alamos Scientific Laboratory, LA-4364 (1970).
- ¹²K.-E. J. Hallin and A. J. Merer, *Can. J. Phys.* **54**, 1157 (1976).
- ¹³J. C. Stephenson, *J. Chem. Phys.* **60**, 4289 (1974).
- ¹⁴C. A. Brau, in *Excimer Lasers*, edited by C. K. Rhodes (Springer, New York, 1979), p. 93.
- ¹⁵T. Nakayama, M. Y. Kitamura, and K. Watanabe, *J. Chem. Phys.* **30**, 1180 (1959).
- ¹⁶R. C. Mitchell and J. P. Simons, *Discuss. Faraday Soc.* **44**, 208 (1967).
- ¹⁷M. D. Moser, E. Wertz, and G. C. Schatz, *J. Chem. Phys.* **78**, 757 (1983).
- ¹⁸A. E. Douglas and K. P. Huber, *Can. J. Phys.* **43**, 74 (1965).
- ¹⁹C. G. Stevens, M. W. Swagel, R. Wallace, and R. N. Zare, *Chem. Phys. Lett.* **18**, 465 (1973).